

# Integrated Principal Components Analysis

Tiffany M. Tang<sup>a</sup> and Genevera I. Allen<sup>b,c</sup>

## Abstract

Data integration, or the strategic analysis of multiple sources of data simultaneously, can often lead to discoveries that may be hidden in individualistic analyses of a single data source. We develop a new statistical data integration method named Integrated Principal Components Analysis (iPCA), which is a model-based generalization of PCA and serves as a practical tool to find and visualize common patterns that occur in multiple datasets. The key idea driving iPCA is the matrix-variate normal model, whose Kronecker product covariance structure captures both individual patterns within each dataset and joint patterns shared by multiple datasets. Building upon this model, we develop several penalized (sparse and non-sparse) covariance estimators for iPCA and study their theoretical properties. We show that our sparse iPCA estimator consistently estimates the underlying joint subspace, and using geodesic convexity, we prove that our non-sparse iPCA estimator converges to the global solution of a non-convex problem. We also demonstrate the practical advantages of iPCA through simulations and a case study application to integrative genomics for Alzheimer's Disease. In particular, we show that the joint patterns extracted via iPCA are highly predictive of a patient's cognition and Alzheimer's diagnosis.

*Keywords: Data integration, data fusion, matrix-variate normal, dimension reduction, integrative genomics*

---

<sup>a</sup>Department of Statistics, University of California, Berkeley, Berkeley, CA

<sup>b</sup>Departments of Statistics, Computer Science, and Electrical and Computer Engineering, Rice University, Houston, TX

<sup>c</sup>Jan and Dan Duncan Neurological Research Institute, Baylor College of Medicine, Houston, TX

# 1 Introduction

Because of the complexity of most natural phenomena, it is unlikely that a single data source encapsulates all information necessary to fully understand the phenomena of interest. For example, meteorologists cannot predict the weather based on temperature alone. Audio is only one component in surveillance efforts, and in science, it is known that DNA is not the sole driver of human health. Thus, it is not surprising that data integration, or the strategic analysis of multiple sources of data simultaneously, can lead to discoveries which are not evident in analyses of a single data source. Returning to the previous examples, meteorologists must integrate data from satellites, ground-based sensors, and numerical models (Ghil and Malanotte-Rizzoli 1991). Audio and video are often combined for surveillance as well as speech recognition (Shivappa et al. 2010), and as new technologies arise in biology, scientists are leveraging data integration to better understand complex biological processes (Lock et al. 2013). In general, by exploiting the diversity and commonalities among different datasets, data integration helps to build a wholistic and perhaps more realistic model of the phenomena of interest. Furthermore, as technological advances fuel the growing number of available datasets, data integration is becoming increasingly necessary in numerous disciplines.

## 1.1 Related Work

Though the data deluge is a recent development, the concept of data integration is certainly not new. For instance, it is a fundamental idea in the classical canonical correlation analysis (CCA) (Hotelling 1936), which infers the relationship between features from two datasets.

More recently, data integration has revolved around factorization methods due to their ease of interpretability and computational feasibility. The framework of coupled matrix and tensor (CMTF) factorizations (Singh and Gordon 2008; Acar et al. 2014) unifies a large class of these factorizations while Joint and Individual Variation Explained (JIVE) (Lock et al. 2013) is another factorization method that is commonly used in integrative genomics. One

general challenge with matrix factorization methods however is that they depend on the rank of the factorized matrices, which is frequently unknown and must be specified a priori.

In contrast to the matrix factorization methods, the generalized SVD (GSVD) provides an exact matrix decomposition for coupled data (Alter et al. 2003; Ponnappalli et al. 2011) and is not dependent on the matrix rank. However, it is limited in scope. The GSVD assumes each matrix has full row rank, excluding integrated problems with both high-dimensional and low-dimensional datasets.

There has also been work on extending principal components analysis (PCA) to integrated data problems. This family of methods is known as the multiblock PCA family, and it includes Multiple Factor Analysis (MFA) (Escofier and Pages 1994; Abdi et al. 2013) and Consensus PCA (Westerhuis et al. 1998). In these methods, each data matrix is normalized according to a specific procedure, then data matrices are concatenated together, and finally, PCA is performed on the normalized concatenated data. Closely related to this is Distributed PCA (Fan et al. 2017), which integrates data that are stored across multiple servers.

Thus far, the existing methods have largely been algorithmic constructions, which lack a rigorous statistical model. As a result, the statistical properties and theoretical foundations of data integration methods are generally unknown. We begin to bridge this gap between data integration methodology and statistical theory by developing a new data integration method, Integrated Principal Components Analysis (iPCA), which extends a model-based framework of PCA to the integrated data setting. The two main building blocks of iPCA are PCA and the matrix-variate normal distribution, which we review next.

## 1.2 Principal Components Analysis

Given a dataset  $\mathbf{X} \in \mathbb{R}^{n \times p}$ , recall that PCA finds orthogonal directions  $\mathbf{v}_1, \dots, \mathbf{v}_m \in \mathbb{R}^p$ , which maximize the covariance  $\mathbf{\Delta} \in \mathcal{S}_{++}^p$ . That is, for each  $j = 1, \dots, m$ ,

$$\mathbf{v}_j = \operatorname{argmax}_{\mathbf{v} \in \mathbb{R}^p} \mathbf{v}^T \mathbf{\Delta} \mathbf{v} \quad \text{subject to } \mathbf{v}^T \mathbf{v} = 1, \quad \mathbf{v}^T \mathbf{v}_i = 0 \quad \forall i < j. \quad (1)$$

It is well-known that the PC loading  $\mathbf{v}_j$  is the eigenvector of  $\mathbf{\Delta}$  with the  $j^{\text{th}}$  largest eigenvalue, and its corresponding PC score is  $\mathbf{u}_j := \mathbf{X} \mathbf{v}_j$ . In practice, since the population covariance  $\mathbf{\Delta}$  is typically unknown, the sample version of PCA plugs in an estimate  $\hat{\mathbf{\Delta}} := \frac{1}{n} \mathbf{X}^T \mathbf{X}$  for  $\mathbf{\Delta}$  in (1) (assuming  $\mathbf{X}$  is column centered). It follows that the PC loadings are the eigenvectors of  $\hat{\mathbf{\Delta}}$ , and the PC scores are the eigenvectors of  $\hat{\mathbf{\Sigma}} := \frac{1}{p} \mathbf{X} \mathbf{X}^T$ . Equivalently, if the SVD gives  $\mathbf{X} = \mathbf{U} \mathbf{D} \mathbf{V}^T$ , then the columns of  $\mathbf{V}$  and  $\mathbf{U}$  are the PC loadings and scores, respectively.

To later establish the link between iPCA and PCA, we point out that  $\hat{\mathbf{\Delta}}$  is the maximum likelihood estimator (MLE) of  $\mathbf{\Delta}$  under the multivariate normal model  $\mathbf{x}_1, \dots, \mathbf{x}_n \stackrel{iid}{\sim} N(\mathbf{0}, \mathbf{\Delta})$ , and  $\hat{\mathbf{\Sigma}}$  is the MLE of  $\mathbf{\Sigma}$  under  $\mathbf{x}'_1, \dots, \mathbf{x}'_p \stackrel{iid}{\sim} N(\mathbf{0}, \mathbf{\Sigma})$ . Here,  $\mathbf{x}_i$  is the  $i^{\text{th}}$  row of  $\mathbf{X}$ , and  $\mathbf{x}'_j$  is the  $j^{\text{th}}$  column of  $\mathbf{X}$ . While this is not the only way of viewing PCA, this framework illustrates two points which we explore further in iPCA: (1) PCA can be framed as maximizing the variance in  $\mathbf{X}$  under a normal model; (2) Eigenvectors correspond to the dominant (or variance-maximizing) patterns in the data.

### 1.3 Matrix-variate Normal Model

The matrix-variate normal distribution (Gupta and Nagar 1999; Dawid 1981) is an extension of the multivariate normal distribution such that the matrix is the fundamental object of study. We say that an  $n \times p$  random matrix  $\mathbf{X}$  follows a matrix-variate normal distribution and write  $\mathbf{X} \sim N_{n,p}(\mathbf{M}, \mathbf{\Sigma} \otimes \mathbf{\Delta})$  if  $\text{vec}(\mathbf{X}^T)$  follows a multivariate normal distribution with Kronecker product covariance structure,  $\text{vec}(\mathbf{X}^T) \sim N(\text{vec}(\mathbf{M}^T), \mathbf{\Sigma} \otimes \mathbf{\Delta})$ , where  $\text{vec}(\mathbf{X}) \in \mathbb{R}^{np}$  is the column vector formed by stacking the columns of  $\mathbf{X}$  below one another. We call  $\mathbf{M} \in \mathbb{R}^{n \times p}$  the mean matrix,  $\mathbf{\Sigma} \in \mathcal{S}_{++}^n$  the row covariance matrix, and  $\mathbf{\Delta} \in \mathcal{S}_{++}^p$  the column covariance matrix, where  $\mathcal{S}_{++}^n$  denotes the set of  $n \times n$  symmetric positive definite matrices.

Intuitively, the row covariance  $\mathbf{\Sigma}$  encodes the dependencies between rows of  $\mathbf{X}$ , and the column covariance  $\mathbf{\Delta}$  encodes the dependencies among the columns of  $\mathbf{X}$ , i.e.  $\mathbf{X}_{i,\cdot} \sim N(\mathbf{M}_{i,\cdot}, \mathbf{\Sigma}_{ii} \mathbf{\Delta})$  and  $\mathbf{X}_{\cdot,j} \sim N(\mathbf{M}_{\cdot,j}, \mathbf{\Delta}_{jj} \mathbf{\Sigma})$ . Given these normally-distributed marginals, it can be shown that if  $\mathbf{\Sigma} = \mathbf{I}$  and  $\mathbf{M} = \mathbf{0}$ , we are in the familiar multivariate normal setting,

$\mathbf{x}_1, \dots, \mathbf{x}_n \stackrel{iid}{\sim} N(\mathbf{0}, \mathbf{\Delta})$ . Similarly, if  $\mathbf{\Delta} = \mathbf{I}$  and  $\mathbf{M} = \mathbf{0}$ , then  $\mathbf{x}'_1, \dots, \mathbf{x}'_p \stackrel{iid}{\sim} N(\mathbf{0}, \mathbf{\Sigma})$ .

An important distinction between the multivariate and matrix-variate normal distributions is that the multivariate normal can only model relationships between elements of a single row or a single column in  $\mathbf{X}$  whereas the matrix-variate normal can model relationships between elements from different rows and columns. The matrix-variate normal is thus far more general than the multivariate normal. With this level of generality, the matrix-variate normal has proven to be a versatile tool in various contexts such as graphical models (Yin and Li 2012; Tsiligkaridis et al. 2013; Zhou 2014a), spatio-temporal models (Greenewald and Hero 2015), and transposable models (Allen and Tibshirani 2010). Our work on iPCA is the first to consider the matrix-variate normal model in light of data integration.

## 1.4 Overview

iPCA is a generalization of PCA for integrated data via matrix-variate normal models, and it serves as a practical tool to identify and visualize joint patterns that are shared by multiple datasets. We formally introduce iPCA in Section 2, and in Section 3, we discuss covariance estimation methods for iPCA and highlight our two main theoretical contributions - proving subspace consistency of the additive  $L_1$  correlation iPCA estimator and proving global convergence of the multiplicative Frobenius iPCA estimator. Beyond these theoretical guarantees, iPCA has several practical advantages: (1) since iPCA is not a matrix factorization method, it is not dependent on the rank of the factorized matrices; instead, iPCA gives ordered, nested, orthogonal PCs as in PCA; (2) iPCA (with the multiplicative Frobenius estimator) converges to the global solution, which is important for reproducibility, and (3) from an interpretability standpoint, iPCA can extract patterns in feature and sample space simultaneously and provides convenient visualizations of these patterns. Furthermore, we will empirically demonstrate in Section 4, through extensive simulations and a case study with integrative genomics for Alzheimer’s Disease, the strong performance of iPCA in practice. Finally, we conclude with a discussion of iPCA and future work in Section 5.

## 2 Integrated PCA

Similar to PCA, iPCA is an unsupervised tool for exploratory data analysis, pattern recognition, and visualization. Unlike PCA however, iPCA extracts dominant joint patterns which are *common* to multiple datasets, not necessarily the variance-maximizing patterns since they might be specific to one dataset. These joint patterns are typically of considerable interest to practitioners as its common occurrence in multiple datasets may point to some foundational mechanism or structure.

Generally speaking, we find these joint patterns by modeling the dependencies between and within datasets via the matrix-variate normal model. The inherent Kronecker product covariance structure enables us to decompose the total covariance of each data matrix into two separable components - an individual column covariance structure which is unique to each dataset and a joint row covariance structure which is shared among all datasets. The joint row covariance structure is our primary interest, and maximizing this joint variation will yield the dominant patterns which are common across all datasets.

### 2.1 Population Model of iPCA

Suppose we observe  $K$  coupled data matrices,  $\mathbf{X}_1, \dots, \mathbf{X}_K$ , of dimensions  $n \times p_1, \dots, n \times p_K$ , where  $n$  is the number of samples and  $p_k$  is the number of features in  $\mathbf{X}_k$ . Throughout this paper, we let  $p := \sum_{k=1}^K p_k$  and  $\tilde{\mathbf{X}} := [\mathbf{X}_1, \dots, \mathbf{X}_K]$ . Suppose also that each of the data matrices has a distinct set of features that are measured on the same  $n$  samples and that all of the rows of  $\mathbf{X}_k$  perfectly align (see Figure 1). Under the iPCA model, we assume that each dataset  $\mathbf{X}_k$  arises from a matrix-variate normal distribution. Namely, for each  $k = 1, \dots, K$ ,

$$\mathbf{X}_k \sim N_{n,p_k}(\mathbf{1}_n \boldsymbol{\mu}_k^T, \boldsymbol{\Sigma} \otimes \boldsymbol{\Delta}_k), \quad (2)$$

where  $\mathbf{1}_n$  is an  $n \times 1$  column vector of ones,  $\boldsymbol{\mu}_k$  is a  $p_k \times 1$  vector of column means specific to  $\mathbf{X}_k$ ,  $\boldsymbol{\Sigma}$  is an  $n \times n$  row covariance matrix that is jointly shared by all data matrices, and

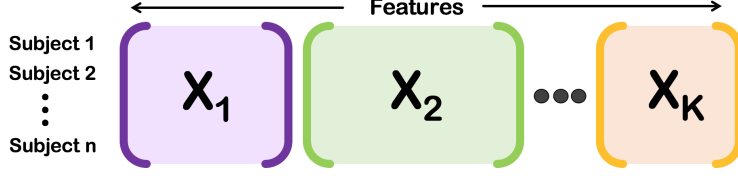


**Figure 1:** Integrated Data Setting for iPCA: We observe  $K$  coupled data matrices, each with a distinct set of features that are measured on the same set of  $n$  samples. Assume that the rows align.

$\Delta_k$  is a  $p_k \times p_k$  column covariance matrix that is specific to  $\mathbf{X}_k$ .

Given the underlying model in (2), we define the population version of iPCA to maximize the row and column covariances. For  $k = 1, \dots, K$ , iPCA solves

$$\mathbf{u}_i = \operatorname{argmax}_{\mathbf{u} \in \mathbb{R}^n} \mathbf{u}^T \Sigma \mathbf{u} \quad \text{subject to } \mathbf{u}^T \mathbf{u} = 1, \quad \mathbf{u}^T \mathbf{u}_l = 0 \quad \forall l < i, \quad (i = 1, \dots, n) \quad (3)$$

$$\mathbf{v}_j^k = \operatorname{argmax}_{\mathbf{v} \in \mathbb{R}^{p_k}} \mathbf{v}^T \Delta_k \mathbf{v} \quad \text{subject to } \mathbf{v}^T \mathbf{v} = 1, \quad \mathbf{v}^T \mathbf{v}_l^k = 0 \quad \forall l < j, \quad (j = 1, \dots, p_k) \quad (4)$$

for which we know the solution to be given by the eigendecompositions of  $\Sigma$  and  $\Delta_k$ . That is,  $\mathbf{u}_i$  is the eigenvector of  $\Sigma$  with the  $i^{\text{th}}$  largest eigenvalue, and  $\mathbf{v}_j^k$  is the eigenvector of  $\Delta_k$  with the  $j^{\text{th}}$  largest eigenvalue. Most notably,  $\mathbf{u}_1$  maximizes the joint variation and is interpreted as the most dominant pattern shared by all  $K$  datasets. We call the columns of  $\mathbf{U} := [\mathbf{u}_1, \dots, \mathbf{u}_n]$  the integrated principal component (iPC) scores and the columns of  $\mathbf{V}_k := [\mathbf{v}_1^k, \dots, \mathbf{v}_{p_k}^k]$  the iPC loadings for the  $k^{\text{th}}$  dataset. Since we are interested in the joint patterns, we primarily plot the iPC scores  $\mathbf{U}$  to visualize the joint patterns in sample space.

*Remark.* The population covariances in (2) are not identifiable (e.g.  $\Sigma \otimes \Delta_k = c \Sigma \otimes \frac{1}{c} \Delta_k$  for  $c \in \mathbb{R}$ ), but the iPC scores and loadings are identifiable since eigenvectors are scale-invariant.

To build intuition for the iPCA model (2), we note that  $\mathbf{1}_n \boldsymbol{\mu}_k^T$  is the matrix of column means. Moreover, by properties of the matrix-variate normal, we interpret  $\Delta_k$  as describing the covariance structure among features in  $\mathbf{X}_k$ , giving rise to patterns unique to  $\mathbf{X}_k$ , and we interpret  $\Sigma$  as describing the common covariance structure among samples, corresponding to joint patterns that are shared by all  $K$  datasets. Hence, maximizing the joint row covariance in (3) yields the dominant patterns among samples, which are common to all  $K$  datasets.

We also point out that if  $K = 1$  and  $\Sigma = \mathbf{I}$ , then  $\mathbf{V}_1$  are the PC loadings from PCA, and if  $K = 1$  and  $\Delta_1 = \mathbf{I}$ , then  $\mathbf{U}$  are the PC scores from PCA. This reveals the fundamental difference between PCA and iPCA - PCA computes the PC loadings and scores by assuming independent samples and features, respectively, while iPCA models the dependencies among samples and features concurrently, making no assumptions on independence.

## 2.2 Sample Version of iPCA

To go from the population iPCA model to the sample version, we simply plug in estimators  $\hat{\Sigma}$  and  $\hat{\Delta}_k$  for  $\Sigma$  and  $\Delta_k$ . The sample version of iPCA can be summarized as follows:

1. **Model** each dataset via a matrix-variate normal model with Kronecker product covariance structure:  $\mathbf{X}_k \sim N_{n,p_k}(\mathbf{1}_n \boldsymbol{\mu}_k^T, \Sigma \otimes \Delta_k)$  for each  $k = 1, \dots, K$ .
2. **Estimate** the covariance matrices  $\Sigma, \Delta_1, \dots, \Delta_K$  to obtain  $\hat{\Sigma}, \hat{\Delta}_1, \dots, \hat{\Delta}_K$ . Methods for covariance estimation will be discussed in detail in Section 3.
3. Compute the **eigenvectors**, say  $\hat{\mathbf{U}} =$  eigenvectors of  $\hat{\Sigma}$  and  $\hat{\mathbf{V}}_k =$  eigenvectors of  $\hat{\Delta}_k$ . We interpret  $\hat{\mathbf{U}}$  as the dominant joint patterns in sample space and  $\hat{\mathbf{V}}_k$  as the dominant patterns in feature space which are specific to  $\mathbf{X}_k$ .
4. **Visualize** the dominant joint patterns by plotting the iPC scores  $\hat{\mathbf{U}}$ .

Figure 2 illustrates a motivating example for when iPCA is advantageous. In the example, strong dependencies among features obscure the true joint patterns among the samples. As a result, applying PCA separately to each of the datasets (panels B-D) fails to reveal the joint signal. iPCA can better recover the joint signal because it exploits the known integrated data structure and extracts the shared information among all three datasets simultaneously.

### 2.2.1 Variance Explained by iPCA

After performing iPCA, one might wonder how to interpret the iPCs. Analogous to PCA, we can define a notion of variance explained.

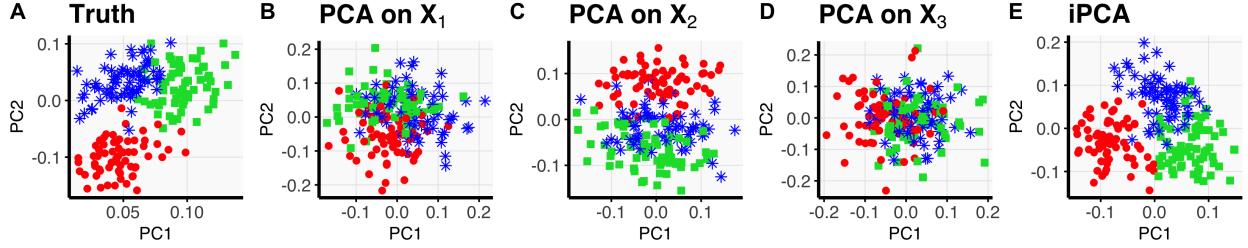


**Figure 2:** Coupled matrices  $\mathbf{X}_1, \mathbf{X}_2, \mathbf{X}_3$  with  $n = 200$ ,  $p_1 = 300$ ,  $p_2 = 500$ ,  $p_3 = 400$  were simulated from the iPCA model (2). Here,  $\Sigma$  and  $\Delta_1, \Delta_2, \Delta_3$  were taken to be as in the base simulation described in Section 4.1. (A) plots the top two eigenvectors of  $\Sigma$ . In separate PCA analyses (B-D), the individual signal in each dataset masks the true joint signal, but (E) iPCA (using the multiplicative Frobenius estimator) exploits the integrated data structure and recovers the true joint signal.

**Definition 1.** Assume that  $\mathbf{X}_k$  has been column centered. We define the cumulative proportion of variance explained in dataset  $\mathbf{X}_k$  by the top  $m$  iPCs to be

$$\text{PVE}_{k,m} := \frac{\|(\mathbf{U}^{(m)})^T \mathbf{X}_k \mathbf{V}_k^{(m)}\|_F^2}{\|\mathbf{X}_k\|_F^2}, \quad (5)$$

where  $\mathbf{U}^{(m)} = [\mathbf{u}_1, \dots, \mathbf{u}_m]$  are the top  $m$  iPC scores, and  $\mathbf{V}_k^{(m)} = [\mathbf{v}_1^k, \dots, \mathbf{v}_m^k]$  are the top  $m$  iPC loadings associated with  $\mathbf{X}_k$ .

**Definition 2.** The marginal proportion of variance explained in dataset  $\mathbf{X}_k$  by the  $m^{\text{th}}$  iPC is defined as  $\text{MPVE}_{k,m} := \text{PVE}_{k,m} - \text{PVE}_{k,m-1}$ .

We verify in Appendix A that  $\text{PVE}_{k,m}$  is a proportion and monotonically increasing as  $m$  increases. Aside from being well-defined, we also show in Appendix A that (5) generalizes the cumulative proportion of variance explained in PCA and hence, is a natural definition.

*Remark.* Unlike PCA, it may be that  $\text{MPVE}_{k,m+1} > \text{MPVE}_{k,m}$  in iPCA. This is because iPCA does not maximize the *total* variance, e.g. if  $\text{MPVE}_{1,2} > \text{MPVE}_{1,1}$ , this simply means that dataset  $\mathbf{X}_1$  contributed more variation to the joint pattern in iPC2 than in iPC1.

## 2.3 Relationship to Existing Methods

Throughout our development of iPCA, we have established the connection between iPCA and PCA, demonstrating that iPCA is indeed a generalization of PCA. We also find it

instructive to draw connections between iPCA and other existing data integration methods.

**Relationship to Multiblock PCA Family** As discussed in Abdi et al. (2013), multiblock PCA methods reduce to performing PCA on the normalized concatenated data  $\tilde{\mathbf{X}}' = [\mathbf{X}'_1, \dots, \mathbf{X}'_K]$ , where each  $\mathbf{X}_k$  has been normalized to  $\mathbf{X}'_k$  according to some procedure. We show in Proposition 1 that performing PCA on the unnormalized concatenated data (referred to as concatenated PCA) is a special case of iPCA, where we assume  $\Delta_k = \mathbf{I}$  for each  $k$ . Proposition 1 can easily be extended to show that multiblock PCA methods are a special case of iPCA for some fixed  $\Delta_1, \dots, \Delta_K$ , and the exact form of  $\Delta_k$  depends on the normalization procedure. For example, since MFA normalizes  $\mathbf{X}_k$  by dividing all of its entries by its largest singular value  $\|\mathbf{X}_k\|_2$ , MFA is a special case of iPCA, where each  $\Delta_k = \|\mathbf{X}_k\|_2 \mathbf{I}$ . Consequently, iPCA can be viewed as a unifying framework for the multiblock PCA family.

**Relationship to Matrix Factorizations** Since coupled matrix factorizations (CMF) decompose the data into the product of a low-rank joint and individual factors, an argument similar to Theorem 2 from Hastie et al. (2015) shows that CMF is closely related to the SVD of the concatenated data. More precisely, one solution of the CMF optimization problem is given by the PC scores and loadings from concatenated PCA, which we know to be a special case of iPCA by Proposition 1. JIVE, on the other hand, is an additive model and decomposes coupled data into the sum of a low-rank joint variation matrix, a low-rank individual variation matrix, and an error matrix. While CMF and iPCA are closely related, JIVE and iPCA are quite different models and are each advantageous in different situations.

### 3 Covariance Estimators for iPCA

Fitting the iPCA model requires estimating the population parameters in (2). As in PCA, we consider maximum likelihood estimation. However, we will see in Section 3.1 that there are substantial challenges with this approach, so we propose new estimators in Section 3.2.

### 3.1 Unpenalized Maximum Likelihood Estimators

Under the iPCA population model (2), the log-likelihood function reduces to

$$\begin{aligned} \ell(\boldsymbol{\mu}_1, \dots, \boldsymbol{\mu}_K, \boldsymbol{\Sigma}^{-1}, \boldsymbol{\Delta}_1^{-1}, \dots, \boldsymbol{\Delta}_K^{-1}) &\propto p \log |\boldsymbol{\Sigma}^{-1}| + n \sum_{k=1}^K \log |\boldsymbol{\Delta}_k^{-1}| \\ &\quad - \sum_{k=1}^K \text{tr} \left( \boldsymbol{\Sigma}^{-1} (\mathbf{X}_k - \mathbf{1}_n \boldsymbol{\mu}_k^T) \boldsymbol{\Delta}_k^{-1} (\mathbf{X}_k - \mathbf{1}_n \boldsymbol{\mu}_k^T)^T \right). \end{aligned} \quad (6)$$

Taking partial derivatives of (6) with respect to each parameter gives the following:

**Lemma 1.** *The unpenalized MLEs of  $\boldsymbol{\mu}_1, \dots, \boldsymbol{\mu}_K, \boldsymbol{\Sigma}, \boldsymbol{\Delta}_1, \dots, \boldsymbol{\Delta}_K$  satisfy*

$$\hat{\boldsymbol{\mu}}_k = \frac{\mathbf{X}_k^T \mathbf{1}_n}{n} \quad \forall k = 1, \dots, K \quad (7)$$

$$\hat{\boldsymbol{\Sigma}} = \frac{1}{p} \sum_{k=1}^K (\mathbf{X}_k - \mathbf{1}_n \hat{\boldsymbol{\mu}}_k^T) \hat{\boldsymbol{\Delta}}_k^{-1} (\mathbf{X}_k - \mathbf{1}_n \hat{\boldsymbol{\mu}}_k^T)^T \quad (8)$$

$$\hat{\boldsymbol{\Delta}}_k = \frac{1}{n} (\mathbf{X}_k - \mathbf{1}_n \hat{\boldsymbol{\mu}}_k^T)^T \hat{\boldsymbol{\Sigma}}^{-1} (\mathbf{X}_k - \mathbf{1}_n \hat{\boldsymbol{\mu}}_k^T) \quad \forall k = 1, \dots, K. \quad (9)$$

Notice that the unpenalized MLE of  $\boldsymbol{\mu}_k$  is the vector of column means of  $\mathbf{X}_k$ , so  $\mathbf{X}_k - \mathbf{1}_n \hat{\boldsymbol{\mu}}_k^T$  is simply  $\mathbf{X}_k$  with its columns centered to mean 0. We can proceed to compute the unpenalized MLEs of  $\boldsymbol{\Sigma}$  and  $\boldsymbol{\Delta}_1, \dots, \boldsymbol{\Delta}_K$  via a Flip-Flop algorithm (also known as block coordinate descent) analogous to Dutilleul (1999), which iteratively optimizes over each of the parameters while keeping all other parameters fixed.

However, because we only have one matrix observation per matrix-variate normal model, existence of the unpenalized MLEs is not guaranteed. In fact, the following theorem essentially implies that the unpenalized MLEs do not exist for all practical purposes.

**Theorem 1.** *(i) If the population means  $\boldsymbol{\mu}_1, \dots, \boldsymbol{\mu}_K$  in (2) are known,  $\text{rank}(\tilde{\mathbf{X}}) = n$ , and  $\text{rank}(\mathbf{X}_k) = p_k$  for  $k = 1, \dots, K$ , then the unpenalized MLEs for  $\boldsymbol{\Sigma}, \boldsymbol{\Delta}_1, \dots, \boldsymbol{\Delta}_K$  exist.*

*(ii) If the population means  $\boldsymbol{\mu}_1, \dots, \boldsymbol{\mu}_K$  in (2) are unknown, then the unpenalized MLEs for  $\boldsymbol{\Sigma}$  and  $\boldsymbol{\Delta}_1, \dots, \boldsymbol{\Delta}_K$  are not positive definite and hence do not exist.*

The proof of Theorem 1 also shows that if the unpenalized MLEs for  $\Sigma$  and  $\Delta_1, \dots, \Delta_K$  exist, then  $p_k \leq n \leq p$  for each  $k = 1, \dots, K$ . Thus in summary, if  $p_k > n$  for some  $k$  or if the population means are unknown (which is almost always the case), then the unpenalized MLEs do not exist. These severe restrictions motivate new covariance estimators.

For example, we can naively estimate  $\Sigma$  and  $\Delta_k$  by setting their counterparts to  $\mathbf{I}$ .

**Proposition 1.** (i) *The MLE for  $\Delta_k$ , assuming that  $\Sigma = \mathbf{I}$ , is*

$$\hat{\Delta}_k = \frac{1}{n} (\mathbf{X}_k - \mathbf{1}_n \hat{\boldsymbol{\mu}}_k^T)^T (\mathbf{X}_k - \mathbf{1}_n \hat{\boldsymbol{\mu}}_k^T). \quad (10)$$

(ii) *Let  $\tilde{\mathbf{M}} = [\mathbf{1}_n \hat{\boldsymbol{\mu}}_1^T \dots \mathbf{1}_n \hat{\boldsymbol{\mu}}_K^T]$ . The MLE for  $\Sigma$ , assuming  $\Delta_k = \mathbf{I}$  for all  $k = 1, \dots, K$ , is*

$$\hat{\Sigma} = \frac{1}{p} \sum_{k=1}^K (\mathbf{X}_k - \mathbf{1}_n \hat{\boldsymbol{\mu}}_k^T) (\mathbf{X}_k - \mathbf{1}_n \hat{\boldsymbol{\mu}}_k^T)^T = \frac{1}{p} (\tilde{\mathbf{X}} - \tilde{\mathbf{M}}) (\tilde{\mathbf{X}} - \tilde{\mathbf{M}})^T. \quad (11)$$

This approach for estimating  $\Sigma$  is the familiar MLE for the concatenated data  $\tilde{\mathbf{X}}$ . Hence, the eigenvectors of  $\hat{\Sigma}$  from (11) are the PC scores from concatenated PCA (i.e. PCA applied to  $\tilde{\mathbf{X}}$ ). While this illuminates another way in which iPCA is related to PCA, we will see in Section 4 that concatenated PCA performs poorly when the datasets are of different scales. In the next section, we discuss more effective methods for estimating  $\Sigma$  and  $\Delta_1, \dots, \Delta_K$ .

### 3.2 Penalized Maximum Likelihood Estimators

Since the unpenalized MLEs do not exist for a large class of problems, we instead look to penalized maximum likelihood estimation. To reduce cluttering of notation, we assume that  $\mathbf{X}_k$  has been column-centered. Then, the penalized maximum likelihood simplifies to

$$\hat{\Sigma}^{-1}, \hat{\Delta}_1^{-1}, \dots, \hat{\Delta}_K^{-1} = \underset{\substack{\Sigma^{-1} \succ 0 \\ \Delta_1^{-1}, \dots, \Delta_K^{-1} \succ 0}}{\operatorname{argmax}} \left\{ p \log |\Sigma^{-1}| + n \sum_{k=1}^K \log |\Delta_k^{-1}| - \sum_{k=1}^K \operatorname{tr} (\Sigma^{-1} \mathbf{X}_k \Delta_k^{-1} \mathbf{X}_k^T) - P(\Sigma^{-1}, \Delta_1^{-1}, \dots, \Delta_K^{-1}) \right\}. \quad (12)$$

Similar to previous work on the penalized matrix-variate normal log-likelihood (Yin and Li 2012; Allen and Tibshirani 2010), we can consider an additive penalty term and define the additive  $L_q$  iPCA penalty to be  $P_q(\boldsymbol{\Sigma}^{-1}, \boldsymbol{\Delta}_1^{-1}, \dots, \boldsymbol{\Delta}_K^{-1}) = \lambda_{\boldsymbol{\Sigma}} \|\boldsymbol{\Sigma}^{-1}\|_q + \sum_{k=1}^K \lambda_k \|\boldsymbol{\Delta}_k^{-1}\|_q$ , where  $\lambda_{\boldsymbol{\Sigma}}, \lambda_1, \dots, \lambda_K > 0$  are tuning parameters. We can take  $\|\cdot\|_q = \|\cdot\|_1, \|\cdot\|_{1,\text{off}}$  to induce sparsity or  $\|\cdot\|_q = \|\cdot\|_F^2$  to induce smoothness. However, solving (12) with these additive penalties is a non-convex problem, for which we can only guarantee a local solution.

Nevertheless, even though (12) is non-convex in Euclidean space, Wiesel (2012) showed that the matrix-variate normal log-likelihood is geodesically convex (g-convex) with respect to the manifold of positive definite matrices. G-convexity is a generalized notion of convexity on a Riemannian manifold, and like convexity, all local minima of g-convex functions are globally optimal. We thus exploit the g-convex properties of the matrix-variate normal log-likelihood and construct a new penalty: the multiplicative Frobenius iPCA penalty  $P^*(\boldsymbol{\Sigma}^{-1}, \boldsymbol{\Delta}_1^{-1}, \dots, \boldsymbol{\Delta}_K^{-1}) = \sum_{k=1}^K \lambda_k \|\boldsymbol{\Sigma}^{-1} \otimes \boldsymbol{\Delta}_k^{-1}\|_F^2$ , which we will show to be g-convex in Theorem 3. Note that because  $\|\mathbf{A} \otimes \mathbf{B}\|_F^2 = \|\mathbf{A}\|_F^2 \|\mathbf{B}\|_F^2$ , the multiplicative penalty can be rewritten as a product  $\|\boldsymbol{\Sigma}^{-1}\|_F^2 \sum_{k=1}^K \lambda_k \|\boldsymbol{\Delta}_k^{-1}\|_F^2$ , giving rise to its name.

The Flip-Flop algorithms for solving (12) with various penalties are derived in Appendix B.2, but in general, for the Frobenius penalties, each Flip-Flop update has a closed form solution determined by a full eigendecomposition. For the  $L_1$  penalties (also known as the Kronecker Graphical Lasso (Tsiligkaridis et al. 2013)), each update can be solved by the graphical lasso (Hsieh et al. 2011). We provide the multiplicative Frobenius Flip-Flop algorithm here in Algorithm 1, but since the other algorithms take similar forms, we leave them to Appendix B.2. The next theorem guarantees numerical convergence of the Flip-Flop algorithms for the multiplicative Frobenius, additive Frobenius, and additive  $L_1$  penalties.

**Theorem 2.** *Suppose that the objective function in (12) is bounded below. Suppose also that either (i)  $P(\boldsymbol{\Sigma}^{-1}, \boldsymbol{\Delta}_1^{-1}, \dots, \boldsymbol{\Delta}_K^{-1})$  is a differentiable convex function with respect to each coordinate or (ii)  $P(\boldsymbol{\Sigma}^{-1}, \boldsymbol{\Delta}_1^{-1}, \dots, \boldsymbol{\Delta}_K^{-1}) = P_0(\boldsymbol{\Sigma}^{-1}) + \sum_{k=1}^K P_k(\boldsymbol{\Delta}_k^{-1})$ , where  $P_i$  is a (non-differentiable) convex function for each  $k = 1, \dots, K$ . If either (i) or (ii) holds, then the*

---

**Algorithm 1** Flip-Flop Algorithm for Multiplicative Frobenius iPCA Estimators
 

---

- 1: Center the columns of  $\mathbf{X}_1, \dots, \mathbf{X}_K$ , and initialize  $\hat{\Sigma}, \hat{\Delta}_1, \dots, \hat{\Delta}_K$  to be positive definite.
  - 2: **while** not converged **do**
  - 3:   Take eigendecomposition:  $\sum_{k=1}^K \mathbf{X}_k \hat{\Delta}_k^{-1} \mathbf{X}_k^T = \mathbf{U} \mathbf{\Gamma} \mathbf{U}^T$
  - 4:   Regularize eigenvalues:  $\phi_i = \frac{1}{2p} \left( \gamma_i + \sqrt{\gamma_i^2 + 8p \sum_{k=1}^K \lambda_k \|\hat{\Delta}_k^{-1}\|_F^2} \right)$
  - 5:   Update  $\hat{\Sigma}^{-1} = \mathbf{U} \mathbf{\Phi}^{-1} \mathbf{U}^T$
  - 6:   **for**  $k = 1, \dots, K$  **do**
  - 7:     Take eigendecomposition:  $\mathbf{X}_k^T \hat{\Sigma}^{-1} \mathbf{X}_k = \mathbf{V} \mathbf{\Phi} \mathbf{V}^T$
  - 8:     Regularize eigenvalues:  $\gamma_i = \frac{1}{2n} \left( \phi_i + \sqrt{\phi_i^2 + 8n \lambda_k \|\hat{\Sigma}^{-1}\|_F^2} \right)$ .
  - 9:     Update  $\hat{\Delta}_k^{-1} = \mathbf{V} \mathbf{\Gamma}^{-1} \mathbf{V}^T$
- }

Update  $\Sigma$
- }

Update  $\Delta_k$
- 

*Flip-Flop algorithm corresponding to (12) converges to a stationary point of the objective.*

While Theorem 2 guarantees convergence to a local solution, we can build upon Wiesel (2012) to prove a much stronger statement for the multiplicative Frobenius iPCA estimator.

**Theorem 3.** *The multiplicative Frobenius iPCA estimator is jointly geodesically convex in  $\Sigma^{-1}$  and  $\Delta_1^{-1}, \dots, \Delta_K^{-1}$ . Because of this, the Flip-Flop algorithm for the multiplicative Frobenius iPCA estimator given in Algorithm 1 converges to the global solution.*

There are currently only a handful of non-convex problems where there exists an achievable global solution, so this guarantee that the multiplicative Frobenius iPCA estimator always reaches a global solution is both extremely rare and highly desirable. In Section 4, we will also see that the multiplicative Frobenius iPCA estimator undoubtedly gives the best empirical performance, indicating that in addition to its theoretical advantages from global convergence, there are significant practical advantages associated with the g-convex penalty. A self-contained review of g-convexity and the proof of Theorem 3 are given in Appendix C.

### 3.2.1 Subspace Consistency of the Additive $L_1$ Correlation iPCA Estimator

In this section, we begin exploring statistical properties of iPCA by proving subspace consistency for a slight variation of the additive  $L_1$  iPCA estimator. Rather than applying the  $L_1$  penalty to the inverse covariances, we can apply the  $L_1$  penalties to the inverse correlation

matrices, as outlined by Algorithm 6 in Appendix D. This approach was adopted in Zhou (2014a) and Rothman et al. (2008), and we extend their idea to integrated data. Throughout this section, we let  $\hat{\Sigma}$  denote the estimate obtained from Algorithm 6, and we refer to it as the additive  $L_1$  correlation iPCA estimator. We will show in Theorem 4 that the one-step additive  $L_1$  correlation iPCA estimator consistently estimates the underlying joint subspace.

Though previous works have studied the convergence of related sparse penalties, none are directly applicable for data integration. For instance, Tsiligkaridis et al. (2013) proved convergence rates for KGLasso but assumed multiple matrix observations per matrix-variate normal model. Since iPCA assumes only one matrix observation per model, the results from Tsiligkaridis et al. (2013) do not apply. In fact, the theory suggests it is difficult to estimate the diagonal of  $\hat{\Sigma}$  consistently with only one matrix observation. This motivated us to follow the approach in Zhou (2014a), where convergence rates were derived for the one-step (noniterative) version of Algorithm 6. Zhou (2014a) assumed that only one matrix instance was observed from the matrix-variate normal distribution, so we extend the proof techniques and results in Zhou (2014a), where  $K = 1$ , to iPCA, where we observe one matrix instance for each of the  $K \geq 1$  distinct matrix-variate normal models.

For simplicity, we assume  $\hat{\Sigma}$  is initialized to the  $n \times n$  identity matrix, and like Zhou (2014a), we analyze the one-step version of Algorithm 6. That is, we stop the algorithm after one iteration of the while loop. For now, we also assume that  $\sqrt{n} \geq p/\sqrt{p_k}$  for each  $k = 1, \dots, K$ , or what is classically known as the “large n” setting. We will later discuss how to adapt our results to the  $\sqrt{n} < p/\sqrt{p_k}$  for each  $k = 1, \dots, K$  case, or the “large p” setting.

We next collect notation. Suppose for each  $k = 1, \dots, K$ , the true population model is given by  $\mathbf{X}_k \sim N_{n,p_k}(\mathbf{0}, \Sigma \otimes \Delta_k)$ , and the true correlation matrices associated to  $\Sigma$  and  $\Delta_k$  are  $\rho(\Sigma)$  and  $\rho(\Delta_k)$ , respectively. For identifiability, define  $\Sigma^* = n \Sigma / \text{tr}(\Sigma)$  and  $\Delta_k^* = \text{tr}(\Sigma) \Delta_k / n$  so that  $\text{tr}(\Sigma^*) = n$  and  $\Sigma^* \otimes \Delta_k^* = \Sigma \otimes \Delta_k$  for each  $k$ . If  $\mathbf{A}$  is a matrix, let  $\|\mathbf{A}\|_2$  denote the operator norm or the maximum singular value of  $\mathbf{A}$ . Let  $\|\mathbf{A}\|_F$  denote the Frobenius norm (i.e.  $\|\mathbf{A}\|_F^2 = \sum_{i,j} a_{ij}^2$ ). Let  $\|\mathbf{A}\|_{0,\text{off}}$  denote the number of non-zero off-

diagonal entries in  $\mathbf{A}$ . Let  $\|\mathbf{A}\|_1 = \sum_{i,j} |a_{ij}|$ , and let  $\|\mathbf{A}\|_{1,\text{off}} = \sum_{i \neq j} |a_{ij}|$ . Write  $\phi_{\min}(\mathbf{A})$  and  $\phi_{\max}(\mathbf{A})$  for the minimum and maximum eigenvalues of  $\mathbf{A}$ . Also write  $a \vee b = \max(a, b)$  and  $a \wedge b = \min(a, b)$ . If  $a = o(b)$ , then  $|a/b| \rightarrow 0$  as  $n, p_1, \dots, p_K \rightarrow \infty$ . If  $a \asymp b$ , then there exists positive constants  $c, C$  such that  $cb \leq a \leq Cb$  as  $n, p_1, \dots, p_K \rightarrow \infty$ .

The following assumptions are needed to establish subspace consistency of  $\hat{\Sigma}$ .

- (A1) Assume that  $\Sigma^{-1}$  and  $\Delta_k^{-1}$  are sparse with respect to each other's dimensions:  $s_{\Sigma} := \|\Sigma^{-1}\|_{0,\text{off}} = o\left(\frac{p^2}{p_k \log(n \vee p_k)}\right)$  and  $s_k := \|\Delta_k^{-1}\|_{0,\text{off}} = o\left(\frac{n}{\log(n \vee p_k)}\right)$  for each  $k = 1, \dots, K$ .
- (A2) Assume that we have uniformly bounded spectra:  $0 < \phi_{\min}(\Sigma) \leq \phi_{\max}(\Sigma) < \infty$  and  $0 < \phi_{\min}(\Delta_k) \leq \phi_{\max}(\Delta_k) < \infty$  for each  $k = 1, \dots, K$ .
- (A3) Assume that the inverse correlation matrices satisfy  $\|\rho(\Sigma)^{-1}\|_1 \asymp n$  and  $\|\rho(\Delta_k)^{-1}\|_1 \asymp p_k$  for each  $k = 1, \dots, K$ .
- (A4) Assume that  $K$  is finite and the growth rate of  $n$  and  $p_1, \dots, p_K$  satisfy  $n \vee p_k = o(\exp(n \wedge p_k))$  for each  $k = 1, \dots, K$ .

*Remarks.* (1) Rather than verifying the sparsity assumption of  $\Sigma^{-1}$  in (A1) and the growth rate (A4) for each  $k = 1, \dots, K$ , it is sufficient to check that  $s_{\Sigma} = o\left(\frac{p^2}{\max_k p_k \log(n \vee \max_k p_k)}\right)$  and  $n \vee \max_k p_k = o(\exp(n \wedge \min_k p_k))$ , respectively.

- (2) (A1) implies that  $\sqrt{\frac{s_k \log(n \vee p_k)}{n}} \rightarrow 0$  and  $\sqrt{\frac{s_{\Sigma} \log(n \vee p_k)}{p_k}} \rightarrow 0$  as  $n, p_1, \dots, p_K \rightarrow \infty$ .

Under these four assumptions, we summarize our main statistical convergence result:

**Theorem 4.** *Suppose that (A1)-(A4) hold and that  $\sqrt{n} \geq \frac{p}{\sqrt{p_k}}$  for each  $k = 1, \dots, K$ .*

*Let  $\hat{\Sigma}$  denote the one-step additive  $L_1$  correlation iPCA estimator, where we choose  $\lambda_{\Sigma} \asymp \sum_{k=1}^K \frac{p_k}{p} \sqrt{\frac{\log(n \vee p_k)}{p_k}}$  and  $\lambda_k \asymp \sqrt{\frac{\log(n \vee p_k)}{n}}$  for each  $k$ . Then with probability  $1 - \sum_{k=1}^K \frac{8}{(n \vee p_k)^2}$ ,*

$$\|\hat{\Sigma} - \Sigma^*\|_2 = O\left(\sum_{k=1}^K \frac{p_k}{p} \sqrt{\frac{(s_{\Sigma} \vee 1) \log(n \vee p_k)}{p_k}}\right), \quad (13)$$

$$\|\hat{\Sigma} - \Sigma^*\|_F = O\left(\sum_{k=1}^K \frac{p_k}{p} \sqrt{\frac{(s_{\Sigma} \vee n) \log(n \vee p_k)}{p_k}}\right). \quad (14)$$

Details of this proof are provided in Appendix D, but the overarching proof idea is to follow Algorithm 6 and sequentially bound each step of the algorithm. Our proof closely resembles Zhou (2014a) with technical differences due to the estimation of  $\Sigma$  from multiple  $\Delta_k$ 's with different  $p_k$ 's. Note when  $K = 1$ , Theorem 4 gives the same rates as Zhou (2014a).

*Remark.* If  $\sqrt{n} < p/\sqrt{p_k}$  for each  $k = 1, \dots, K$  (i.e. the “large  $p$ ” setting), then we modify Algorithm 6 to first initialize an estimate for  $\Sigma$ , next estimate  $\Delta_k$ , and then obtain the final estimate of  $\Sigma$ . The same convergence rates can be obtained for the “large  $p$ ” setting by using this modified algorithm. The only additional assumption required here is a bound on  $|\rho(\Sigma)_{ij}|$ , namely,  $|\rho(\Sigma)_{ij}| = O(\sqrt{np_k}/p)$  for each  $k = 1, \dots, K$  and  $i \neq j$ .

Therefore, in either the large  $n$  or the large  $p$  setting, we have a one-step Flip-Flop algorithm such that under certain assumptions, the estimate of  $\Sigma$  converges in the operator and Frobenius norms at rates given by (13) and (14). Convergence in the operator norm, in particular, has two direct consequences. By Weyl’s Theorem (Horn and Johnson 2012), the eigenvalues of  $\hat{\Sigma}$  are consistent, and by a variant of the Davis-Kahan  $\sin \theta$  theorem (Yu et al. 2015), the eigenvectors of  $\hat{\Sigma}$  are consistent. Since eigenvectors of  $\hat{\Sigma}$  define the estimated iPCA subspace, this in turn implies subspace consistency.

### 3.2.2 Selecting Penalty Parameters

In practice, it is important to select penalty parameters for (12) in a principled data-driven manner. We propose to do this via a missing data imputation framework.

Let  $\Lambda$  denote the space of penalty parameters, and let  $\lambda := (\lambda_\Sigma, \lambda_1, \dots, \lambda_K)$  be a specific choice of penalty parameters in  $\Lambda$ . The idea is to first randomly leave out scattered elements from each  $\mathbf{X}_k$ . Then, for each  $\lambda \in \Lambda$ , impute the missing elements via an EM-like algorithm, similar to Allen and Tibshirani (2010). Finally, select the  $\lambda$  which minimizes the error between the imputed values and the observed values. Further details, technical derivations, and numerical results regarding our imputation method and penalty parameter selection are provided in Appendix E.

- Remarks.* (i) If  $K$  is large or the datasets are large, it might be computationally intractable to try all combinations of penalty parameters in  $\mathbf{\Lambda}$ . In these cases, we can select the penalty parameters in a greedy manner: first fix  $\lambda_1, \dots, \lambda_K$  and optimize over  $\lambda_{\Sigma}$ , then fix  $\lambda_{\Sigma}, \lambda_2, \dots, \lambda_K$  and optimize  $\lambda_1$ , and so forth, and we stop after optimizing  $\lambda_K$ .
- (ii) Our imputation procedure may also be used to perform iPCA in missing data scenarios.

## 4 Empirical Results

In the following simulations and case study, we evaluate iPCA against individual PCAs on each of the datasets  $\mathbf{X}_k$ , concatenated PCA, distributed PCA, JIVE, and MFA. Note that many data integration methods from the multitask PCA family are known to perform similarly to MFA (Abdi et al. 2013), so we only include MFA to minimize redundancy. We also omit CMF, as it performs similarly to concatenated PCA, and the GSVD since it is not applicable for integrated data with both low-dimensional and high-dimensional datasets.

Within the class of iPCA estimators, we focus our attention on the additive and multiplicative Frobenius iPCA estimators, but to also represent the sparse estimators, we include the most commonly used sparse estimator, the additive  $L_1$  penalty ( $\|\cdot\|_{1,\text{off}}$ ) applied to the inverse covariance matrices. In order to reduce the computational burden, we stop the  $L_1$  Flip-Flop algorithm after one iteration, and we select the iPCA penalty parameters in a greedy manner, as discussed in Section 3.2.2.

### 4.1 Simulations

The base simulation is set up as follows: Three coupled data matrices,  $\mathbf{X}_1, \mathbf{X}_2, \mathbf{X}_3$ , with  $n = 150$ ,  $p_1 = 300$ ,  $p_2 = 500$ ,  $p_3 = 400$ , were simulated according to the iPCA Kronecker covariance model (2). Here,  $\Sigma$  is taken to be a spiked covariance with the top two factors forming three clusters as shown in Figure 2A;  $\Delta_1$  is an autoregressive Toeplitz matrix with entry  $(i, j)$  given by  $.9^{|i-j|}$ ;  $\Delta_2$  is the observed covariance matrix of miRNA data from TCGA

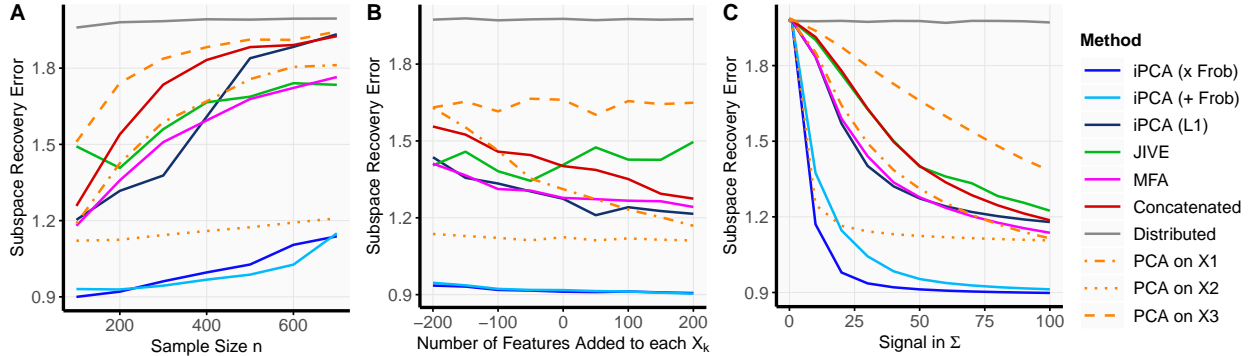


**Figure 3:** *Subspace recovery as simulation parameters vary from the base simulation: (A) As the number of samples increases, it becomes more difficult to estimate the joint row subspace; (B) As the number of features increases, it becomes slightly easier to estimate the joint row subspace; (C) Performance drastically improves as the strength of the joint signal in  $\Sigma$  (i.e. the top singular value of  $\Sigma$ ) increases. Moreover, in almost every scenario, the multiplicative and additive Frobenius iPCA estimators outperform their competitors.*

ovarian cancer (Network 2011); and  $\Delta_3$  is a block-diagonal matrix with five equally-sized blocks. We also ensured that the largest eigenvalue of each  $\Delta_k$  was larger than that of  $\Sigma$  so that the joint patterns are intentionally obscured by individualistic patterns. From this base simulation, we systematically varied the parameters - number of samples, number of features, and strength of the joint signal in  $\Sigma$  (i.e.  $\|\Sigma\|_2$ ) - one at a time while keeping everything else constant.

We evaluate the performance of various methods using the subspace recovery error: If the true subspace of  $\Sigma$  was simulated to be of dimension  $d$  with the orthogonal eigenbasis  $\mathbf{u}_1, \dots, \mathbf{u}_d$  and the top  $d$  eigenvectors of the estimate  $\hat{\Sigma}$  are given by  $\hat{\mathbf{u}}_1, \dots, \hat{\mathbf{u}}_d$ , then the subspace recovery error is defined to be  $\frac{1}{d} \|\hat{\mathbf{U}}\hat{\mathbf{U}}^T - \mathbf{U}\mathbf{U}^T\|_F^2$ , where  $\mathbf{U} = [\mathbf{u}_1, \dots, \mathbf{u}_d]$  and  $\hat{\mathbf{U}} = [\hat{\mathbf{u}}_1, \dots, \hat{\mathbf{u}}_d]$ . This metric simply quantifies the distance between the true subspace of  $\Sigma$  and the estimated subspace from  $\hat{\Sigma}$ . We note that a lower subspace recovery error implies higher estimation accuracy, and in the base simulation,  $d = 2$ . Although there are other metrics like canonical angles, which also quantify the distance between subspaces, these metrics behave similarly to the subspace recovery error, so we omit the results for brevity.

The average subspace recovery error, measured over 50 trials, from various simulations are shown in Figure 3. We clearly see that the additive and multiplicative Frobenius iPCA estimators consistently outperformed all other methods. Since  $\Sigma$  was not simulated to be

sparse, it is no surprise that the Frobenius iPCA estimators outperformed the  $L_1$  iPCA estimator. It is also expected that distributed PCA performs poorly since the  $\Delta_k$ 's are not all identical, violating its basic assumption. What may be surprising is that doing PCA on  $\mathbf{X}_2$  performed better than its competitors, excluding the Frobenius iPCA estimators. We speculate that this is because the observed covariance  $\Delta_2$  happened to be a very low-rank matrix, and because  $\Delta_2$  was low-rank, the signal from  $\Sigma$  most likely dominated much of the variation in the second PC. Looking ahead at Figure 4A, as Laplacian error was added to the simulated data, PCA on  $\mathbf{X}_2$  failed to recover the true signal since the Laplacian error increasingly contributed to the variation in the data. We also point out that MFA always yielded a lower error than concatenated PCA in Figure 3, indicating that there is value in normalizing datasets to be on comparable scales. On the other hand, we must be weary of this normalization process. In the case of these simulations, PCA on  $\mathbf{X}_2$  outperformed MFA, illustrating that normalization can sometimes remove important information.

To verify that these simulation results are not heavily dependent by the base simulation setup of  $\Sigma$  and  $\Delta_k$ , we also ran simulations, varying the dimension  $d$  of the true joint subspace  $\mathbf{U}$  and the number of datasets  $K$ . We provide these results in Appendix F.

Beyond simulating from the iPCA model (2), we check for robustness from the two main iPCA assumptions - normality and Kronecker covariance structure. To deviate from normality, we add Laplacian noise to the base simulation setup, and to depart from the Kronecker covariance structure, we simulate data from the JIVE model. The results are summarized in Figure 4, and we leave the simulation details to Appendix F.

As seen in Figure 4A, the Frobenius iPCA estimators appear to be relatively robust to the non-Gaussian noise and outperformed their competitors even as the standard deviation of added Laplacian errors increased. From the simulations under the JIVE model in Figure 4B, we see that as the amount of noise increases, JIVE given the known ranks yields the lowest error, as expected. But similar to how JIVE was comparable to competing methods under the iPCA model (Figure 3), the iPCA estimators are comparable to competing methods for

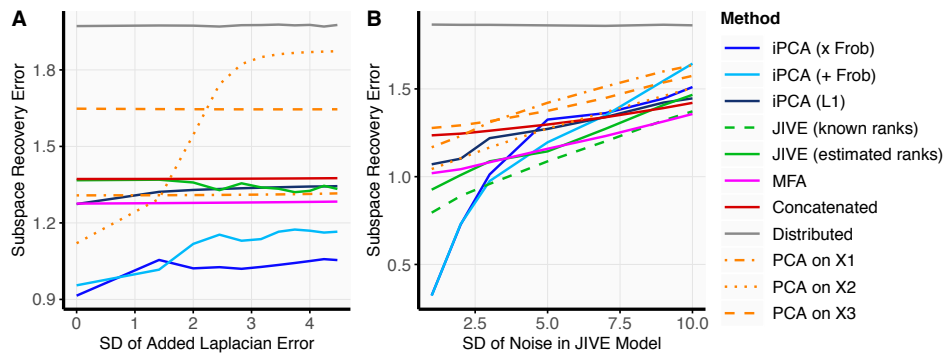


**Figure 4:** *Robustness Simulations: (A) As Laplacian error is increasingly added to the simulated datasets, the Frobenius iPCA estimators appear to be robust to the departures from Gaussianity; (B) As the amount of noise in the JIVE model increases, iPCA seems to be comparable to existing methods, illustrating its relative robustness to departures from the Kronecker product model.*

high noise levels under the JIVE model. At low noise levels however, the Frobenius iPCA estimators are able to recover the true joint subspace better than JIVE with the known ranks. Further investigation into this peculiar behavior reveals that the Frobenius iPCA estimators give lower subspace recovery errors but larger approximation errors  $\|\Sigma - \hat{\Sigma}\|_F^2$ , compared to JIVE with the known ranks. This brings up a subtle, but important distinction - iPCA revolves around estimating the underlying subspace, determined by eigenvectors, while JIVE focuses on minimizing the matrix approximation error. These are inherently different objectives, and it is common for iPCA to estimate the eigenvectors well at the cost of a poor matrix approximation due to the regularized eigenvalues.

## 4.2 Case Study: Integrative Genomics of Alzheimer’s Disease

A key motivating example for our research is in integrative genomics, where the goal is to combine genetic information from different, yet related, technologies in order to better understand the genetic basis of particular diseases. In particular, apart from the APOE gene, little is known about the genomic basis of Alzheimer’s Disease (AD) and the genes which contribute to dominant expression patterns in AD. Thus, in this case study, we delve into the integrative genomics of AD and jointly analyze miRNA expression, gene expression via RNASeq, and DNA methylation data obtained from the Religious Orders Study Memory

and Aging Project (ROSMAP) Study (Mostafavi et al. 2018). The ROSMAP study is a longitudinal clinical-pathological cohort study of aging and AD, consisting of  $n = 507$  subjects with data across all three datasets of interest, and it is uniquely positioned for the study of AD since its genomics data is collected from post-mortem brain tissue from the dorsolateral prefrontal cortex of the brain, an area known to play an important role in cognitive functions.

The ROSMAP data originally contained 309 miRNAs, 41,809 genes, and 420,132 CpG sites, so we aggressively preprocessed the number of features in the RNASeq and methylation datasets to manageable sizes. First, we transformed the methylation data to m-values and log-transformed the RNASeq counts, as is common in most analyses for these data types. Then, we removed batch (experimental) effects from both datasets via ComBat (Johnson et al. 2007). We next filtered the features by taking those with the highest variance (top 20,000 genes for RNASeq and top 50,000 CpG sites for methylation). Then, we performed univariate filtering and kept the features with the highest association to clinician’s diagnosis. This left us with  $p_1 = 309$ ,  $p_2 = 900$ ,  $p_3 = 1250$  in the miRNA, RNASeq, and methylation datasets, respectively.

For our analysis, we consider two clinical outcome variables: clinician’s diagnosis and global cognition score. The clinician’s diagnosis is the last clinical evaluation prior to the patient’s death and is a categorical variable with three levels - Alzheimer’s Disease (AD), mild cognitive impairment (MCI), and no cognitive impairment (NCI). Global cognition score, a continuous variable, is the average of 19 cognitive tests and is the last cognitive testing score prior to death. While the clinician’s diagnosis is sometimes subjective, global cognition score is viewed as a more objective measure of cognition. Our goal is to find common patterns among patients, which occur in all three datasets, and to understand whether these joint patterns are predictive of AD, as measured by clinician’s diagnosis and global cognition score.

To this end, we run iPCA and other existing methods to extract dominant patterns from the ROSMAP data. Figure 5 shows the PC plots obtained from the various methods - each

point represents a subject and is colored by either clinician’s diagnosis or cognition score.

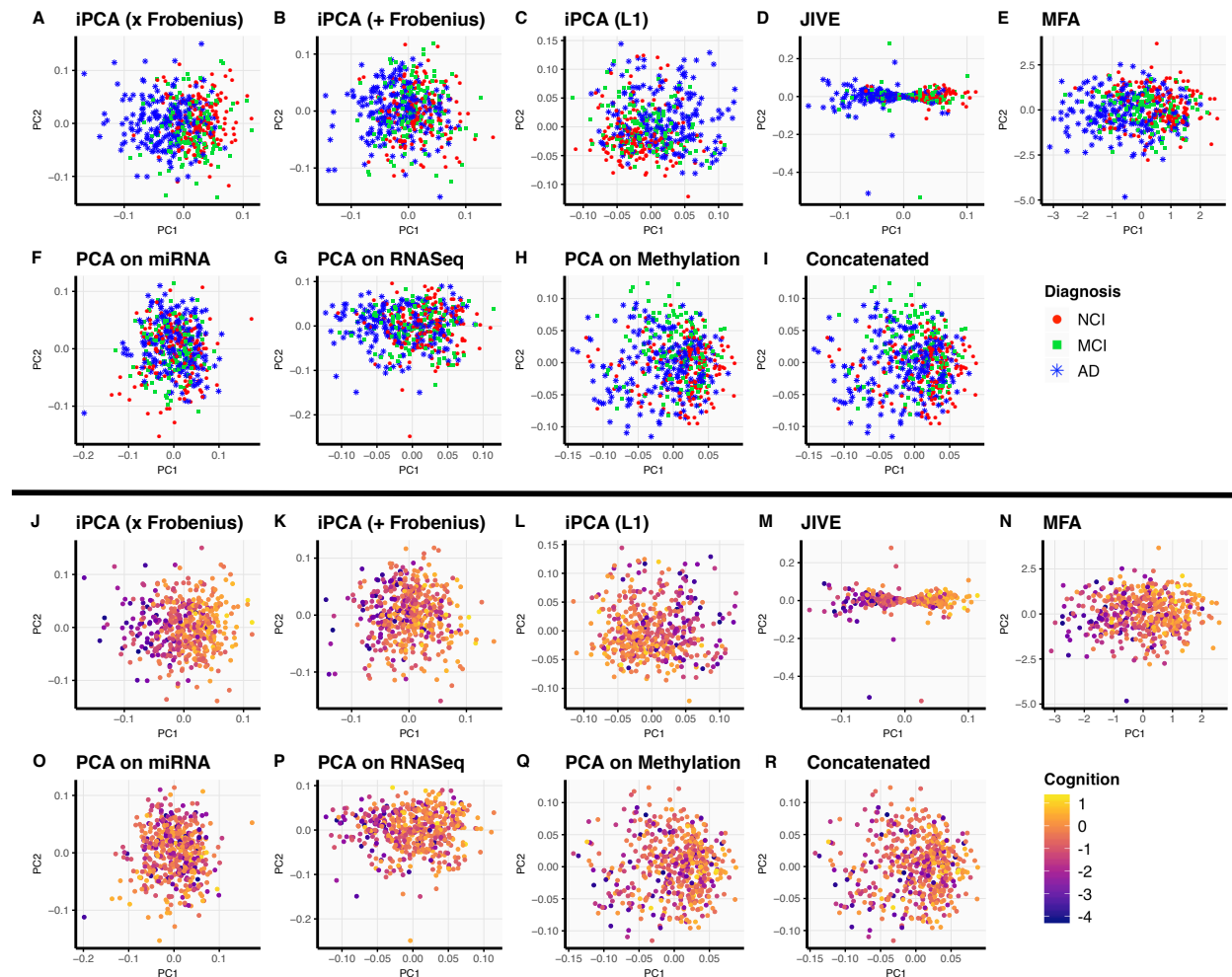


**Figure 5:** We plot the first two (integrated) principal components from various methods applied to the ROSMAP data. Each point represents a subject, colored by the clinician’s diagnosis in panels A-I and by global cognition score in panels J-R.

Since visuals are a subjective measure of performance, we quantify it by taking the top PCs and using them as predictors in a random forest to predict the outcome of interest. For the random forest, we split the ROSMAP data into a training ( $n = 375$ ) and test set ( $n = 132$ ) and used the default random forest settings in R. The test errors, averaged over 100 random training/test splits, are shown in Figure 6. From Figure 6, it is clear that the joint patterns extracted from iPCA using the multiplicative Frobenius penalty were the most predictive of the clinician’s diagnosis of AD and the patient’s global cognition score. Moreover, most of the predictive power can be attributed to the first three iPCs, which we

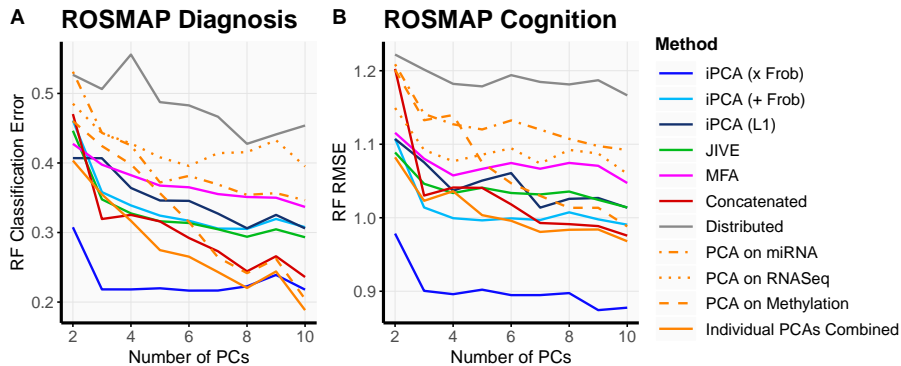


**Figure 6:** We took the top PCs and used them as predictor variables in a random forest to predict (A) the clinician’s diagnosis and (B) the global cognition score. The average test error from the random forests over 100 random splits are shown as the number of PCs used in the random forests increases.

visualize in Figure 7A-B. We also note that the top iPCs from iPCA with the multiplicative Frobenius penalties were more predictive than combining the PCs from the three individual PCAs performed on each dataset. This showcases empirically that a joint analysis of the integrated datasets can be advantageous over three disparate analyses.

Beyond the high predictive power of iPCA with the multiplicative Frobenius penalty, it is perhaps more important for scientists to be able to interpret the iPCA results. One way is through the proportion of variance explained by the joint iPCs, as defined in Section 2.2.1. Figure 7C shows the marginal proportions for the top 5 iPCs. It reveals that the RNASeq dataset contributed the most variation in the joint patterns found by iPC1 and iPC2, and the miRNA dataset contributed the most variation in iPC3. More interestingly, even though iPC2 and iPC3 have relatively small variances, iPCA is able to pick out these weak joint signals, which we found to be predictive of AD. This reiterates that the most variable patterns in the data are not necessarily the most relevant patterns for the question at hand. In this case, our goal was to find joint patterns which occur in all three datasets, and since the joint signal is not the most dominant source of variation in each dataset, no individualistic PCA analysis would have identified the joint signal found by iPCA.

We conclude our ROSMAP analysis by extracting the top genetic features which are associated to the joint patterns shown in Figure 7. Since iPCA provides an estimate of both  $\Sigma$  and  $\Delta_k$ , we can select the top features by applying sparse PCA to each  $\hat{\Delta}_k$  obtained from

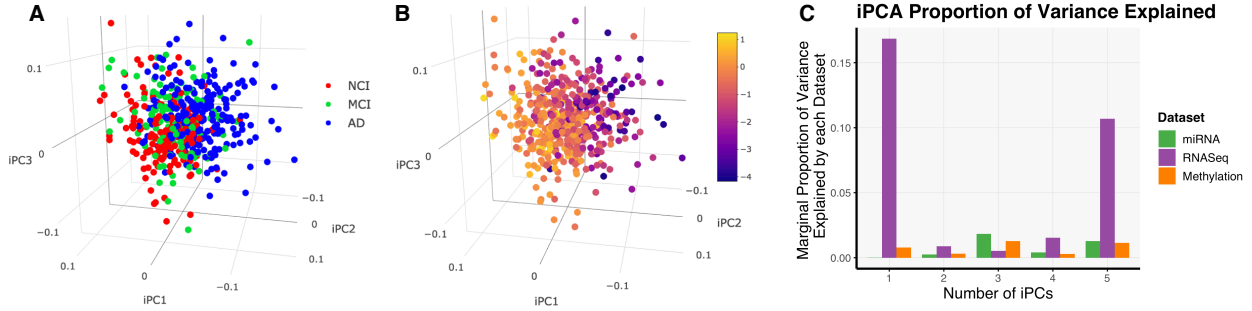


**Figure 7:** (A)-(B) We show the top 3 iPCs obtained from iPCA with the multiplicative Frobenius estimator; the points are colored by clinician’s diagnosis and global cognition score in (A) and (B), respectively. (C) We plot the marginal proportion of variance explained by the top iPCs in each dataset in the ROSMAP analysis (using the multiplicative Frobenius iPCA estimator).

iPCA. Table 1 lists the top miRNAs, genes, and genes affiliated with the selected CpG sites obtained from sparse PCA. Here, we used the `sparseEigen` R package (Benidis et al. 2016) and chose the tuning parameter such that there were only 12 non-zero features.

Because the RNASeq data contributed most of the variation in iPC1, we did a literature search on the top five genes extracted by sparse PCA on  $\hat{\Delta}_2$ . Out of the top five genes, we found evidence in the biological literature, which links four of the five genes (the exception being SVOP) to AD (Carrette et al. 2003; Li et al. 2017; Han et al. 2014; Espuny-Camacho et al. 2017). While this is only a preliminary investigation into the importance of the genetic features obtained from iPCA, it is encouraging evidence and may potentially hint at candidate genes for future research.

**Table 1:** Top genetic features obtained by applying Sparse PCA to each  $\hat{\Delta}_k$  in ROSMAP analysis (using the multiplicative Frobenius iPCA estimator)

	miRNA	RNASeq	Methylation
1	miR 216a	VGF	TMCO6
2	miR 127 3p	SVOP	PHF3
3	miR 124	PCDHGC5	BRUNOL4
4	miR 30c	ADCYAP1	OSCP1
5	miR 143	LINC01007	GRIN2B
6	miR 27a	FRMPD2L1	CASP9
7	miR 603	SLC30A3	ZFP91; LPXN; ZFP91-CNTF
8	miR 423 3p	NCALD	CNP
9	miR 204	S100A4	YWHAE
10	miR 128	AZGP1	C11orf73
11	miR 193a 3p	PAK1	TMED10
12	ebv miRBART14	MAL2	RELL1

## 5 Discussion

As showcased in the simulation study and the Alzheimer’s Disease case study, iPCA is not simply a theoretical construct that generalizes PCA to the integrated data setting. iPCA is also a useful tool in practice to discover interesting joint patterns which occur in multiple datasets. We believe that iPCA’s strong performance is due in part to the appropriateness of the iPCA model for many integrated data problems. The iPCA model assumes that the variation in each dataset is a function of the dependencies among samples and the dependencies among features, and because each dataset is measured on the same set of samples, then the dependencies among samples should be the same across all datasets. We encode these shared sample dependencies as  $\Sigma$  and the individualistic feature dependencies as  $\Delta_k$ . Then, whereas ordinary PCA estimates each  $\Delta_k$  independently of  $\Sigma$ , iPCA estimates  $\Sigma$  and  $\Delta_k$  jointly, inherently accounting for the effects of the other factor.

While there are many different penalized iPCA estimators, we recommend that if the covariance matrices are not known to be sparse, practitioners should strongly consider using the multiplicative Frobenius iPCA estimator. The simulations show that the Frobenius penalties are relatively robust to departures from model assumptions, and in theory, the multiplicative Frobenius penalized estimator requires one less penalty parameter to tune and always converges to the global solution. Though it is not obvious as to why the multiplicative Frobenius iPCA estimator drastically outperforms the other data integration methods in the ROSMAP case study, we speculate that it is related to g-convexity and convergence to the global solution. If not this, then it might be that the multiplicative Frobenius penalty simply gives the appropriate scalings and interactions between penalty parameters and covariance estimates. We leave this as open question for future research.

Still, there are many other open avenues for future exploration. Analogous to PCA, one might imagine similar fruitful extensions of iPCA to higher-order data, functional data, and other structured applications. One could continue exploring g-convex penalties in different contexts and problems. Another interesting area for future research would be to develop

a general framework to prove the consistency of g-convex estimators using the intrinsic manifold space, rather than the Euclidean space. We believe this intersection of g-convexity and statistical theory is a particularly ripe area of future research, but overall, in this work, we developed a theoretically sound and practical tool for performing dimension reduction in the integrated data setting, thus facilitating wholistic analyses at a large scale.

## **Acknowledgements**

The authors acknowledge support from NSF DMS-1264058, NSF DMS-1554821 and NSF NeuroNex-1707400. The authors thank Dr. Joshua Shulman and Dr. David Bennett for help acquiring the ROS/MAP data and acknowledge support from NIH P30AG10161, RF1AG15819, R01AG17917, and R01AG36042 for this data. The authors also thank Dr. Zhandong Liu and Dr. Ying-Wooi Wan for help with processing and interpreting the ROS/MAP data.

# Integrated Principal Components Analysis: Supplementary Materials

Tiffany M. Tang, Genevera I. Allen

The supplementary materials are structured as follows. In Appendix A, we verify that the variance explained by iPCA is a well-defined definition. In Appendix B, we provide the proofs, derivations, and algorithms related to the unpenalized and penalized MLEs for iPCA. We then review geodesic convexity and prove the global convergence property of the multiplicative Frobenius iPCA estimator in Appendix C. In Appendix D, we prove the subspace consistency of the onse-step additive  $L1$  correlation iPCA estimator. We discuss the penalty parameter selection in Appendix E, and we conclude with additional simulation details in Appendix F.

## A Variance Explained by iPCA

To ensure that the cumulative proportion of variance explained from Definition 1 is a well-defined concept, we check that  $PVE_{k,m}$  is a proportion and is an increasing function as  $m$  increases. This implies that the marginal proportion of variance explained given in Definition 2 is also a proportion.

**Lemma 2.** *The cumulative proportion of variance explained in  $\mathbf{X}_k$  by the top  $m$  iPCs, as defined in (5), satisfies the following properties: for each  $k = 1, \dots, K$  and  $m = 1, \dots, \min\{n, p_k\}$ ,*

$$(i) \quad 0 \leq PVE_{k,m} \leq 1;$$

$$(ii) \quad PVE_{k,m-1} \leq PVE_{k,m}.$$

*Proof.* (i) Since the Frobenius norm is always non-negative, it is clear that  $PVE_{k,m} \geq 0$ . So it suffices to show that  $PVE_{k,m} \leq 1$ , or equivalently,  $\|(\mathbf{U}^{(m)})^T \mathbf{X}_k \mathbf{V}_k^{(m)}\|_F^2 \leq \|\mathbf{X}_k\|_F^2$ .

By definition of the Frobenius norm, we have that

$$\begin{aligned} \|(\mathbf{U}^{(m)})^T \mathbf{X}_k \mathbf{V}_k^{(m)}\|_F^2 &= \sum_{i=1}^m \sum_{j=1}^m \left( (\mathbf{U}^{(m)})^T \mathbf{X}_k \mathbf{V}_k^{(m)} \right)_{ij}^2 \\ &= \sum_{i=1}^m \sum_{j=1}^m \left( \sum_{q=1}^n \sum_{r=1}^{p_k} (\mathbf{U}^{(m)})_{iq}^T \mathbf{X}_{k,qr} \mathbf{V}_{k,rj}^{(m)} \right)^2 \\ &\stackrel{[1]}{\leq} \sum_{i=1}^n \sum_{j=1}^{p_k} \left( \sum_{q=1}^n \sum_{r=1}^{p_k} \mathbf{U}_{iq}^T \mathbf{X}_{k,qr} \mathbf{V}_{k,rj} \right)^2 \\ &= \|\mathbf{U}^T \mathbf{X}_k \mathbf{V}_k\|_F^2 \\ &\stackrel{[2]}{=} \|\mathbf{X}_k\|_F^2. \end{aligned}$$

Here, [2] holds by the orthogonality of  $\mathbf{U}$  and  $\mathbf{V}_k$ , and [1] follows from the facts that  $m \leq \min\{n, p_k\}$ ,  $\mathbf{U}^{(m)}$  and  $\mathbf{V}_k^{(m)}$  are precisely the first  $m$  columns of  $\mathbf{U}$  and  $\mathbf{V}_k$  respectively, and the summand is non-negative. This concludes the proof of part (i).

(ii) We follow a similar argument as part (i) to see that

$$\begin{aligned} \|(\mathbf{U}^{(m-1)})^T \mathbf{X}_k \mathbf{V}_k^{(m-1)}\|_F^2 &= \sum_{i=1}^{m-1} \sum_{j=1}^{m-1} \left( \sum_{q=1}^n \sum_{r=1}^{p_k} (\mathbf{U}^{(m-1)})_{iq}^T \mathbf{X}_{k,qr} \mathbf{V}_{k,rj}^{(m-1)} \right)^2 \\ &\leq \sum_{i=1}^m \sum_{j=1}^m \left( \sum_{q=1}^n \sum_{r=1}^{p_k} (\mathbf{U}^{(m)})_{iq}^T \mathbf{X}_{k,qr} \mathbf{V}_{k,rj}^{(m)} \right)^2 \\ &= \|(\mathbf{U}^{(m)})^T \mathbf{X}_k \mathbf{V}_k^{(m)}\|_F^2. \end{aligned}$$

This implies that  $\text{PVE}_{k,m-1} \leq \text{PVE}_{k,m}$ . □

Next, we claim that Definition 1 is a generalization of the cumulative proportion of variance explained in PCA. Recall that in PCA, if  $\mathbf{X} = \mathbf{U} \mathbf{D} \mathbf{V}^T$  is the SVD of  $\mathbf{X}$ , then the cumulative proportion of variance explained by the top  $m$  PCs is  $(\sum_{i=1}^m d_i^2) / (\sum_{i=1}^p d_i^2)$ , where  $\mathbf{D} = \text{diag}(d_1, \dots, d_p)$ . We can rewrite this as

$$\frac{\sum_{i=1}^m d_i^2}{\sum_{i=1}^p d_i^2} = \frac{\|\mathbf{D}^{(m)}\|_F^2}{\|\mathbf{X}\|_F^2} = \frac{\|(\mathbf{U}^{(m)})^T \mathbf{X} \mathbf{V}^{(m)}\|_F^2}{\|\mathbf{X}\|_F^2} \quad (15)$$

using properties of the SVD. Since  $\mathbf{U}$  are the PC scores, and  $\mathbf{V}$  are the PC loadings from PCA, then Definition 1 is indeed a natural definition in the sense that it generalizes the PCA cumulative proportion of variance explained.

## B Covariance Estimation for iPCA

In this section, we provide the proofs and derivations related to the unpenalized and penalized maximum likelihood estimators under the iPCA model.

### B.1 Unpenalized Maximum Likelihood Estimators

We begin this section by deriving the log-likelihood equation associated with the iPCA population model (2).

Recall that the probability density function for each matrix-variate normal model ( $k = 1, \dots, K$ ) is given by

$$\begin{aligned} f(\mathbf{X}_k | \boldsymbol{\mu}_k, \boldsymbol{\Sigma}, \boldsymbol{\Delta}_k) &= (2\pi)^{-\frac{np_k}{2}} |\boldsymbol{\Sigma}|^{-\frac{p_k}{2}} |\boldsymbol{\Delta}_k|^{-\frac{n}{2}} \times \\ &\quad \exp\left(-\frac{1}{2} \text{tr}\left(\boldsymbol{\Sigma}^{-1} (\mathbf{X}_k - \mathbf{1}_n \boldsymbol{\mu}_k^T) \boldsymbol{\Delta}_k^{-1} (\mathbf{X}_k - \mathbf{1}_n \boldsymbol{\mu}_k^T)^T\right)\right). \end{aligned}$$

Hence, the log-likelihood function is

$$\begin{aligned}
\ell(\boldsymbol{\mu}_1, \dots, \boldsymbol{\mu}_K, \boldsymbol{\Sigma}^{-1}, \boldsymbol{\Delta}_1^{-1}, \dots, \boldsymbol{\Delta}_K^{-1}) &= \sum_{k=1}^K \left[ -\frac{np_k}{2} \log(2\pi) + \frac{p_k}{2} \log |\boldsymbol{\Sigma}^{-1}| + \frac{n}{2} \log |\boldsymbol{\Delta}_k^{-1}| \right. \\
&\quad \left. - \frac{1}{2} \text{tr} \left( \boldsymbol{\Sigma}^{-1} (\mathbf{X}_k - \mathbf{1}_n \boldsymbol{\mu}_k^T) \boldsymbol{\Delta}_k^{-1} (\mathbf{X}_k - \mathbf{1}_n \boldsymbol{\mu}_k^T)^T \right) \right] \\
&\propto p \log |\boldsymbol{\Sigma}^{-1}| + n \sum_{k=1}^K \log |\boldsymbol{\Delta}_k^{-1}| \\
&\quad - \sum_{k=1}^K \text{tr} \left( \boldsymbol{\Sigma}^{-1} (\mathbf{X}_k - \mathbf{1}_n \boldsymbol{\mu}_k^T) \boldsymbol{\Delta}_k^{-1} (\mathbf{X}_k - \mathbf{1}_n \boldsymbol{\mu}_k^T)^T \right).
\end{aligned}$$

The unpenalized MLEs are designed to solve the optimization problem

$$\underset{\substack{\boldsymbol{\mu}_1, \dots, \boldsymbol{\mu}_K \\ \boldsymbol{\Sigma}^{-1}, \boldsymbol{\Delta}_1^{-1}, \dots, \boldsymbol{\Delta}_K^{-1}}}{\text{argmin}} \quad -\ell(\boldsymbol{\mu}_1, \dots, \boldsymbol{\mu}_K, \boldsymbol{\Sigma}^{-1}, \boldsymbol{\Delta}_1^{-1}, \dots, \boldsymbol{\Delta}_K^{-1}) \quad (16)$$

**Lemma 1.** *The unpenalized MLEs of  $\boldsymbol{\mu}_1, \dots, \boldsymbol{\mu}_K, \boldsymbol{\Sigma}, \boldsymbol{\Delta}_1, \dots, \boldsymbol{\Delta}_K$  satisfy*

$$\hat{\boldsymbol{\mu}}_k = \frac{\mathbf{X}_k^T \mathbf{1}_n}{n} \quad \forall k = 1, \dots, K \quad (7)$$

$$\hat{\boldsymbol{\Sigma}} = \frac{1}{p} \sum_{k=1}^K (\mathbf{X}_k - \mathbf{1}_n \hat{\boldsymbol{\mu}}_k^T) \hat{\boldsymbol{\Delta}}_k^{-1} (\mathbf{X}_k - \mathbf{1}_n \hat{\boldsymbol{\mu}}_k^T)^T \quad (8)$$

$$\hat{\boldsymbol{\Delta}}_k = \frac{1}{n} (\mathbf{X}_k - \mathbf{1}_n \hat{\boldsymbol{\mu}}_k^T)^T \hat{\boldsymbol{\Sigma}}^{-1} (\mathbf{X}_k - \mathbf{1}_n \hat{\boldsymbol{\mu}}_k^T) \quad \forall k = 1, \dots, K. \quad (9)$$

*Proof.* To compute the MLE of  $\boldsymbol{\mu}_k$ , we expand the trace term in the log-likelihood equation and take partial derivatives to obtain the gradient equation

$$\frac{\partial \ell}{\partial \boldsymbol{\mu}_k} = 2 \boldsymbol{\Delta}_k^{-1} \mathbf{X}_k^T \boldsymbol{\Sigma}^{-1} \mathbf{1}_n - 2 \boldsymbol{\Delta}_k^{-1} \boldsymbol{\mu}_k \mathbf{1}_n^T \boldsymbol{\Sigma}^{-1} \mathbf{1}_n = \mathbf{0}.$$

By invertibility of  $\boldsymbol{\Sigma}^{-1}$  and  $\boldsymbol{\Delta}_k^{-1}$ , it follows that

$$\begin{aligned}
\mathbf{X}_k^T - \hat{\boldsymbol{\mu}}_k \mathbf{1}_n^T &= \mathbf{0} \\
\implies \hat{\boldsymbol{\mu}}_k &= \frac{\mathbf{X}_k^T \mathbf{1}_n}{n}.
\end{aligned}$$

In other words,  $\hat{\boldsymbol{\mu}}_k$  is the vector of column means of  $\mathbf{X}_k$ .

Now, taking the partial derivatives of the log-likelihood equation with respect to  $\boldsymbol{\Sigma}^{-1}$

and  $\Delta_k^{-1}$  respectively yields the gradient equations:

$$\begin{aligned}\frac{\partial \ell}{\partial \Sigma^{-1}} &= p \Sigma - \sum_{k=1}^K (\mathbf{X}_k - \mathbf{1}_n \boldsymbol{\mu}_k^T) \Delta_k^{-1} (\mathbf{X}_k - \mathbf{1}_n \boldsymbol{\mu}_k^T)^T \\ \frac{\partial \ell}{\partial \Delta_k^{-1}} &= n \Delta_k - (\mathbf{X}_k - \mathbf{1}_n \boldsymbol{\mu}_k^T)^T \Sigma^{-1} (\mathbf{X}_k - \mathbf{1}_n \boldsymbol{\mu}_k^T).\end{aligned}$$

Setting the gradient equations equal to  $\mathbf{0}$  gives the desired result.  $\square$

We can compute the unpenalized MLEs via Algorithm 2, assuming that  $\boldsymbol{\mu}_1, \dots, \boldsymbol{\mu}_K$  are known and that the unpenalized MLEs exist.

---

**Algorithm 2** Flip-Flop Algorithm for iPCA Unpenalized MLEs

---

- 1: Assume that  $\boldsymbol{\mu}_1, \dots, \boldsymbol{\mu}_K$  are known and that the unpenalized MLEs exist
  - 2: Initialize  $\hat{\Sigma}, \hat{\Delta}_1, \dots, \hat{\Delta}_K$  to be symmetric positive definite.
  - 3: Set  $\bar{\mathbf{X}}_k = \mathbf{X}_k - \mathbf{1}_n \boldsymbol{\mu}_k^T$  for each  $k = 1, \dots, K$
  - 4: **while** not converged **do**
  - 5:     Update  $\hat{\Sigma} = \frac{1}{p} \sum_{k=1}^K \bar{\mathbf{X}}_k \hat{\Delta}_k^{-1} \bar{\mathbf{X}}_k^T$
  - 6:     **for**  $k = 1, \dots, K$  **do**
  - 7:         Update  $\hat{\Delta}_k = \frac{1}{n} \bar{\mathbf{X}}_k^T \hat{\Sigma}^{-1} \bar{\mathbf{X}}_k$
- 

The next theorem provides very restrictive conditions for which the unpenalized MLEs exist, but in almost all practical cases, the unpenalized maximum likelihood problem is ill-posed for iPCA.

**Theorem 1.** (i) *If the population means  $\boldsymbol{\mu}_1, \dots, \boldsymbol{\mu}_K$  in (2) are known,  $\text{rank}(\tilde{\mathbf{X}}) = n$ , and  $\text{rank}(\mathbf{X}_k) = p_k$  for  $k = 1, \dots, K$ , then the unpenalized MLEs for  $\Sigma, \Delta_1, \dots, \Delta_K$  exist.*

(ii) *If the population means  $\boldsymbol{\mu}_1, \dots, \boldsymbol{\mu}_K$  in (2) are unknown, then the unpenalized MLEs for  $\Sigma$  and  $\Delta_1, \dots, \Delta_K$  are not positive definite and hence do not exist.*

*Proof.* (i) Without loss of generality, we may assume that  $\boldsymbol{\mu}_1 = \dots = \boldsymbol{\mu}_K = \mathbf{0}$ . It is easy to see that  $\hat{\Sigma}$  and  $\hat{\Delta}_1, \dots, \hat{\Delta}_K$  are symmetric positive semidefinite. We next claim that  $\hat{\Sigma}$  and  $\hat{\Delta}_1, \dots, \hat{\Delta}_K$  are full rank and hence positive definite. To prove this claim, we proceed by induction on the unpenalized Flip-Flop iteration counter  $m$ . Let  $\hat{\Sigma}^m$  and  $\hat{\Delta}_k^m$  denote the  $m^{\text{th}}$  Flip-Flop update of  $\hat{\Sigma}$  and  $\hat{\Delta}_k$ , respectively.

Clearly, the base case holds since  $\Sigma^0$  and  $\Delta_1^0, \dots, \Delta_K^0$  are initialized to be symmetric positive definite. So suppose  $\Sigma^m$  and  $\Delta_1^m, \dots, \Delta_K^m$  are full rank.

Then the unpenalized Flip-Flop iterates at the  $(m+1)^{\text{th}}$ -update step are

$$\begin{aligned}\hat{\Sigma}^{m+1} &= \frac{1}{p} \sum_{k=1}^K \mathbf{X}_k (\hat{\Delta}_k^m)^{-1} \mathbf{X}_k^T = \frac{1}{p} \tilde{\mathbf{X}} (\tilde{\Delta}^m)^{-1} \tilde{\mathbf{X}}^T \\ \hat{\Delta}_k^{m+1} &= \frac{1}{n} \mathbf{X}_k^T (\hat{\Sigma}^{m+1})^{-1} \mathbf{X}_k\end{aligned}$$

where  $\tilde{\mathbf{X}} = [\mathbf{X}_1, \dots, \mathbf{X}_K]$  and  $\tilde{\Delta}^m = \text{diag}(\hat{\Delta}_1^m, \dots, \hat{\Delta}_K^m)$ .

Therefore, we have that

$$\text{rank}\left(\hat{\Sigma}^{m+1}\right) = \text{rank}\left(\tilde{\mathbf{X}}(\tilde{\Delta}^m)^{-1}\tilde{\mathbf{X}}^T\right) = \text{rank}\left(\tilde{\mathbf{X}}(\tilde{\Delta}^m)^{-\frac{1}{2}}\right) = \text{rank}(\tilde{\mathbf{X}}) = n.$$

Here, the second equality holds because  $\text{rank}(\mathbf{A}^T \mathbf{A}) = \text{rank}(\mathbf{A}) = \text{rank}(\mathbf{A}^T)$ . The third equality holds because  $(\tilde{\Delta}^m)^{-\frac{1}{2}}$  is full rank (i.e.  $\text{rank} = p$ ) by the inductive hypothesis, and the last equality holds by hypothesis. Thus,  $\hat{\Sigma}^{m+1}$  is positive definite.

Similarly, for each  $k = 1, \dots, K$ ,

$$\text{rank}\left(\hat{\Delta}_k^{m+1}\right) = \text{rank}\left(\mathbf{X}_k^T(\hat{\Sigma}^{m+1})^{-1}\mathbf{X}_k\right) = \text{rank}(\mathbf{X}_k) = p_k.$$

So for each  $k = 1, \dots, K$ ,  $\hat{\Delta}_k^{m+1}$  is positive definite.

By induction,  $\hat{\Sigma}^m, \hat{\Delta}_1^m, \dots, \hat{\Delta}_K^m \succ 0$  for each iterate of Algorithm 2, and by Corollary 1, Algorithm 2 converges to the global solution of (16). Thus, the unpenalized MLEs for  $\Sigma$  and  $\Delta_1^{-1}, \dots, \Delta_K^{-1}$  exist under the assumptions given in part (i).

(ii) Assume that the population means of (2) are unknown. In this case, we must estimate  $\boldsymbol{\mu}_1, \dots, \boldsymbol{\mu}_K$  as well as  $\Sigma$  and  $\Delta_1, \dots, \Delta_K$ . By Lemma 1,  $\hat{\boldsymbol{\mu}}_k$  is the vector of column means of  $\mathbf{X}_k$ , so suppose that we have centered each data matrix  $\mathbf{X}_k$  to have column means  $\mathbf{0}$ . Then the unpenalized MLEs for  $\Sigma$  and  $\Delta_1, \dots, \Delta_K$  are obtained by

$$\begin{aligned}\hat{\Sigma} &= \frac{1}{p} \sum_{k=1}^K \mathbf{X}_k \hat{\Delta}_k^{-1} \mathbf{X}_k^T = \frac{1}{p} \tilde{\mathbf{X}} \tilde{\Delta}^{-1} \tilde{\mathbf{X}}^T, \\ \hat{\Delta}_k &= \frac{1}{n} \mathbf{X}_k^T \hat{\Sigma}^{-1} \mathbf{X}_k,\end{aligned}$$

where  $\tilde{\Delta} := \text{diag}(\hat{\Delta}_1, \dots, \hat{\Delta}_K)$ .

Now, suppose for the sake of contradiction that there exists  $n, p_1, \dots, p_k$  such that  $\Sigma^{-1}$  and  $\Delta_1^{-1}, \dots, \Delta_K^{-1}$  are symmetric positive definite. By the same argument as in part (i),  $\text{rank}(\hat{\Sigma}) = \text{rank}(\tilde{\mathbf{X}})$ , but since each  $\mathbf{X}_k$  has been centered to have column means  $\mathbf{0}$ , then the  $n$  rows of  $\tilde{\mathbf{X}}$  are linearly dependent. Hence,  $\text{rank}(\hat{\Sigma}) = \text{rank}(\tilde{\mathbf{X}}) < n$ , which implies that  $\hat{\Sigma}$  can never be positive definite, a contradiction. Therefore, if the population mean of (2) is unknown, then the unpenalized MLEs never exist.  $\square$

*Remark.* Notice that if the unpenalized MLEs for  $\Sigma, \Delta_1, \dots, \Delta_K$  exist, then

$$\begin{aligned}n &\stackrel{[1]}{=} \text{rank}(\hat{\Sigma}) \stackrel{[2]}{=} \text{rank}(\tilde{\mathbf{X}}) \stackrel{[3]}{\leq} \min\{n, p\} \\ p_k &\stackrel{[1]}{=} \text{rank}(\hat{\Delta}_k) \stackrel{[2]}{=} \text{rank}(\mathbf{X}_k) \stackrel{[3]}{\leq} \min\{n, p_k\} \quad \forall k = 1, \dots, K\end{aligned}$$

where [1] follows from positive definiteness of  $\hat{\Sigma}$  and  $\hat{\Delta}_k$ , [2] follows the same argument as in the proof of Theorem 1, and [3] holds by properties of rank and the dimensions of  $\tilde{\mathbf{X}}$  and  $\mathbf{X}_k$ . Hence, if the unpenalized MLEs for  $\Sigma, \Delta_1, \dots, \Delta_K$  exist, it must be that  $p_k \leq n \leq p$  for each  $k = 1, \dots, K$ .

Proposition 1 can be proved in the same way as Lemma 1, so we omit the proof.

## B.2 Penalized Maximum Likelihood Estimators

In this section, we develop Flip-Flop algorithms and analyze the convergence results for both Frobenius and  $L_1$  penalties. For the sake of notation, let

$$\begin{aligned} -\ell_P(\boldsymbol{\Sigma}^{-1}, \boldsymbol{\Delta}_1^{-1}, \dots, \boldsymbol{\Delta}_K^{-1}) &= -p \log |\boldsymbol{\Sigma}^{-1}| - n \sum_{k=1}^K \log |\boldsymbol{\Delta}_k^{-1}| + \sum_{k=1}^K \text{tr}(\boldsymbol{\Sigma}^{-1} \mathbf{X}_k \boldsymbol{\Delta}_k^{-1} \mathbf{X}_k^T) \\ &\quad + P(\boldsymbol{\Sigma}^{-1}, \boldsymbol{\Delta}_1^{-1}, \dots, \boldsymbol{\Delta}_K^{-1}) \end{aligned}$$

We give the overarching framework of the Flip-Flop algorithms in Algorithm 3, and we show in Theorem 2 that Algorithm 3 can be used to find a local solution of (12) for a certain class of penalties, which includes the additive Frobenius, multiplicative Frobenius, and additive  $L_1$  penalties. The main idea behind the proof is to use convexity and view Algorithm 3 as a block coordinate descent algorithm so that each update of the Flip-Flop algorithm is a descent direction.

---

### Algorithm 3 Outline of Flip-Flop Algorithm for Penalized iPCA Covariance Estimators

---

- 1: Center the columns of  $\mathbf{X}_1, \dots, \mathbf{X}_K$ , and initialize  $\hat{\boldsymbol{\Sigma}}, \hat{\boldsymbol{\Delta}}_1, \dots, \hat{\boldsymbol{\Delta}}_K$  to be positive definite.
  - 2: **while** not converged **do**
  - 3:     Update  $\boldsymbol{\Sigma}$  while fixing all other variables:  

$$\hat{\boldsymbol{\Sigma}}^{-1} = \underset{\boldsymbol{\Sigma}^{-1} \succ 0}{\text{argmin}} \quad -\ell_P(\boldsymbol{\Sigma}^{-1}, \hat{\boldsymbol{\Delta}}_1^{-1}, \dots, \hat{\boldsymbol{\Delta}}_K^{-1})$$
  - 4:     **for**  $k = 1, \dots, K$  **do**
  - 5:         Update  $\boldsymbol{\Delta}_k$  while fixing all other variables:  

$$\hat{\boldsymbol{\Delta}}_k^{-1} = \underset{\boldsymbol{\Delta}_k^{-1} \succ 0}{\text{argmin}} \quad -\ell_P(\hat{\boldsymbol{\Sigma}}^{-1}, \hat{\boldsymbol{\Delta}}_1^{-1}, \dots, \hat{\boldsymbol{\Delta}}_{k-1}^{-1}, \boldsymbol{\Delta}_k^{-1}, \hat{\boldsymbol{\Delta}}_{k+1}^{-1}, \dots, \hat{\boldsymbol{\Delta}}_K^{-1})$$
- 

**Theorem 2.** *Suppose that the objective function in (12) is bounded below. Suppose also that either (i)  $P(\boldsymbol{\Sigma}^{-1}, \boldsymbol{\Delta}_1^{-1}, \dots, \boldsymbol{\Delta}_K^{-1})$  is a differentiable convex function with respect to each coordinate or (ii)  $P(\boldsymbol{\Sigma}^{-1}, \boldsymbol{\Delta}_1^{-1}, \dots, \boldsymbol{\Delta}_K^{-1}) = P_0(\boldsymbol{\Sigma}^{-1}) + \sum_{k=1}^K P_k(\boldsymbol{\Delta}_k^{-1})$ , where  $P_i$  is a (non-differentiable) convex function for each  $k = 1, \dots, K$ . If either (i) or (ii) holds, then the Flip-Flop algorithm corresponding to (12) converges to a stationary point of the objective.*

*Proof.* Suppose either  $P(\boldsymbol{\Sigma}^{-1}, \boldsymbol{\Delta}_1^{-1}, \dots, \boldsymbol{\Delta}_K^{-1})$  is a differentiable convex function with respect to each coordinate or  $P(\boldsymbol{\Sigma}^{-1}, \boldsymbol{\Delta}_1^{-1}, \dots, \boldsymbol{\Delta}_K^{-1}) = P_0(\boldsymbol{\Sigma}^{-1}) + \sum_{k=1}^K P_k(\boldsymbol{\Delta}_k^{-1})$  where  $P_i$  is a (non-differentiable) convex function for each  $i = 1, \dots, K$ .

Let  $\ell(\boldsymbol{\Sigma}^{-1}, \boldsymbol{\Delta}_1^{-1}, \dots, \boldsymbol{\Delta}_K^{-1}) = p \log |\boldsymbol{\Sigma}^{-1}| + n \sum_{k=1}^K \log |\boldsymbol{\Delta}_k^{-1}| - \sum_{k=1}^K \text{tr}(\boldsymbol{\Sigma}^{-1} \mathbf{X}_k \boldsymbol{\Delta}_k^{-1} \mathbf{X}_k^T)$ . Since the domain of  $-\ell$  is open and  $-\ell$  is Gateaux-differentiable on its domain, then  $-\ell_P$  is regular in the domain of  $-\ell_P$  by Lemma 3.1 in Tseng (2001).

Note also that since the log-determinant is a strictly concave function on the set of symmetric positive definite matrices, the trace function is linear, and the penalty term is convex with respect to each coordinate by hypothesis, then

- $-\ell_P$  is strictly convex in  $\Sigma^{-1}$  with  $\Delta_1^{-1}, \dots, \Delta_K^{-1}$  fixed, and
- for each  $k = 1, \dots, K$ ,  $-\ell_P$  is strictly convex in  $\Delta_k^{-1}$  with  $\Sigma^{-1}, \Delta_j^{-1}, j \neq k$  fixed.

Because  $-\ell_P$  is regular and strictly convex with respect to each coordinate, it follows that the Flip-Flop algorithm corresponding to (12) converges to a stationary point of the objective function by Theorem 4.1(c) in Tseng (2001).  $\square$

In the following sections, we will derive the specific form of the Flip-Flop updates for each of the penalized iPCA estimators.

### B.2.1 Additive Frobenius Penalized Flip-Flop Estimator

To compute the additive Frobenius penalized estimator, we solve

$$\hat{\Sigma}^{-1}, \hat{\Delta}_1^{-1}, \dots, \hat{\Delta}_K^{-1} = \underset{\substack{\Sigma^{-1} \succ 0 \\ \Delta_1^{-1}, \dots, \Delta_K^{-1} \succ 0}}{\operatorname{argmax}} \left\{ p \log |\Sigma^{-1}| + n \sum_{k=1}^K \log |\Delta_k^{-1}| - \sum_{k=1}^K \operatorname{tr} (\Sigma^{-1} \mathbf{X}_k \Delta_k^{-1} \mathbf{X}_k^T) - \lambda_\Sigma \|\Sigma^{-1}\|_F^2 - \sum_{k=1}^K \lambda_k \|\Delta_k^{-1}\|_F^2 \right\}. \quad (17)$$

The gradient equations corresponding to (17) are given by

$$p \hat{\Sigma} - \sum_{k=1}^K \mathbf{X}_k \hat{\Delta}_k^{-1} \mathbf{X}_k^T - 2\lambda_\Sigma \hat{\Sigma}^{-1} = 0, \quad (18)$$

$$n \hat{\Delta}_k - \mathbf{X}_k^T \hat{\Sigma}^{-1} \mathbf{X}_k - 2\lambda_k \hat{\Delta}_k^{-1} = 0 \quad \forall k = 1, \dots, K. \quad (19)$$

From (18) and (19), we can rewrite  $\hat{\Sigma}$  and  $\hat{\Delta}_1, \dots, \hat{\Delta}_K$  in terms of one another.

**Proposition 2.** *If gradient equations (18) and (19) are satisfied, then*

$$\hat{\Sigma} = \left( \frac{2\lambda_\Sigma}{p} \mathbf{I} + \frac{1}{4p^2} \left( \sum_{k=1}^K \mathbf{X}_k \hat{\Delta}_k^{-1} \mathbf{X}_k^T \right)^2 \right)^{\frac{1}{2}} + \frac{1}{2p} \sum_{k=1}^K \mathbf{X}_k \hat{\Delta}_k^{-1} \mathbf{X}_k^T \quad (20)$$

$$\hat{\Delta}_k = \left( \frac{2\lambda_k}{n} \mathbf{I} + \frac{1}{4n^2} (\mathbf{X}_k^T \hat{\Sigma}^{-1} \mathbf{X}_k)^2 \right)^{\frac{1}{2}} + \frac{1}{2n} \mathbf{X}_k^T \hat{\Sigma}^{-1} \mathbf{X}_k \quad \forall k = 1, \dots, K \quad (21)$$

*Proof.* Define  $\hat{\mathbf{S}}_\Sigma = \sum_{k=1}^K \mathbf{X}_k \hat{\Delta}_k^{-1} \mathbf{X}_k^T$ , and right multiply (18) by  $\hat{\Sigma}$  to obtain

$$p \hat{\Sigma}^2 - \hat{\mathbf{S}}_\Sigma \hat{\Sigma} - 2\lambda_\Sigma \mathbf{I} = \mathbf{0} \quad (22)$$

$$\implies \hat{\Sigma}^2 - \frac{1}{p} \hat{\mathbf{S}}_\Sigma \hat{\Sigma} + \frac{1}{4p^2} \hat{\mathbf{S}}_\Sigma^2 = \frac{2\lambda_\Sigma}{p} \mathbf{I} + \frac{1}{4p^2} \hat{\mathbf{S}}_\Sigma^2. \quad (23)$$

On the other hand, we can multiply (18) by  $\hat{\Sigma}$  on the left to obtain

$$p\hat{\Sigma}^2 - \hat{\Sigma}\hat{\mathbf{S}}_{\Sigma} - 2\lambda_{\Sigma}\mathbf{I} = \mathbf{0} \quad (24)$$

$$\implies \hat{\Sigma}^2 - \frac{1}{p}\hat{\Sigma}\hat{\mathbf{S}}_{\Sigma} + \frac{1}{4p^2}\hat{\mathbf{S}}_{\Sigma}^2 = \frac{2\lambda_{\Sigma}}{p}\mathbf{I} + \frac{1}{4p^2}\hat{\mathbf{S}}_{\Sigma}^2. \quad (25)$$

So adding (23) and (25) then dividing by 2 gives

$$\begin{aligned} \hat{\Sigma}^2 - \frac{1}{2p}\hat{\mathbf{S}}_{\Sigma}\hat{\Sigma} - \frac{1}{2p}\hat{\Sigma}\hat{\mathbf{S}}_{\Sigma} + \frac{1}{4p^2}\hat{\mathbf{S}}_{\Sigma}^2 &= \frac{2\lambda_{\Sigma}}{p}\mathbf{I} + \frac{1}{4p^2}\hat{\mathbf{S}}_{\Sigma}^2 \\ \implies \left(\hat{\Sigma} - \frac{1}{2p}\hat{\mathbf{S}}_{\Sigma}\right)^2 &= \frac{2\lambda_{\Sigma}}{p}\mathbf{I} + \frac{1}{4p^2}\hat{\mathbf{S}}_{\Sigma}^2. \end{aligned}$$

Since  $\frac{2\lambda_{\Sigma}}{p}\mathbf{I} + \frac{1}{4p^2}\hat{\mathbf{S}}_{\Sigma}^2$  is positive definite, it has a unique square root. Thus,

$$\hat{\Sigma} = \left(\frac{2\lambda_{\Sigma}}{p}\mathbf{I} + \frac{1}{4p^2}\hat{\mathbf{S}}_{\Sigma}^2\right)^{1/2} + \frac{1}{2p}\hat{\mathbf{S}}_{\Sigma}.$$

We can similarly rearrange (19) and complete the square to obtain (21).  $\square$

We now have the machinery to prove Proposition 3, which gives us the form of each update in the additive Frobenius Flip-Flop algorithm.

**Proposition 3.**  $\hat{\Sigma}$  and  $\hat{\Delta}_1, \dots, \hat{\Delta}_K$  are solutions to the gradient equations in (18) and (19) if and only if

$$\hat{\Sigma} = \mathbf{U} \left[ \frac{1}{2p} \left( \Gamma + (\Gamma^2 + 8\lambda_{\Sigma}p\mathbf{I})^{\frac{1}{2}} \right) \right] \mathbf{U}^T \quad (26)$$

$$\text{and } \hat{\Delta}_k = \mathbf{V}_k \left[ \frac{1}{2n} \left( \Phi_k + (\Phi_k^2 + 8\lambda_{kn}\mathbf{I})^{\frac{1}{2}} \right) \right] \mathbf{V}_k^T \quad \forall k = 1, \dots, K, \quad (27)$$

where  $\mathbf{U}, \mathbf{V}_k, \Gamma$ , and  $\Phi_k$  are defined by the eigendecompositions  $\sum_{k=1}^K \mathbf{X}_k \hat{\Delta}_k^{-1} \mathbf{X}_k^T = \mathbf{U} \Gamma \mathbf{U}^T$  and  $\mathbf{X}_k^T \hat{\Sigma}^{-1} \mathbf{X}_k = \mathbf{V}_k \Phi_k \mathbf{V}_k^T$ .

*Proof.* ( $\implies$ ) Suppose that  $\hat{\Sigma}$  and  $\hat{\Delta}_1, \dots, \hat{\Delta}_K$  are solutions to the gradient equations in (18) and (19). We will first show that the eigenvectors of  $\hat{\Sigma}$  and  $\sum_{k=1}^K \mathbf{X}_k \hat{\Delta}_k^{-1} \mathbf{X}_k^T$  are equivalent.

Let  $\mathbf{u}$  be an eigenvector of  $\hat{\Sigma}$  with the corresponding eigenvalue  $\phi$ . Then, by (18),

$$\sum_{k=1}^K \mathbf{X}_k \hat{\Delta}_k^{-1} \mathbf{X}_k^T \mathbf{u} = (p\hat{\Sigma} - 2\lambda_{\Sigma}\hat{\Sigma}^{-1}) \mathbf{u} = (p\phi - 2\lambda_{\Sigma}\phi^{-1}) \mathbf{u}.$$

Therefore,  $\mathbf{u}$  is an eigenvector of  $\sum_{k=1}^K \mathbf{X}_k \hat{\Delta}_k^{-1} \mathbf{X}_k^T$  with the eigenvalue  $p\phi - 2\lambda_{\Sigma}\phi^{-1}$ .

Conversely, suppose  $\mathbf{u}$  is an eigenvector of  $\sum_{k=1}^K \mathbf{X}_k \hat{\Delta}_k^{-1} \mathbf{X}_k^T$  with eigenvalue  $\gamma$ . Then

$$\left( \frac{2\lambda_{\Sigma}}{p}\mathbf{I} + \frac{1}{4p^2} \left( \sum_{k=1}^K \mathbf{X}_k \hat{\Delta}_k^{-1} \mathbf{X}_k^T \right)^2 \right) \mathbf{u} = \left( \frac{2\lambda_{\Sigma}}{p} + \frac{1}{4p^2}\gamma^2 \right) \mathbf{u}.$$

This implies that

$$\left( \frac{2\lambda_{\Sigma}}{p} \mathbf{I} + \frac{1}{4p^2} \left( \sum_{k=1}^K \mathbf{X}_k \hat{\Delta}_k^{-1} \mathbf{X}_k^T \right)^2 \right)^{\frac{1}{2}} \mathbf{u} = \left( \frac{2\lambda_{\Sigma}}{p} + \frac{1}{4p^2} \gamma^2 \right)^{\frac{1}{2}} \mathbf{u}. \quad (28)$$

So by Proposition 2 and (28), we have that

$$\hat{\Sigma} \mathbf{u} = \left[ \left( \frac{2\lambda_{\Sigma}}{p} \mathbf{I} + \frac{1}{4p^2} \left( \sum_{k=1}^K \mathbf{X}_k \hat{\Delta}_k^{-1} \mathbf{X}_k^T \right)^2 \right)^{\frac{1}{2}} + \frac{1}{2p} \sum_{k=1}^K \mathbf{X}_k \hat{\Delta}_k^{-1} \mathbf{X}_k^T \right] \mathbf{u} \quad (29)$$

$$= \left[ \left( \frac{2\lambda_{\Sigma}}{p} + \frac{1}{4p^2} \gamma^2 \right)^{\frac{1}{2}} + \frac{1}{2p} \gamma \right] \mathbf{u} \quad (30)$$

$$= \left[ \frac{1}{2p} \left( \gamma + \sqrt{\gamma^2 + 8\lambda_{\Sigma} p} \right) \right] \mathbf{u}, \quad (31)$$

so  $\mathbf{u}$  is indeed an eigenvector of  $\hat{\Sigma}$  with the eigenvalue  $\frac{1}{2p} \left( \gamma + \sqrt{\gamma^2 + 8\lambda_{\Sigma} p} \right)$ .

Since the eigenvectors of  $\hat{\Sigma}$  and  $\sum_{k=1}^K \mathbf{X}_k \hat{\Delta}_k^{-1} \mathbf{X}_k^T$  are equivalent and (31) gives us the exact connection between their eigenvalues, it follows that

$$\hat{\Sigma} = \mathbf{U} \left[ \frac{1}{2p} \left( \Gamma + (\Gamma^2 + 8\lambda_{\Sigma} p \mathbf{I})^{\frac{1}{2}} \right) \right] \mathbf{U}^T,$$

where  $\mathbf{U}, \Gamma$  are defined by the eigendecomposition  $\sum_{k=1}^K \mathbf{X}_k \hat{\Delta}_k^{-1} \mathbf{X}_k^T = \mathbf{U} \Gamma \mathbf{U}^T$ .

This same logic can be used to show that for each  $k = 1, \dots, K$ ,

$$\hat{\Delta}_k = \mathbf{V}_k \left[ \frac{1}{2n} \left( \Phi_k + (\Phi_k^2 + 8\lambda_k n \mathbf{I})^{\frac{1}{2}} \right) \right] \mathbf{V}_k^T,$$

where  $\mathbf{V}_k, \Phi_k$  are defined by the eigendecomposition  $\mathbf{X}_k^T \hat{\Sigma}^{-1} \mathbf{X}_k = \mathbf{V}_k \Phi_k \mathbf{V}_k^T$ . We omit the proof since it uses the same argument as above.

( $\Leftarrow$ ) Now suppose that  $\hat{\Sigma}$  and  $\hat{\Delta}_1, \dots, \hat{\Delta}_K$  satisfy equations (26) and (27).

Since we know  $\left[ \frac{1}{2p} \left( \gamma + \sqrt{\gamma^2 + 8\lambda_{\Sigma} p} \right) \right]^{-1} = \frac{1}{4\lambda_{\Sigma}} \left( \sqrt{\gamma^2 + 8\lambda_{\Sigma} p} - \gamma \right)$ , it follows that  $\left[ \frac{1}{2p} \left( \Gamma + (\Gamma^2 + 8\lambda_{\Sigma} p \mathbf{I})^{\frac{1}{2}} \right) \right]^{-1} = \frac{1}{4\lambda_{\Sigma}} \left( (\Gamma^2 + 8\lambda_{\Sigma} p \mathbf{I})^{\frac{1}{2}} - \Gamma \right)$ . Therefore,

$$\begin{aligned} p\hat{\Sigma} - \sum_{k=1}^K \mathbf{X}_k \hat{\Delta}_k^{-1} \mathbf{X}_k^T - 2\lambda_{\Sigma} \hat{\Sigma}^{-1} &= p \mathbf{U} \left[ \frac{1}{2p} \left( \Gamma + (\Gamma^2 + 8\lambda_{\Sigma} p \mathbf{I})^{\frac{1}{2}} \right) \right] \mathbf{U}^T - \mathbf{U} \Gamma \mathbf{U}^T \\ &\quad - 2\lambda_{\Sigma} \mathbf{U} \left[ \frac{1}{2p} \left( \Gamma + (\Gamma^2 + 8\lambda_{\Sigma} p \mathbf{I})^{\frac{1}{2}} \right) \right]^{-1} \mathbf{U}^T \\ &= \mathbf{U} \left[ \frac{1}{2} \left( \Gamma + (\Gamma^2 + 8\lambda_{\Sigma} p \mathbf{I})^{\frac{1}{2}} \right) \right] \mathbf{U}^T - \mathbf{U} \Gamma \mathbf{U}^T \end{aligned}$$

$$\begin{aligned}
& - \mathbf{U} \left[ \frac{1}{2} \left( (\mathbf{\Gamma}^2 + 8\lambda_{\Sigma} p \mathbf{I})^{\frac{1}{2}} - \mathbf{\Gamma} \right) \right] \mathbf{U}^T \\
& = 0.
\end{aligned}$$

Similarly, one can substitute in (27) and follow the same argument to show that (19) is also satisfied.  $\square$

As a consequence of Proposition 3, each update step in the additive Frobenius Flip-Flop algorithm can be solved by taking a full eigendecomposition and then regularizing the eigenvalues. This algorithm is given in Algorithm 4.

---

**Algorithm 4** Flip-Flop Algorithm for Additive Frobenius Penalized iPCA Estimators

---

- 1: Center the columns of  $\mathbf{X}_1, \dots, \mathbf{X}_K$ , and initialize  $\hat{\Sigma}, \hat{\Delta}_1, \dots, \hat{\Delta}_K$  to be positive definite.
- 2: **while** not converged **do**
- 3:   Take eigendecomposition:  $\sum_{k=1}^K \mathbf{X}_k \hat{\Delta}_k^{-1} \mathbf{X}_k^T = \mathbf{U} \mathbf{\Gamma} \mathbf{U}^T$
- 4:   Regularize eigenvalues:  $\phi_i = \frac{1}{2p} \left( \gamma_i + \sqrt{\gamma_i^2 + 8\lambda_{\Sigma} p} \right)$
- 5:   Update  $\hat{\Sigma}^{-1} = \mathbf{U} \mathbf{\Phi}^{-1} \mathbf{U}^T$
- 6:   **for**  $k = 1, \dots, K$  **do**
- 7:     Take eigendecomposition:  $\mathbf{X}_k^T \hat{\Sigma}^{-1} \mathbf{X}_k = \mathbf{V} \mathbf{\Phi} \mathbf{V}^T$
- 8:     Regularize eigenvalues:  $\gamma_i = \frac{1}{2n} \left( \phi_i + \sqrt{\phi_i^2 + 8\lambda_k n} \right)$ .
- 9:     Update  $\hat{\Delta}_k^{-1} = \mathbf{V} \mathbf{\Gamma}^{-1} \mathbf{V}^T$

### B.2.2 Multiplicative Frobenius Penalized Flip-Flop Estimator

The derivation of the multiplicative Frobenius Flip-Flop algorithm is very similar to the previous derivation with the additive Frobenius penalty. Thus, we omit most of the details and simply provide a sketch of the derivation.

Recall that the multiplicative Frobenius penalized estimator solves

$$\begin{aligned}
\hat{\Sigma}^{-1}, \hat{\Delta}_1^{-1}, \dots, \hat{\Delta}_K^{-1} = \underset{\substack{\Sigma^{-1} \succ 0 \\ \Delta_1^{-1}, \dots, \Delta_K^{-1} \succ 0}}{\operatorname{argmax}} \left\{ p \log |\Sigma^{-1}| + n \sum_{k=1}^K \log |\Delta_k^{-1}| - \sum_{k=1}^K \operatorname{tr} (\Sigma^{-1} \mathbf{X}_k \Delta_k^{-1} \mathbf{X}_k^T) \right. \\
\left. - \|\Sigma^{-1}\|_F^2 \sum_{k=1}^K \lambda_k \|\Delta_k^{-1}\|_F^2 \right\}, \tag{32}
\end{aligned}$$

for which the gradient equations are

$$p \hat{\Sigma} - \sum_{k=1}^K \mathbf{X}_k \hat{\Delta}_k^{-1} \mathbf{X}_k^T - 2 \hat{\Sigma}^{-1} \sum_{k=1}^K \lambda_k \|\hat{\Delta}_k^{-1}\|_F^2 = 0, \tag{33}$$

$$n \hat{\Delta}_k - \mathbf{X}_k^T \hat{\Sigma}^{-1} \mathbf{X}_k - 2 \lambda_k \hat{\Delta}_k^{-1} \|\hat{\Sigma}^{-1}\|_F^2 = 0 \quad \forall k = 1, \dots, K. \tag{34}$$

Assuming these gradient equations (33) and (34) are satisfied, we can write

$$\hat{\Sigma} = \left( \frac{2 \sum_{k=1}^K \lambda_k \|\hat{\Delta}_k^{-1}\|_F^2}{p} \mathbf{I} + \frac{1}{4p^2} \left( \sum_{k=1}^K \mathbf{X}_k \hat{\Delta}_k^{-1} \mathbf{X}_k^T \right)^2 \right)^{\frac{1}{2}} + \frac{1}{2p} \sum_{k=1}^K \mathbf{X}_k \hat{\Delta}_k^{-1} \mathbf{X}_k^T, \quad (35)$$

$$\hat{\Delta}_k = \left( \frac{2\lambda_k \|\hat{\Sigma}^{-1}\|_F^2}{n} \mathbf{I} + \frac{1}{4n^2} (\mathbf{X}_k^T \hat{\Sigma}^{-1} \mathbf{X}_k)^2 \right)^{\frac{1}{2}} + \frac{1}{2n} \mathbf{X}_k^T \hat{\Sigma}^{-1} \mathbf{X}_k \quad \forall k = 1, \dots, K. \quad (36)$$

We then can follow the same argument in Proposition 3 to show that  $\hat{\Sigma}$  and  $\hat{\Delta}_1, \dots, \hat{\Delta}_K$  are solutions to the multiplicative Frobenius gradient equations (33) and (34) if and only if

$$\hat{\Sigma} = \mathbf{U} \left[ \frac{1}{2p} \left( \mathbf{\Gamma} + \left( \mathbf{\Gamma}^2 + 8p \sum_{k=1}^K \lambda_k \|\hat{\Delta}_k^{-1}\|_F^2 \mathbf{I} \right)^{\frac{1}{2}} \right) \right] \mathbf{U}^T \quad (37)$$

$$\text{and } \hat{\Delta}_k = \mathbf{V}_k \left[ \frac{1}{2n} \left( \Phi_k + (\Phi_k^2 + 8n\lambda_k \|\hat{\Sigma}^{-1}\|_F^2 \mathbf{I})^{\frac{1}{2}} \right) \right] \mathbf{V}_k^T \quad \forall k = 1, \dots, K, \quad (38)$$

where  $\mathbf{U}, \mathbf{V}_k, \mathbf{\Gamma}$ , and  $\Phi_k$  are defined by the eigendecompositions  $\sum_{k=1}^K \mathbf{X}_k \hat{\Delta}_k^{-1} \mathbf{X}_k^T = \mathbf{U} \mathbf{\Gamma} \mathbf{U}^T$  and  $\mathbf{X}_k^T \hat{\Sigma}^{-1} \mathbf{X}_k = \mathbf{V}_k \Phi_k \mathbf{V}_k^T$ . This gives rise to the Flip Flop algorithm for solving the multiplicative Frobenius penalized estimators, as given in Algorithm 1.

### B.2.3 Additive $L_1$ Penalized Flip-Flop Estimator

If the inverse covariance matrices are known to have a sparse underlying structure, then we can apply an  $L_1$  penalty, rather than the Frobenius penalty, to induce this sparsity. Note that while it is possible to use a multiplicative  $L_1$  penalty, the multiplicative  $L_1$  penalty is not known to be geodesically convex and is not separable (as defined in Tseng (2001)). Thus, we primarily consider the additive  $L_1$  penalized iPCA estimator:

$$\hat{\Sigma}^{-1}, \hat{\Delta}_1^{-1}, \dots, \hat{\Delta}_K^{-1} = \underset{\substack{\Sigma^{-1} \succ 0 \\ \Delta_1^{-1}, \dots, \Delta_K^{-1} \succ 0}}{\text{argmax}} \left\{ p \log |\Sigma^{-1}| + n \sum_{k=1}^K \log |\Delta_k^{-1}| - \sum_{k=1}^K \text{tr} (\Sigma^{-1} \mathbf{X}_k \Delta_k^{-1} \mathbf{X}_k^T) - \lambda_{\Sigma} \|\Sigma^{-1}\|_{1,\text{off}} - \sum_{k=1}^K \lambda_k \|\Delta_k^{-1}\|_{1,\text{off}} \right\}. \quad (39)$$

Note that  $\|\cdot\|_{1,\text{off}}$  penalizes the off-diagonal entries (i.e.  $\|\mathbf{A}\|_{1,\text{off}} = \sum_{i \neq j} |a_{ij}|$ ), but it is also possible to use the ordinary  $L_1$  norm  $\|\cdot\|_1$ .

For fixed  $\hat{\Delta}_1, \dots, \hat{\Delta}_K$ , the Flip-Flop update for  $\hat{\Sigma}$  is seen to be

$$\hat{\Sigma}^{-1} = \underset{\Sigma^{-1} \succ 0}{\text{argmin}} -p \log |\Sigma^{-1}| + \text{tr} \left( \Sigma^{-1} \left( \sum_{k=1}^K \mathbf{X}_k \hat{\Delta}_k^{-1} \mathbf{X}_k^T \right) \right) + \lambda_{\Sigma} \|\Sigma^{-1}\|_{1,\text{off}}, \quad (40)$$

and similarly for fixed  $\hat{\Sigma}$  and  $\hat{\Delta}_j$ ,  $j \neq k$ , the update for  $\hat{\Delta}_k$  is

$$\hat{\Delta}_k^{-1} = \underset{\Delta_k^{-1} \succ 0}{\operatorname{argmin}} -n \log |\Delta_k^{-1}| + \operatorname{tr}(\Delta_k^{-1} \mathbf{X}_k^T \hat{\Sigma}^{-1} \mathbf{X}_k) + \lambda_k \|\Delta_k^{-1}\|_{1,\text{off}}. \quad (41)$$

Both of which can be solved via the graphical lasso algorithm (Hsieh et al. 2011). Plugging in these updates to the framework laid out in Algorithm 3, we give the additive  $L_1$  Flip-Flop algorithm in Algorithm 5.

---

**Algorithm 5** Flip-Flop Algorithm for Additive  $L_1$  Penalized iPCA Covariance Estimators

---

- 1: Center the columns of  $\mathbf{X}_1, \dots, \mathbf{X}_K$ , and initialize  $\hat{\Sigma}$ ,  $\hat{\Delta}_1, \dots, \hat{\Delta}_K$  to be positive definite.
- 2: **while** not converged **do**
- 3:     Put  $\mathbf{A} = \frac{1}{p} \sum_{k=1}^K \mathbf{X}_k \Delta_k^{-1} \mathbf{X}_k^T$
- 4:     Apply graphical lasso:
 
$$\hat{\Sigma}^{-1} = \underset{\Sigma^{-1}}{\operatorname{argmin}} -\log |\Sigma^{-1}| + \operatorname{tr}(\mathbf{A} \Sigma^{-1}) + \frac{\lambda_{\Sigma}}{p} \|\Sigma^{-1}\|_{1,\text{off}}$$
- 5:     **for**  $k = 1, \dots, K$  **do**
- 6:         Put  $\mathbf{A}_k := \frac{1}{n} \mathbf{X}_k^T \Sigma^{-1} \mathbf{X}_k$
- 7:         Apply graphical lasso:
 
$$\hat{\Delta}_k^{-1} = \underset{\Delta_k^{-1}}{\operatorname{argmin}} -\log |\Delta_k^{-1}| + \operatorname{tr}(\mathbf{A}_k \Delta_k^{-1}) + \frac{\lambda_k}{n} \|\Delta_k^{-1}\|_{1,\text{off}}$$

} Update  $\Sigma$

} Update  $\Delta_k$

---

## C Geodesic Convexity and the Multiplicative Frobenius iPCA Estimator

Because of the central role that geodesic convexity plays in the multiplicative Frobenius iPCA estimator, we give a self-contained introduction to geodesic convexity in Appendix C.1. This review provides the necessary concepts and tools to prove the theorems in Appendix C.2. For a more comprehensive review, we refer to Rapcsák (1991) and Vishnoi (2018).

### C.1 Introduction to Geodesic Convexity

Convex optimization problems arise frequently in a variety of machine learning applications such as regression, matrix completion, and clustering, to name a few examples. Beyond its widespread applications, convex problems are well-understood theoretically and can be reliably solved in polynomial-time. As a result, machine learning tasks are often formulated as convex problems in Euclidean space to guarantee fast convergence to a global solution. Convexity, however, is not limited to Euclidean spaces. Many tools which we know and love from convex optimization can be extended to geodesic convexity (g-convexity) on Riemannian manifolds. In this general Riemannian setting, there are several applications in which we have g-convexity but not convexity (Zhang and Sra 2016).

Before formally defining geodesic convexity, we first recall some useful concepts from metric geometry. A *metric space* is a pair  $(X, d)$  of a set  $X$  and a distance function  $d$  that

satisfies positivity, symmetry, and the triangle inequality. A *path*  $\gamma$  is a continuous mapping from  $[0, 1]$  to  $X$ , and the *length*  $\ell$  of a path  $\gamma$  is defined as  $\ell(\gamma) := \sup\{\sum_{i=1}^n d(\gamma(t_{i-1}), \gamma(t_i)) : 0 = t_0 < \dots < t_n = 1, n \in \mathbb{N}\}$ . A metric space is a *length space* if  $d(x, y) = \inf \ell(\gamma)$  where the infimum is taken over all paths  $\gamma : [0, 1] \rightarrow X$  joining  $x$  and  $y$ .

**Definition 3.** Let  $(X, d)$  be a length space. A path  $\gamma : [0, 1] \rightarrow X$  is a **geodesic** if for every  $t \in [0, 1]$  there exists an interval  $[a, b] \subset [0, 1]$  which contains a neighborhood of  $t$  and  $\gamma|_{[a, b]}$  is a shortest path from  $\gamma(a)$  to  $\gamma(b)$ . Put simply, a geodesic is a path which locally minimizes length.

Note that geodesics minimize length locally, but not globally. A canonical example of geodesics are the great circles on a sphere.

This concept of a geodesic generalizes the notion of a line in Euclidean space to general (nonlinear) length spaces. By replacing lines by geodesics in the definition of convexity, we can extend convexity to g-convexity in a straightforward manner.

**Definition 4.** Let  $\mathcal{M}$  be a Riemannian manifold. A function  $f : \mathcal{M} \rightarrow \mathbb{R}$  is **geodesically convex** if for any  $x, y \in \mathcal{M}$ , geodesic  $\gamma$  such that  $\gamma(0) = x$  and  $\gamma(1) = y$ , and  $t \in [0, 1]$ , it holds that

$$f(\gamma(t)) \leq (1 - t)f(x) + tf(y).$$

The only caveat is that the underlying space must be a Riemannian manifold. To prevent a long winded detour into the details of Riemannian geometry, we avoid the full technical definition and simply think of a Riemannian manifold as a real differentiable manifold equipped with the notion of an inner product. We need the structure of a Riemannian manifold in order to meaningfully perform algebraic operations in our space.

In summary, by extending the notion of a line to a geodesic, we can easily translate the notion of convexity on a Euclidean space to geodesic convexity on a Riemannian manifold. We next give a series of known properties regarding geodesic convexity that will be of use in the following proofs (Wiesel 2012; Vishnoi 2018). Many of these properties are analogous to the familiar convex setting.

**Theorem 5.** *Any local minima of a geodesically convex function is a global minima.*

**Proposition 4.** *The following operations preserve geodesic convexity:*

- (i) *(Addition) If  $f$  and  $g$  are  $g$ -convex functions, then  $f + g$  is  $g$ -convex.*
- (ii) *(Kronecker Products) Suppose  $f$  is a real-valued,  $g$ -convex function on  $\mathbb{S}_{++}^d$ , and  $\mathbf{Q}_j \in \mathbb{S}_{++}^{d_j}$  for each  $j = 1, \dots, J$  such that  $\prod_{j=1}^J d_j = d$ . Then*

$$g(\mathbf{Q}_1, \dots, \mathbf{Q}_K) = f(\mathbf{Q}_1 \otimes \dots \otimes \mathbf{Q}_K)$$

*is jointly  $g$ -convex in  $\{\mathbf{Q}_j\}_{j=1}^J \in \mathbb{S}_{++}^{d_1} \times \dots \times \mathbb{S}_{++}^{d_K}$ .*

The proof of Proposition 4(i) is straightforward from the definition of  $g$ -convex functions, and Proposition 4(ii) is proved in Wiesel (2012).

*Remark.* (Example 4.9 in Vishnoi (2018)) Consider the manifold of positive definite matrices  $\mathbb{S}_{++}^n$ . For  $\mathbf{Q}_0, \mathbf{Q}_1 \in \mathbb{S}_{++}^n$ , the geodesic joining  $\mathbf{Q}_0$  to  $\mathbf{Q}_1$  can be parameterized as

$$\mathbf{Q}_t = \mathbf{Q}_0^{\frac{1}{2}} \left( \mathbf{Q}_0^{-\frac{1}{2}} \mathbf{Q}_1 \mathbf{Q}_0^{-\frac{1}{2}} \right)^t \mathbf{Q}_0^{\frac{1}{2}} \quad \forall t \in [0, 1]. \quad (42)$$

## C.2 Global Convergence of the Multiplicative Frobenius iPCA Estimator

We now have the tools to start proving global convergence of the multiplicative iPCA estimator. The roadmap of this proofs is as follows. First, we prove that the negative log-likelihood is g-convex. Then, we prove that the multiplicative Frobenius penalty is g-convex. Since the sum of g-convex functions is g-convex, this implies that the multiplicative iPCA estimator is a g-convex optimization problem. Furthermore, since the Flip-Flop algorithm was proven to converge in Theorem 2, it follows that the multiplicative Frobenius iPCA estimator converges to the global solution as a consequence of geodesic convexity!

Without loss of generality, we assume that each dataset  $\mathbf{X}_k$  has been column-centered for the remainder of this section.

**Lemma 3.** *The negative log-likelihood of our model, (6), is jointly geodesically convex in  $\Sigma^{-1}, \Delta_1^{-1}, \dots, \Delta_K^{-1}$  with respect to  $\mathbb{S}_{++}^n \times \mathbb{S}_{++}^{p_1} \times \dots \times \mathbb{S}_{++}^{p_K}$ .*

*Proof.* Let  $\tilde{\mathbf{X}} = [\mathbf{X}_1, \dots, \mathbf{X}_K] \in \mathbb{R}^{n \times p}$  and define

$$\tilde{\Delta} = \begin{bmatrix} \Delta_1 & 0 & \dots & 0 \\ 0 & \Delta_2 & \dots & 0 \\ \vdots & \vdots & \ddots & \vdots \\ 0 & 0 & \dots & \Delta_K \end{bmatrix}$$

Since  $\tilde{\Delta}$  is a block diagonal matrix, then  $|\tilde{\Delta}| = \prod_{k=1}^K |\Delta_k|$  and  $|\tilde{\Delta}^{-1}| = \prod_{k=1}^K |\Delta_k^{-1}|$ . This implies that

$$\sum_{k=1}^K \log |\Delta_k^{-1}| = \log \left( \prod_{k=1}^K |\Delta_k^{-1}| \right) = \log |\tilde{\Delta}^{-1}|. \quad (43)$$

Also, using this new parameterization,

$$\sum_{k=1}^K \text{tr}(\mathbf{X}_k \Delta_k^{-1} \mathbf{X}_k^T \Sigma^{-1}) = \text{tr}(\tilde{\mathbf{X}} \tilde{\Delta}^{-1} \tilde{\mathbf{X}}^T \Sigma^{-1}) = \text{vec}(\tilde{\mathbf{X}})^T (\tilde{\Delta}^{-1} \otimes \Sigma^{-1}) \text{vec}(\tilde{\mathbf{X}}). \quad (44)$$

Using (43) and (44), we rewrite the negative log-likelihood as

$$\begin{aligned} -\ell(\Sigma^{-1}, \Delta_1^{-1}, \dots, \Delta_K^{-1}) &\propto -p \log |\Sigma^{-1}| - n \sum_{k=1}^K \log |\Delta_k^{-1}| + \sum_{k=1}^K \text{tr}(\mathbf{X}_k \Delta_k^{-1} \mathbf{X}_k^T \Sigma^{-1}) \\ &= -p \log |\Sigma^{-1}| - n \log |\tilde{\Delta}^{-1}| + \text{vec}(\tilde{\mathbf{X}})^T (\tilde{\Delta}^{-1} \otimes \Sigma^{-1}) \text{vec}(\tilde{\mathbf{X}}) \end{aligned}$$

$$\begin{aligned}
&= -\log(|\Sigma^{-1}|^p |\tilde{\Delta}^{-1}|^n) + \text{vec}(\tilde{\mathbf{X}})^T (\tilde{\Delta}^{-1} \otimes \Sigma^{-1}) \text{vec}(\tilde{\mathbf{X}}) \\
&= \log(|\tilde{\Delta}^{-1} \otimes \Sigma^{-1}|^{-1}) + \text{vec}(\tilde{\mathbf{X}})^T (\tilde{\Delta}^{-1} \otimes \Sigma^{-1}) \text{vec}(\tilde{\mathbf{X}}).
\end{aligned}$$

Next, consider the manifold  $\mathbb{S}_{++}^{np}$ , and let the function  $f : \mathbb{S}_{++}^{np} \rightarrow \mathbb{R}$  be given by

$$f(\mathbf{Q}) = \log(|\mathbf{Q}|^{-1}) + \text{vec}(\tilde{\mathbf{X}})^T \mathbf{Q} \text{vec}(\tilde{\mathbf{X}}).$$

Since  $f$  is the sum of geodesically convex functions on  $\mathbb{S}_{++}^{np}$  (Wiesel 2012), and  $-\ell(\Sigma^{-1}, \tilde{\Delta}^{-1}) = f(\tilde{\Delta}^{-1} \otimes \Sigma^{-1})$ , then by Proposition 4, the negative log-likelihood is jointly geodesically convex in  $\Sigma^{-1}, \Delta_1^{-1}, \dots, \Delta_K^{-1}$  with respect to  $\mathbb{S}_{++}^n \times \mathbb{S}_{++}^{p_1} \times \dots \times \mathbb{S}_{++}^{p_K}$ .  $\square$

**Corollary 1.** *If the Flip-Flop estimators for the un-penalized log-likelihood exist, then they converge to the global solution of (16).*

*Proof.* Recall that the Flip-Flop algorithm yields the iterates:

1.  $\hat{\Sigma} = \frac{1}{p} \sum_{k=1}^K \mathbf{X}_k \hat{\Delta}_k^{-1} \mathbf{X}_k^T = \text{argmax}_{\Sigma} \ell(\Sigma, \hat{\Delta}_1, \dots, \hat{\Delta}_K)$
2. For each  $k = 1, \dots, K$ ,  
 $\hat{\Delta}_k = \frac{1}{n} \mathbf{X}_k^T (\hat{\Sigma})^{-1} \mathbf{X}_k = \text{argmax}_{\Delta_k} \ell(\hat{\Sigma}, \hat{\Delta}_1, \dots, \hat{\Delta}_{k-1}, \Delta_k, \hat{\Delta}_{k+1}, \dots, \hat{\Delta}_K)$

Thus, each update of the Flip-Flop algorithm monotonically increases the log-likelihood  $\ell$ . Assuming that the MLEs exist and are bounded, this Flip-Flop algorithm converges to a local maximum. Furthermore, since  $\ell$  is jointly geodesically concave in  $\Sigma^{-1}, \Delta_1^{-1}, \dots, \Delta_K^{-1}$ , then all local maxima are global maxima so that the Flip-Flop estimators for the un-penalized log-likelihood converge to the global solution.  $\square$

**Lemma 4.** *The multiplicative Frobenius norm penalty,  $\|\Sigma^{-1}\|_F^2 \sum_{k=1}^K \lambda_k \|\Delta_k^{-1}\|_F^2$ , is jointly geodesically convex in  $\Sigma^{-1}, \Delta_1^{-1}, \dots, \Delta_K^{-1}$  with respect to  $\mathbb{S}_{++}^n \times \mathbb{S}_{++}^{p_1} \times \dots \times \mathbb{S}_{++}^{p_K}$ .*

*Proof.* Since  $\text{tr}(\mathbf{A} \otimes \mathbf{B}) = \text{tr}(\mathbf{A})\text{tr}(\mathbf{B})$  and  $\|\mathbf{A}\|_F^2 = \text{tr}(\mathbf{A}^T \mathbf{A})$ , then

$$P(\Sigma^{-1}, \Delta_1^{-1}, \dots, \Delta_K^{-1}) := \|\Sigma^{-1}\|_F^2 \sum_{k=1}^K \lambda_k \|\Delta_k^{-1}\|_F^2 \quad (45)$$

$$= \sum_{k=1}^K \lambda_k \text{tr}(\Sigma^{-2}) \text{tr}(\Delta_k^{-2}) \quad (46)$$

$$= \sum_{k=1}^K \lambda_k \text{tr}(\Delta_k^{-2} \otimes \Sigma^{-2}) \quad (47)$$

$$= \sum_{k=1}^K \lambda_k \|\Delta_k^{-1} \otimes \Sigma^{-1}\|_F^2 \quad (48)$$

$$= \sum_{k=1}^K \|(\sqrt{\lambda_k} \Delta_k^{-1}) \otimes \Sigma^{-1}\|_F^2 \quad (49)$$

$$= \|\bar{\Delta}^{-1} \otimes \Sigma^{-1}\|_F^2, \quad (50)$$

where

$$\bar{\Delta} = \begin{bmatrix} \frac{1}{\sqrt{\lambda_1}} \Delta_1 & 0 & \cdots & 0 \\ 0 & \frac{1}{\sqrt{\lambda_2}} \Delta_2 & \cdots & 0 \\ \vdots & \vdots & \ddots & \vdots \\ 0 & 0 & \cdots & \frac{1}{\sqrt{\lambda_K}} \Delta_K \end{bmatrix}.$$

We will next show that the function  $f : \mathbb{S}_{++}^{np} \rightarrow \mathbb{R}$  defined by

$$f(\mathbf{Q}^\alpha) := \|\mathbf{Q}^\alpha\|_F^2 = \text{tr}((\mathbf{Q}^\alpha)^T \mathbf{Q}^\alpha) = \text{tr}((\mathbf{Q}^\alpha)^2), \quad \alpha \in \{\pm 1\} \quad (51)$$

is geodesically convex in  $\mathbf{Q} \in \mathbb{S}_{++}^{np}$ . That is, let  $\mathbf{Q}_0, \mathbf{Q}_1 \in \mathbb{S}_{++}^{np}$  be given, and let  $\mathbf{Q}_t$  be the geodesic between  $\mathbf{Q}_0$  and  $\mathbf{Q}_1$  as given in (42). We want to show that  $f(\mathbf{Q}_t^\alpha)$  is a convex function with respect to  $t$ .

So consider the eigendecomposition  $\mathbf{Q}_0^{-\frac{1}{2}} \mathbf{Q}_1 \mathbf{Q}_0^{-\frac{1}{2}} = \mathbf{U} \mathbf{D} \mathbf{U}^T$ , where  $\mathbf{U}$  is an orthogonal matrix and  $\mathbf{D}$  is a diagonal matrix with diagonal entries  $d_i$ . Then for all  $t \in [0, 1]$ , it follows from (51) that

$$f(\mathbf{Q}_t^\alpha) = \text{tr}(\mathbf{Q}_t^\alpha \mathbf{Q}_t^\alpha) \quad (52)$$

$$= \text{tr}(\mathbf{Q}_0^{\frac{\alpha}{2}} (\mathbf{Q}_0^{-\frac{1}{2}} \mathbf{Q}_1 \mathbf{Q}_0^{-\frac{1}{2}})^{\alpha t} \mathbf{Q}_0^\alpha (\mathbf{Q}_0^{-\frac{1}{2}} \mathbf{Q}_1 \mathbf{Q}_0^{-\frac{1}{2}})^{\alpha t} \mathbf{Q}_0^{\frac{\alpha}{2}}) \quad (53)$$

$$= \text{tr}(\mathbf{Q}_0^{\frac{\alpha}{2}} (\mathbf{U} \mathbf{D} \mathbf{U}^T)^{\alpha t} \mathbf{Q}_0^\alpha (\mathbf{U} \mathbf{D} \mathbf{U}^T)^{\alpha t} \mathbf{Q}_0^{\frac{\alpha}{2}}) \quad (54)$$

$$= \text{tr}(\mathbf{Q}_0^{\frac{\alpha}{2}} \mathbf{U} \mathbf{D}^{\alpha t} \mathbf{U}^T \mathbf{Q}_0^\alpha \mathbf{U} \mathbf{D}^{\alpha t} \mathbf{U}^T \mathbf{Q}_0^{\frac{\alpha}{2}}) \quad (55)$$

$$= \text{tr}(\mathbf{D}^{\alpha t} \mathbf{U}^T \mathbf{Q}_0^\alpha \mathbf{U} \mathbf{D}^{\alpha t} \mathbf{U}^T \mathbf{Q}_0^\alpha \mathbf{U}) \quad (56)$$

$$= \text{tr}(\mathbf{D}^{\alpha t} \mathbf{A} \mathbf{D}^{\alpha t} \mathbf{A}), \quad (57)$$

where  $\mathbf{A} := \mathbf{U}^T \mathbf{Q}_0^\alpha \mathbf{U}$ .

Because  $\mathbf{A}$  is symmetric and  $(\mathbf{D}^{\alpha t} \mathbf{A})_{ij} = d_i^{\alpha t} a_{ij}$ , then

$$(\mathbf{D}^{\alpha t} \mathbf{A} \mathbf{D}^{\alpha t} \mathbf{A})_{ij} = \sum_{l=1}^{np} ((\mathbf{D}^{\alpha t} \mathbf{A})_{il} (\mathbf{D}^{\alpha t} \mathbf{A})_{lj}) = \sum_{l=1}^{np} (d_i^{\alpha t} a_{il} d_l^{\alpha t} a_{lj}) = \sum_{l=1}^{np} (d_i^{\alpha t} a_{il} d_l^{\alpha t} a_{jl}).$$

Plugging this into (57) gives

$$f(\mathbf{Q}_t^\alpha) = \sum_{i=1}^{np} (\mathbf{D}^{\alpha t} \mathbf{A} \mathbf{D}^{\alpha t} \mathbf{A})_{ii} = \sum_{i=1}^{np} \sum_{l=1}^{np} (d_i^{\alpha t} a_{il} d_l^{\alpha t} a_{il}) = \sum_{i=1}^{np} \sum_{l=1}^{np} (a_{il}^2 (d_i d_l)^{\alpha t}).$$

Note that since  $\mathbf{Q}_0$  and  $\mathbf{Q}_1$  are positive definite, then  $\mathbf{Q}_0^{-\frac{1}{2}} \mathbf{Q}_1 \mathbf{Q}_0^{-\frac{1}{2}}$  is positive definite. Thus,  $d_i > 0$  for each  $i = 1, \dots, np$ , and because  $d_i > 0$  for each  $i = 1, \dots, np$ ,  $f(\mathbf{Q}_t^\alpha) = \sum_{i=1}^{np} \sum_{l=1}^{np} (a_{il}^2 (d_i d_l)^{\alpha t})$  is a convex function in  $t$ . This proves  $f$  is g-convex in  $\mathbf{Q} \in \mathbb{S}_{++}^{np}$ .

Since  $f$  is g-convex in  $\mathbf{Q} \in \mathbb{S}_{++}^{np}$  and  $P(\Sigma^{-1}, \bar{\Delta}^{-1}) = f(\bar{\Delta}^{-1} \otimes \Sigma^{-1})$  from (50), then the multiplicative Frobenius norm penalty  $P$  is g-convex in  $\Sigma^{-1}, \Delta_1^{-1}, \dots, \Delta_K^{-1}$  by Proposition 4(ii).  $\square$

**Theorem 3.** *The multiplicative Frobenius iPCA estimator is jointly geodesically convex*

in  $\Sigma^{-1}$  and  $\Delta_1^{-1}, \dots, \Delta_K^{-1}$ . Because of this, the Flip-Flop algorithm for the multiplicative Frobenius iPCA estimator given in Algorithm 1 converges to the global solution.

*Proof.* From Lemma 3 and Lemma 4, we see that the objective function corresponding to the multiplicative Frobenius penalized estimator in (32) is the sum of jointly g-convex functions. Thus, the multiplicative Frobenius penalized estimator is also jointly geodesically convex in  $\Sigma^{-1}$  and  $\Delta_1^{-1}, \dots, \Delta_K^{-1}$ .

Recall we have already proved that Algorithm 1 converges to a stationary point in Theorem 2. Since the multiplicative Frobenius iPCA estimator is geodesically convex, then all local optima are global optima, and the Flip-Flop algorithm for the multiplicative Frobenius iPCA estimator converges to the global solution of (32).  $\square$

*Remark.* The multiplicative Frobenius iPCA estimator is unique in the sense that the Kronecker production solution  $\hat{\Sigma} \otimes \hat{\Delta}_k$  is unique.

## D Subspace Consistency of the Additive $L_1$ Correlation iPCA Estimator

Before proving rates of convergence for the additive  $L_1$  correlation iPCA estimator given by the one-step version of Algorithm 6, we first introduce notation and outline the steps to prove the main result established in Theorem 8.

---

### Algorithm 6 Flip-Flop Algorithm for Additive $L_1$ Correlation-Penalized iPCA Estimators

---

- 1: Center the columns of  $\mathbf{X}_1, \dots, \mathbf{X}_K$ , and initialize  $\hat{\Sigma}, \hat{\Delta}_1, \dots, \hat{\Delta}_K$  to be positive definite.
- 2: **while** not converged **do**
- 3:   **for**  $k = 1, \dots, K$  **do**
- 4:     Compute sample covariance matrix:  $\hat{\mathbf{S}}_k = \frac{1}{n} \mathbf{X}_k^T \hat{\Sigma}^{-1} \mathbf{X}_k$
- 5:     Get standard deviation estimate:  $\hat{\mathbf{W}}_k = \text{diag}(\hat{\mathbf{S}}_k)^{1/2}$
- 6:     Convert to sample correlation matrix:  $\hat{\mathbf{S}}_{\rho,k} = \hat{\mathbf{W}}_k^{-1} \hat{\mathbf{S}}_k \hat{\mathbf{W}}_k^{-1}$
- 7:     Apply graphical lasso to estimate correlation matrix:
 
$$\hat{\Delta}_{\rho,k}^{-1} = \underset{\Delta_{\rho,k}^{-1}}{\text{argmin}} \quad -\log |\Delta_{\rho,k}^{-1}| + \text{tr}(\hat{\mathbf{S}}_{\rho,k} \Delta_{\rho,k}^{-1}) + \lambda_k \|\Delta_{\rho,k}^{-1}\|_{1,\text{off}}$$
- 8:     Convert back to covariance estimate:  $\hat{\Delta}_k = \hat{\mathbf{W}}_k \hat{\Delta}_{\rho,k} \hat{\mathbf{W}}_k$
- 9:   Compute sample covariance matrix:  $\hat{\mathbf{S}}_{\Sigma} = \frac{1}{p} \sum_{k=1}^K \mathbf{X}_k \hat{\Delta}_k^{-1} \mathbf{X}_k^T$
- 10:   Get standard deviation estimate:  $\hat{\mathbf{W}}_{\Sigma} = \text{diag}(\hat{\mathbf{S}}_{\Sigma})^{1/2}$
- 11:   Convert to sample correlation matrix:  $\hat{\mathbf{S}}_{\rho,\Sigma} = \hat{\mathbf{W}}_{\Sigma}^{-1} \hat{\mathbf{S}}_{\Sigma} \hat{\mathbf{W}}_{\Sigma}^{-1}$
- 12:   Apply graphical lasso to estimate correlation matrix:
 
$$\hat{\Sigma}_{\rho}^{-1} = \underset{\Sigma_{\rho}^{-1}}{\text{argmin}} \quad -\log |\Sigma_{\rho}^{-1}| + \text{tr}(\hat{\mathbf{S}}_{\rho,\Sigma} \Sigma_{\rho}^{-1}) + \lambda_{\Sigma} \|\Sigma_{\rho}^{-1}\|_{1,\text{off}}$$
- 13:   Convert back to covariance estimate:  $\hat{\Sigma} = \hat{\mathbf{W}}_{\Sigma} \hat{\Sigma}_{\rho} \hat{\mathbf{W}}_{\Sigma}$

---

Assume that for each  $k = 1, \dots, K$ , the true population model is given by  $\mathbf{X}_k \sim N_{n,p_k}(\mathbf{M}, \Sigma \otimes \Delta_k)$ , where  $\Sigma = (\sigma_{ij})$  and  $\Delta_k = (\delta_{k,ij})$ . Without loss of generality, we may

also assume that  $\mathbf{M} = \mathbf{0}$ . For the purpose of identifiability, define  $\Sigma^* = (\sigma_{*,ij}) = n \Sigma / \text{tr}(\Sigma)$  and  $\Delta_k^* = (\delta_{k,ij}^*) = \text{tr}(\Sigma) \Delta_k / n$  so that  $\text{tr}(\Sigma^*) = n$  and  $\Sigma^* \otimes \Delta_k^* = \Sigma \otimes \Delta_k$  for each  $k$ . Let  $\rho(\Sigma)$  and  $\rho(\Delta_k)$  denote the true correlation matrices corresponding to  $\Sigma$  and  $\Delta_k$ , respectively. Define  $\text{vec}(\mathbf{A})$  to be the vectorization operator which creates a column vector from the matrix  $\mathbf{A}$  by stacking the columns of  $\mathbf{A}$  below one another. Then for each  $k = 1, \dots, K$ , put  $\tilde{\mathbf{S}}_k = \text{vec}(\mathbf{X}_k) \text{vec}(\mathbf{X}_k)^T$  and  $\bar{\mathbf{S}}_k = \text{vec}(\mathbf{X}_k)^T \text{vec}(\mathbf{X}_k)$ . Let  $\tilde{\mathbf{S}}_k^{r,q}$  denote the  $r, q^{\text{th}}$  block of size  $n \times n$  of  $\tilde{\mathbf{S}}_k$ , and let  $\bar{\mathbf{S}}_k^{r,q}$  denote the  $r, q^{\text{th}}$  block of size  $p_k \times p_k$  of  $\bar{\mathbf{S}}_k$ . If  $\mathbf{A}$  is a matrix, let  $\|\mathbf{A}\|_2$  denote the operator norm or the maximum singular value of  $\mathbf{A}$ , let  $\|\mathbf{A}\|_F$  denote the Frobenius norm (i.e.  $\|\mathbf{A}\|_F^2 = \sum_{i,j} a_{ij}^2$ ), let  $\|\mathbf{A}\|_{0,\text{off}}$  denote the number of non-zero non-diagonal entries in  $\mathbf{A}$ , let  $\|\mathbf{A}\|_1 = \sum_{i,j} |a_{ij}|$ , and let  $\|\mathbf{A}\|_{1,\text{off}} = \sum_{i \neq j} |a_{ij}|$ . Denote the stable rank of  $\mathbf{A}$  by  $r(\mathbf{A}) = \|\mathbf{A}\|_F^2 / \|\mathbf{A}\|_2^2$ . Let us also write for a real symmetric matrix  $\mathbf{A}$ ,  $\phi_{\min}(\mathbf{A})$  to be the minimum eigenvalue of  $\mathbf{A}$ . Define  $\sigma_{\min} = \min_i \sigma_{ii}$ ,  $\sigma_{\max} = \max_i \sigma_{ii}$ ,  $\delta_{k,\min} = \min_i \delta_{k,ii}$ ,  $\delta_{k,\max} = \max_i \delta_{k,ii}$ , and similarly for  $\sigma_{*,\min}$ ,  $\sigma_{*,\max}$ ,  $\delta_{k,\min}^*$ , and  $\delta_{k,\max}^*$ . Note that by (A2) and positive definiteness of  $\Sigma$  and  $\Delta_k$ , we have that  $0 < \sigma_{\min} \leq \sigma_{\max} \leq \|\Sigma\|_2 < \infty$  and  $0 < \delta_{k,\min} \leq \delta_{k,\max} \leq \|\Delta_k\|_2 < \infty$ . Also write  $a \vee b = \max(a, b)$  and  $a \wedge b = \min(a, b)$ . If  $a = o(b)$ , then  $|a/b| \rightarrow 0$  as  $n, p_1, \dots, p_K \rightarrow \infty$ . If  $a \asymp b$ , then there exists positive constants  $c, C$  such that  $cb \leq a \leq Cb$  as  $n, p_1, \dots, p_K \rightarrow \infty$ . Lastly, we will adopt the notation defined in Algorithm 6 for the remainder of this section.

The overall idea of our convergence proof is to follow the steps in Algorithm 6 and sequentially bound each step in the algorithm. First, the error from line 8 of Algorithm 6 can be bounded by adapting results from Rothman et al. (2008). Then, in Lemma 5, we bound the error between  $\Sigma^*$  and the sample covariance estimate  $\hat{\mathbf{S}}_\Sigma$  defined in the step 9. Following the Flip-Flop algorithm, we next bound the error between  $\rho(\Sigma)$  and the sample correlation estimate  $\hat{\mathbf{S}}_{\rho,\Sigma}$  from step 11 in Theorem 7. Finally, in Theorem 8, we prove the rate of convergence in the operator and Frobenius norms for  $\hat{\Sigma}^{-1}$  and  $\hat{\Sigma}$  as defined in step 13 of the algorithm. Two direct consequences of convergence in the operator norm are consistent eigenvalues and eigenvectors of  $\hat{\Sigma}$ , which we will discuss following the proofs.

## D.1 Preliminaries

The main driver behind Lemma 5 is a large deviation inequality, namely Theorem 13.1 from Zhou (2014b). As this is an important result used multiple times in the proof of Lemma 5, we state Theorem 13.1 from Zhou (2014b) below in a slightly different form for convenience.

**Theorem 6.** *Assume that  $n \vee p_k \geq 2$ . Let  $\mathbf{M}$  be an  $n \times n$  matrix and  $\mathbf{N}$  be a  $p_k \times p_k$  matrix such that  $\frac{1}{n} \|\mathbf{M}\|_F^2 < \infty$  and  $\frac{1}{p_k} \|\mathbf{N}\|_F^2 < \infty$ . Define  $\tau_k = 2C\tilde{K}^2 \log^{1/2}(n \vee p_k)$ , where  $C := \frac{1}{\sqrt{c}} \vee \frac{1}{c} \vee 1$  and  $\tilde{K}$  and  $c$  are the constants from Theorem 12.1 in Zhou (2014b).*

(i) *If the stable ranks satisfy  $r(\Sigma^{1/2} \mathbf{M} \Sigma^{1/2}) \geq 4 \log(n \vee p_k)$  and  $r(\Delta_k^{1/2} \mathbf{N} \Delta_k^{1/2}) \geq 4 \log(n \vee p_k)$ , then with probability  $1 - \frac{3}{(n \vee p_k)^2}$ , we have that*

$$\left\| \text{diag}(\Delta_k)^{-1/2} \left( \frac{1}{n} \sum_{q=1}^n \sum_{r=1}^n \mathbf{M}_{qr} \bar{\mathbf{S}}_k^{r,q} \right) \text{diag}(\Delta_k)^{-1/2} - \frac{\text{tr}(\Sigma \mathbf{M})}{n} \rho(\Delta_k) \right\|_\infty \leq D_k \tau_k$$

$$\text{and } \left\| \text{diag}(\boldsymbol{\Sigma})^{-1/2} \left( \frac{1}{p} \sum_{q=1}^{p_k} \sum_{r=1}^{p_k} \mathbf{N}_{qr} \tilde{\mathbf{S}}_k^{rq} \right) \text{diag}(\boldsymbol{\Sigma})^{-1/2} - \frac{\text{tr}(\boldsymbol{\Delta}_k \mathbf{N})}{p} \rho(\boldsymbol{\Sigma}) \right\|_{\infty} \leq D'_k \tau_k,$$

where  $D_k = \frac{1}{n} \left\| \boldsymbol{\Sigma}^{1/2} \mathbf{M} \boldsymbol{\Sigma}^{1/2} \right\|_F$  and  $D'_k = \frac{1}{p} \left\| \boldsymbol{\Delta}_k^{1/2} \mathbf{N} \boldsymbol{\Delta}_k^{1/2} \right\|_F$ .

(ii) If  $n \vee p_k = o(\text{expn} \wedge p_k)$ , then with probability  $1 - \frac{3}{(n \vee p_k)^2}$ , the above inequalities hold with  $D_k = \frac{2}{\sqrt{n}} \left\| \boldsymbol{\Sigma} \right\|_2 \left\| \mathbf{M} \right\|_2$  and  $D'_k = \frac{2\sqrt{p_k}}{p} \left\| \boldsymbol{\Delta}_k \right\|_2 \left\| \mathbf{N} \right\|_2$ .

We refer to Zhou (2014b) for the proof of this theorem, but if one looks at the interior of this proof, we obtain the following useful result, presented in Corollary 2.

To simplify notation, let  $\mathcal{E}_{\boldsymbol{\Delta}}(k, \mathbf{M})$  denote the event

$$\left\{ \left\| \text{diag}(\boldsymbol{\Delta}_k)^{-1/2} \left( \frac{1}{n} \sum_{q=1}^n \sum_{r=1}^n \mathbf{M}_{qr} \bar{\mathbf{S}}_k^{rq} \right) \text{diag}(\boldsymbol{\Delta}_k)^{-1/2} - \frac{\text{tr}(\boldsymbol{\Sigma} \mathbf{M})}{n} \rho(\boldsymbol{\Delta}_k) \right\|_{\infty} \leq \frac{2}{\sqrt{n}} \left\| \boldsymbol{\Sigma} \right\|_2 \left\| \mathbf{M} \right\|_2 \tau_k \right\},$$

let  $\mathcal{E}_{\boldsymbol{\Sigma}}(k, \mathbf{N})$  denote the event

$$\left\{ \left\| \text{diag}(\boldsymbol{\Sigma})^{-1/2} \left( \frac{1}{p} \sum_{q=1}^{p_k} \sum_{r=1}^{p_k} \mathbf{N}_{qr} \tilde{\mathbf{S}}_k^{rq} \right) \text{diag}(\boldsymbol{\Sigma})^{-1/2} - \frac{\text{tr}(\boldsymbol{\Delta}_k \mathbf{N})}{p} \rho(\boldsymbol{\Sigma}) \right\|_{\infty} \leq \frac{2\sqrt{p_k}}{p} \left\| \boldsymbol{\Delta}_k \right\|_2 \left\| \mathbf{N} \right\|_2 \tau_k \right\},$$

and define for each  $k = 1, \dots, K$ ,

$$\nu_{n,k} := \frac{2}{\sqrt{n}} \tau_k = 4C\tilde{K}^2 \sqrt{\frac{\log(n \vee p_k)}{n}} \quad (58)$$

$$\nu_{p_k} := \frac{2\sqrt{p_k}}{p} \tau_k = 4C\tilde{K}^2 \frac{\sqrt{p_k \log(n \vee p_k)}}{p} = 4C\tilde{K}^2 \frac{p_k}{p} \sqrt{\frac{\log(n \vee p_k)}{p_k}}. \quad (59)$$

**Corollary 2.** *Assume the same conditions and notation as Theorem 6. Also suppose that  $n \vee p_k = o(\text{expn} \wedge p_k)$ . Then under the event  $\mathcal{E}_{\boldsymbol{\Delta}}(k, \mathbf{M})$ , we have that*

$$\left| \left( \frac{1}{n} \sum_{q=1}^n \sum_{r=1}^n \mathbf{M}_{qr} \bar{\mathbf{S}}_k^{rq} \right)_{ij} - \frac{\text{tr}(\boldsymbol{\Sigma} \mathbf{M})}{n} \delta_{k,ij} \right| \leq \nu_{n,k} \left\| \boldsymbol{\Sigma} \right\|_2 \left\| \mathbf{M} \right\|_2 \sqrt{\delta_{k,ii} \delta_{k,jj}} \quad \forall i, j, \quad (60)$$

and under the event  $\mathcal{E}_{\boldsymbol{\Sigma}}(k, \mathbf{N})$ , we have that

$$\left| \left( \frac{1}{p} \sum_{q=1}^{p_k} \sum_{r=1}^{p_k} \mathbf{N}_{qr} \tilde{\mathbf{S}}_k^{rq} \right)_{ij} - \frac{\text{tr}(\boldsymbol{\Delta}_k \mathbf{N})}{p} \sigma_{ij} \right| \leq \nu_{p_k} \left\| \boldsymbol{\Delta}_k \right\|_2 \left\| \mathbf{N} \right\|_2 \sqrt{\sigma_{ii} \sigma_{jj}} \quad \forall i, j. \quad (61)$$

We now have the necessary large deviation inequalities to prove Lemma 5, a generalization of Lemma 6.1 from Zhou (2014a). Though the proof of Lemma 5 closely resembles that of Lemma 6.1 from Zhou (2014a), modifications must be made as iPCA considers multiple distinct matrix-variate normal models while Zhou (2014a) considers only one matrix-variate

normal model. For clarity, we give our proof in its entirety and refer to results in Zhou (2014a) when necessary.

**Lemma 5.** *Suppose that (A1)-(A4) hold. Let  $\hat{\Delta}_{\rho,k}$  and  $\hat{\Delta}_k$  be obtained as in steps 7 and 8 in Algorithm 6, where we choose*

$$\lambda_k = \frac{2\alpha_k}{\epsilon(1-\alpha_k)} \geq \frac{3\alpha_k}{1-\alpha_k} \quad \text{for } \alpha_k = A\nu_{n,k} \text{ where } A = \frac{\sqrt{n}\|\Sigma\|_F}{\text{tr}(\Sigma)} \quad (62)$$

and  $\epsilon \in (0, 2/3)$ . Then on event  $\mathcal{E}^*$ , we have for  $\hat{\mathbf{S}}_\Sigma$  defined in step 9 of Algorithm 6,

$$\left| (\hat{\mathbf{S}}_\Sigma - \Sigma^*)_{ij} \right| \leq \sum_{k=1}^K \frac{p_k}{p} \left[ 4C\tilde{K}^2 \sqrt{\sigma_{*,ii}\sigma_{*,jj}} \sqrt{\frac{\log(n \vee p_k)}{p_k}} (1 + o(1)) \right] + \sum_{k=1}^K |\sigma_{*,ij}| \tilde{\mu}_k \quad (63)$$

$$= \sum_{k=1}^K \left[ \sqrt{\sigma_{*,ii}\sigma_{*,jj}} \nu_{p_k} (1 + o(1)) + |\sigma_{*,ij}| \tilde{\mu}_k \right], \quad (64)$$

where

$$\tilde{\mu}_k := \lambda_k \frac{\|\hat{\Delta}_{\rho,k}^{-1}\|_{1,\text{off}}}{p} + \frac{\alpha_k}{1-\alpha_k} \frac{\|\hat{\Delta}_{\rho,k}^{-1}\|_1}{p} \leq \mu_k, \quad (65)$$

$$\mu_k := \lambda_k \frac{\|\rho(\Delta_k)^{-1}\|_{1,\text{off}}}{p} + \frac{\alpha_k}{1-\alpha_k} \frac{\|\rho(\Delta_k)^{-1}\|_1}{p} + o(\lambda_k). \quad (66)$$

Moreover,  $\mathbb{P}(\mathcal{E}^*) \geq 1 - \sum_{k=1}^K \frac{8}{(n \vee p_k)^2}$ .  
To put simply, with high probability,

$$\|\hat{\mathbf{S}}_\Sigma - \Sigma^*\|_\infty \leq \sum_{k=1}^K \frac{p_k}{p} \left[ 4C\tilde{K}^2 \sigma_{*,\max} \sqrt{\frac{\log(n \vee p_k)}{p_k}} (1 + o(1)) \right] + \sum_{k=1}^K \sigma_{*,\max} \mu_k \quad (67)$$

$$= \sigma_{*,\max} \sum_{k=1}^K [\nu_{p_k} (1 + o(1)) + \mu_k]. \quad (68)$$

*Proof.* For each  $k = 1, \dots, K$ , define

$$\begin{aligned} \mathbf{R}_{\Sigma,k} &:= [\delta_{k,11} \text{vec}(\Sigma) \dots \delta_{k,1p_k} \text{vec}(\Sigma) \dots \delta_{k,p_k p_k} \text{vec}(\Sigma)] \equiv \text{vec}(\Sigma) \otimes \text{vec}(\Delta_k)^T \\ \hat{\mathbf{R}}_{\Sigma,k} &:= \left[ \text{vec}(\tilde{\mathbf{S}}_k^{11}) \dots \text{vec}(\tilde{\mathbf{S}}_k^{1p_k}) \dots \text{vec}(\tilde{\mathbf{S}}_k^{p_k p_k}) \right]. \end{aligned}$$

Then one can verify as in Zhou (2014a) that

$$\text{vec}(\Sigma^*) = \frac{1}{p} \sum_{k=1}^K \mathbf{R}_{\Sigma,k} \text{vec}((\Delta_k^*)^{-1}) \quad \text{and} \quad \text{vec}(\hat{\mathbf{S}}_\Sigma) = \frac{1}{p} \sum_{k=1}^K \hat{\mathbf{R}}_{\Sigma,k} \text{vec}(\hat{\Delta}_k^{-1}). \quad (69)$$

The equalities from (69) thus yield

$$\text{vec}(\hat{\mathbf{S}}_{\Sigma} - \Sigma^*) = \frac{1}{p} \sum_{k=1}^K \hat{\mathbf{R}}_{\Sigma,k} \text{vec}(\hat{\Delta}_k^{-1}) - \frac{1}{p} \sum_{k=1}^K \mathbf{R}_{\Sigma,k} \text{vec}((\Delta_k^*)^{-1}) \quad (70)$$

$$\begin{aligned} &= \frac{1}{p} \sum_{k=1}^K \hat{\mathbf{R}}_{\Sigma,k} \text{vec}(\hat{\Delta}_k^{-1}) - \frac{1}{p} \sum_{k=1}^K \mathbf{R}_{\Sigma,k} \text{vec}((\Delta_k^*)^{-1}) \\ &\quad + \frac{1}{p} \sum_{k=1}^K \hat{\mathbf{R}}_{\Sigma,k} \text{vec}((\Delta_k^*)^{-1}) - \frac{1}{p} \sum_{k=1}^K \hat{\mathbf{R}}_{\Sigma,k} \text{vec}((\Delta_k^*)^{-1}) \end{aligned} \quad (71)$$

$$= \frac{1}{p} \sum_{k=1}^K \left[ (\hat{\mathbf{R}}_{\Sigma,k} - \mathbf{R}_{\Sigma,k}) \text{vec}((\Delta_k^*)^{-1}) + \hat{\mathbf{R}}_{\Sigma,k} \text{vec}(\hat{\Delta}_k^{-1} - (\Delta_k^*)^{-1}) \right]. \quad (72)$$

For each  $k = 1, \dots, K$ , define  $\Theta_k := \hat{\Delta}_k - \Delta_k^*$  and  $\tilde{\Theta}_k := \hat{\Delta}_k^{-1} - (\Delta_k^*)^{-1}$ , and notice that  $\tilde{\Theta}_k = -\hat{\Delta}_k^{-1} \Theta_k (\Delta_k^*)^{-1}$ . Then

$$\hat{\mathbf{R}}_{\Sigma,k} \text{vec}(\tilde{\Theta}_k) = \hat{\mathbf{R}}_{\Sigma,k} \text{vec}(\tilde{\Theta}_k) + \mathbf{R}_{\Sigma,k} \text{vec}(\tilde{\Theta}_k) - \mathbf{R}_{\Sigma,k} \text{vec}(\tilde{\Theta}_k) \quad (73)$$

$$= \mathbf{R}_{\Sigma,k} \text{vec}(\tilde{\Theta}_k) + (\hat{\mathbf{R}}_{\Sigma,k} - \mathbf{R}_{\Sigma,k}) \text{vec}(\tilde{\Theta}_k) \quad (74)$$

$$= \mathbf{R}_{\Sigma,k} \text{vec}(-\hat{\Delta}_k^{-1} \Theta_k (\Delta_k^*)^{-1}) + (\hat{\mathbf{R}}_{\Sigma,k} - \mathbf{R}_{\Sigma,k}) \text{vec}(-\hat{\Delta}_k^{-1} \Theta_k (\Delta_k^*)^{-1}). \quad (75)$$

Putting (72) and (75) together gives

$$\begin{aligned} \text{vec}(\hat{\mathbf{S}}_{\Sigma} - \Sigma^*) &= \sum_{k=1}^K \left[ \frac{1}{p} (\hat{\mathbf{R}}_{\Sigma,k} - \mathbf{R}_{\Sigma,k}) \text{vec}((\Delta_k^*)^{-1}) + \frac{1}{p} \mathbf{R}_{\Sigma,k} \text{vec}(-\hat{\Delta}_k^{-1} \Theta_k (\Delta_k^*)^{-1}) \right. \\ &\quad \left. + \frac{1}{p} (\hat{\mathbf{R}}_{\Sigma,k} - \mathbf{R}_{\Sigma,k}) \text{vec}(-\hat{\Delta}_k^{-1} \Theta_k (\Delta_k^*)^{-1}) \right] \end{aligned} \quad (76)$$

$$=: \sum_{k=1}^K (\mathbf{U}_{1,k} + \mathbf{U}_{2,k} + \mathbf{U}_{3,k}), \quad (77)$$

where the matrix correspondent for each of the above terms will be denoted by  $\mathbf{M}_{1,k}$ ,  $\mathbf{M}_{2,k}$ , and  $\mathbf{M}_{3,k}$ , respectively. We will proceed to bound each of the terms separately.

In order to bound  $\mathbf{U}_{1,k}$ , notice that by definition of  $\mathbf{R}_{\Sigma,k}$  and  $\hat{\mathbf{R}}_{\Sigma,k}$ ,

$$\mathbf{U}_{1,k} = \frac{1}{p} (\hat{\mathbf{R}}_{\Sigma,k} - \mathbf{R}_{\Sigma,k}) \text{vec}((\Delta_k^*)^{-1}) \quad (78)$$

$$= \frac{1}{p} \sum_{q=1}^{p_k} \sum_{r=1}^{p_k} \text{vec}(\tilde{\mathbf{S}}_k^{qr} - \delta_{k,qr} \Sigma) [(\Delta_k^*)^{-1}]_{qr} \quad (79)$$

$$= \frac{1}{p} \sum_{q=1}^{p_k} \sum_{r=1}^{p_k} \text{vec}(\tilde{\mathbf{S}}_k^{qr}) [(\Delta_k^*)^{-1}]_{qr} - \frac{\text{tr}(\Delta_k (\Delta_k^*)^{-1})}{p} \text{vec}(\Sigma) \quad (80)$$

$$= \frac{1}{p} \sum_{q=1}^{p_k} \sum_{r=1}^{p_k} \text{vec}(\tilde{\mathbf{S}}_k^{qr}) [(\mathbf{\Delta}_k^*)^{-1}]_{qr} - \frac{p_k}{p} \text{vec}(\mathbf{\Sigma}^*) \quad (81)$$

$$\implies \mathbf{M}_{1,k} = \frac{1}{p} \sum_{q=1}^{p_k} \sum_{r=1}^{p_k} \tilde{\mathbf{S}}_k^{qr} [(\mathbf{\Delta}_k^*)^{-1}]_{qr} - \frac{p_k}{p} \mathbf{\Sigma}^*. \quad (82)$$

Define  $\mathcal{E}_{0,k}$  to be the event  $\mathcal{E}_{\mathbf{\Delta}}(k, (\mathbf{\Sigma}^*)^{-1}) \cap \mathcal{E}_{\mathbf{\Sigma}}(k, (\mathbf{\Delta}_k^*)^{-1})$ . Then by Corollary 2, under the event  $\mathcal{E}_{0,k}$ , we have  $|(\mathbf{M}_{1,k})_{ij}| \leq \nu_{p_k} \sqrt{\sigma_{*,ii} \sigma_{*,jj}}$ . Moreover, by Theorem 6,  $\mathbb{P}(\mathcal{E}_{0,k}) \geq 1 - \frac{3}{(n \vee p_k)^2}$ .

Next, we will bound the second term  $\mathbf{U}_{2,k}$ . As in Zhou (2014b), we can write

$$\mathbf{U}_{2,k} = \frac{1}{p} \mathbf{R}_{\mathbf{\Sigma},k} \text{vec}(-\hat{\mathbf{\Delta}}_k^{-1} \mathbf{\Theta}_k (\mathbf{\Delta}_k^*)^{-1}) = \frac{1}{p} \text{tr}(-\hat{\mathbf{\Delta}}_k^{-1} \mathbf{\Theta}_k) \text{vec}(\mathbf{\Sigma}^*), \quad (83)$$

$$\text{and } \mathbf{M}_{2,k} = \frac{1}{p} \text{tr}(-\hat{\mathbf{\Delta}}_k^{-1} \mathbf{\Theta}_k) \mathbf{\Sigma}^*. \quad (84)$$

By Claim 17.3 in Zhou (2014b), it follows that that under event  $\mathcal{X}_{0,k} := \mathcal{E}_{\mathbf{\Sigma}}(k, \mathbf{I}) \cap \mathcal{E}_{\mathbf{\Delta}}(k, \mathbf{I})$ ,

$$\lambda_k \|\hat{\mathbf{\Delta}}_{\rho,k}^{-1}\|_{1,\text{off}} - \frac{\alpha_k}{1 - \alpha_k} \|\hat{\mathbf{\Delta}}_{\rho,k}^{-1}\|_1 \leq \text{tr}(\mathbf{\Theta}_k \hat{\mathbf{\Delta}}_k^{-1}) \leq \lambda_k \|\hat{\mathbf{\Delta}}_{\rho,k}^{-1}\|_{1,\text{off}} + \frac{\alpha_k}{1 - \alpha_k} \|\hat{\mathbf{\Delta}}_{\rho,k}^{-1}\|_1 \quad (85)$$

Thus,

$$|\text{tr}(-\mathbf{\Theta}_k \hat{\mathbf{\Delta}}_k^{-1})| \leq \lambda_k \|\hat{\mathbf{\Delta}}_{\rho,k}^{-1}\|_{1,\text{off}} + \frac{\alpha_k}{1 - \alpha_k} \|\hat{\mathbf{\Delta}}_{\rho,k}^{-1}\|_1, \quad (86)$$

which implies that on  $\mathcal{X}_{0,k}$ ,

$$|(\mathbf{M}_{2,k})_{ij}| \leq \frac{|\sigma_{*,ij}|}{p} \left( \lambda_k \|\hat{\mathbf{\Delta}}_{\rho,k}^{-1}\|_{1,\text{off}} + \frac{\alpha_k}{1 - \alpha_k} \|\hat{\mathbf{\Delta}}_{\rho,k}^{-1}\|_1 \right) = |\sigma_{*,ij}| \tilde{\mu}_k. \quad (87)$$

Additionally, by Theorem 6,  $\mathbb{P}(\mathcal{X}_{0,k}) \geq 1 - \frac{3}{(n \vee p_k)^2}$ .

To bound the final term  $\mathbf{U}_{3,k}$ , we follow the same logic as (78)-(81) to obtain

$$\mathbf{U}_{3,k} = \frac{1}{p} (\hat{\mathbf{R}}_{\mathbf{\Sigma},k} - \mathbf{R}_{\mathbf{\Sigma},k}) \text{vec}(\tilde{\mathbf{\Theta}}_k) \quad (88)$$

$$= \frac{1}{p} \sum_{q=1}^{p_k} \sum_{r=1}^{p_k} \text{vec}(\tilde{\mathbf{S}}_k^{qr}) [\tilde{\mathbf{\Theta}}_k]_{qr} - \frac{\text{tr}(\mathbf{\Delta}_k \tilde{\mathbf{\Theta}}_k)}{p} \text{vec}(\mathbf{\Sigma}), \quad (89)$$

$$\text{and } \mathbf{M}_{3,k} = \frac{1}{p} \sum_{q=1}^{p_k} \sum_{r=1}^{p_k} \tilde{\mathbf{S}}_k^{qr} [\tilde{\mathbf{\Theta}}_k]_{qr} - \frac{\text{tr}(\mathbf{\Delta}_k \tilde{\mathbf{\Theta}}_k)}{p} \mathbf{\Sigma}. \quad (90)$$

Define  $\mathcal{E}_{1,k} := \mathcal{E}_{\mathbf{\Sigma}}(k, \tilde{\mathbf{\Theta}}_k)$ . By the proof of Theorem 6,  $\mathbb{P}(\mathcal{E}_{1,k} | \mathcal{X}_{0,k}) \geq 1 - \frac{2}{(n \vee p_k)^2}$ . On the other hand, under the event  $\mathcal{E}_{1,k}$ , Corollary 2 gives  $|(\mathbf{M}_{3,k})_{ij}| \leq \nu_{p_k} \|\mathbf{\Delta}_k\|_2 \|\tilde{\mathbf{\Theta}}_k\|_2 \sqrt{\sigma_{ii} \sigma_{jj}}$ .

We next bound  $\|\tilde{\mathbf{\Theta}}_k\|_2$  using Corollary 10.1 from Zhou (2014b), so assuming that  $\mathcal{X}_{0,k}$

holds, then

$$\|\tilde{\Theta}_k\|_2 \leq C' \lambda_k \frac{\sqrt{s_k \vee 1}}{\delta_{k,\min}^* \phi_{\min}^2(\rho(\Delta_k))}. \quad (91)$$

In summary, under the event  $\mathcal{E}^* := \cap_{k=1}^K (\mathcal{E}_{0,k} \cap \mathcal{E}_{1,k} \cap \mathcal{X}_{0,k})$ , we have that

$$|(\hat{\mathbf{S}}_{\Sigma} - \Sigma^*)_{ij}| \leq \sum_{k=1}^K (|(\mathbf{M}_{1,k})_{ij}| + |(\mathbf{M}_{2,k})_{ij}| + |(\mathbf{M}_{3,k})_{ij}|) \quad (92)$$

$$\begin{aligned} &\leq \sum_{k=1}^K \left[ \nu_{p_k} \sqrt{\sigma_{*,ii} \sigma_{*,jj}} + |\sigma_{*,ij}| \tilde{\mu}_k \right. \\ &\quad \left. + \nu_{p_k} \|\Delta_k\|_2 \left( C' \lambda_k \frac{\sqrt{s_k \vee 1}}{\delta_{k,\min}^* \phi_{\min}^2(\rho(\Delta_k))} \right) \sqrt{\sigma_{ii} \sigma_{jj}} \right] \quad (93) \end{aligned}$$

$$\begin{aligned} &= \sum_{k=1}^K \left[ \nu_{p_k} \sqrt{\sigma_{*,ii} \sigma_{*,jj}} + |\sigma_{*,ij}| \tilde{\mu}_k \right. \\ &\quad \left. + \nu_{p_k} \|\Delta_k\|_2 \left( C' \lambda_k \frac{\sqrt{s_k \vee 1}}{\delta_{k,\min}^* \phi_{\min}^2(\rho(\Delta_k))} \right) \sqrt{\sigma_{*,ii} \sigma_{*,jj}} \right] \quad (94) \end{aligned}$$

$$\leq \sum_{k=1}^K \left[ \nu_{p_k} \sqrt{\sigma_{*,ii} \sigma_{*,jj}} (1 + o(1)) + |\sigma_{*,ij}| \tilde{\mu}_k \right] \quad (95)$$

under the assumptions.

Furthermore, applying the union bound implies that  $\mathbb{P}(\mathcal{E}^*) \geq 1 - \sum_{k=1}^K \frac{8}{(n \vee p_k)^2}$ . Assuming that event  $\mathcal{X}_{0,k}$  holds,  $\tilde{\mu}_k \leq \mu_k$  is a consequence of Corollary 17.4 from Zhou (2014b), and this concludes the proof.  $\square$

It is important to point out that in our choice of  $\lambda_k$  in (62),  $A$  can be considered a constant under the bounded spectrum assumption (A2). In addition, (A1) implies that  $\sqrt{\frac{\log(n \vee p_k)}{n}} \rightarrow 0$  as  $n, p_k \rightarrow \infty$ . Therefore, since  $\lambda_k$  is on the order of  $A \sqrt{\frac{\log(n \vee p_k)}{n}}$ ,  $\lambda_k \rightarrow 0$  as  $n, p_k \rightarrow \infty$  (for  $k = 1, \dots, K$ ).

Next, stepping through Algorithm 6, we bound the error between the correlation estimate  $\hat{\mathbf{S}}_{\rho, \Sigma}$  and the true correlation matrix  $\rho(\Sigma)$ .

**Theorem 7.** *Suppose the conditions in Lemma 5 hold. Define  $\tilde{\eta}_k := \nu_{p_k} (1 + o(1)) + \tilde{\mu}_k$ . Then under event  $\mathcal{E}^*$ , we have for  $\hat{\mathbf{S}}_{\rho, \Sigma}$  defined in step 11 in Algorithm 6 and  $i \neq j$ ,*

$$\begin{aligned} \left| \left( \hat{\mathbf{S}}_{\rho, \Sigma} - \rho(\Sigma) \right)_{ij} \right| &\leq \sum_{k=1}^K \frac{p_k}{p} \left[ \frac{4C \tilde{K}^2 \sqrt{\frac{\log(n \vee p_k)}{p_k}} (1 + o(1)) (1 + |\rho(\Sigma)_{ij}|)}{1 - \sum_{k=1}^K \tilde{\eta}_k} \right] \\ &\quad + \frac{2|\rho(\Sigma)_{ij}| \sum_{k=1}^K \tilde{\mu}_k}{1 - \sum_{k=1}^K \tilde{\eta}_k} \quad (96) \end{aligned}$$

$$= \sum_{k=1}^K \left[ \frac{\nu_{p_k}(1+o(1))(1+|\rho(\boldsymbol{\Sigma})_{ij}|)}{1-\sum_{k=1}^K \tilde{\eta}_k} + \frac{2|\rho(\boldsymbol{\Sigma})_{ij}|\tilde{\mu}_k}{1-\sum_{k=1}^K \tilde{\eta}_k} \right] \quad (97)$$

$$\leq \frac{2\sum_{k=1}^K \eta_k}{1-\sum_{k=1}^K \eta_k}, \quad \text{where } \eta_k := \nu_{p_k}(1+o(1)) + \mu_k. \quad (98)$$

*Proof.* Because  $\tilde{\mu}_k \leq \mu_k$  by Lemma 5 and  $|\rho(\boldsymbol{\Sigma})_{ij}| \leq 1$  for all  $i, j$ , it is clear that

$$\sum_{k=1}^K \left[ \frac{\nu_{p_k}(1+o(1))(1+|\rho(\boldsymbol{\Sigma})_{ij}|)}{1-\sum_{k=1}^K \tilde{\eta}_k} + \frac{2|\rho(\boldsymbol{\Sigma})_{ij}|\tilde{\mu}_k}{1-\sum_{k=1}^K \tilde{\eta}_k} \right] \leq \frac{2\sum_{k=1}^K \tilde{\eta}_k}{1-\sum_{k=1}^K \tilde{\eta}_k} \leq \frac{2\sum_{k=1}^K \eta_k}{1-\sum_{k=1}^K \eta_k}. \quad (99)$$

Therefore, it suffices to show (96).

Assume throughout this proof that event  $\mathcal{E}^*$  holds. Then by Lemma 5,

$$\left| \frac{[\hat{\mathbf{S}}_{\boldsymbol{\Sigma}}]_{ii}}{\sigma_{*,ii}} - 1 \right| \leq \sum_{k=1}^K [\nu_{p_k}(1+o(1)) + \tilde{\mu}_k] = \sum_{k=1}^K \tilde{\eta}_k, \quad (100)$$

which implies

$$\frac{[\hat{\mathbf{S}}_{\boldsymbol{\Sigma}}]_{ii}}{\sigma_{*,ii}} \geq 1 - \sum_{k=1}^K \tilde{\eta}_k \implies \sqrt{\frac{\sigma_{*,ii}}{[\hat{\mathbf{S}}_{\boldsymbol{\Sigma}}]_{ii}}} \leq \sqrt{\frac{1}{1-\sum_{k=1}^K \tilde{\eta}_k}} \quad (101)$$

for all  $i$ . On the other hand, for  $i \neq j$ , Lemma 5 gives

$$\left| \left( \frac{\hat{\mathbf{S}}_{\boldsymbol{\Sigma}}}{\sqrt{\sigma_{*,ii}\sigma_{*,jj}}} - \rho(\boldsymbol{\Sigma}) \right)_{ij} \right| = \left| \left( \frac{\hat{\mathbf{S}}_{\boldsymbol{\Sigma}}}{\sqrt{\sigma_{*,ii}\sigma_{*,jj}}} - \frac{\boldsymbol{\Sigma}^*}{\sqrt{\sigma_{*,ii}\sigma_{*,jj}}} \right)_{ij} \right| \quad (102)$$

$$\leq \sum_{k=1}^K \left( \nu_{p_k}(1+o(1)) + \frac{|\sigma_{*,ij}|}{\sqrt{\sigma_{*,ii}\sigma_{*,jj}}} \tilde{\mu}_k \right) \quad (103)$$

$$= \sum_{k=1}^K (\nu_{p_k}(1+o(1)) + |\rho(\boldsymbol{\Sigma})_{ij}|\tilde{\mu}_k), \quad (104)$$

Thus, for  $i \neq j$ ,

$$\left| \left( \hat{\mathbf{S}}_{\rho, \boldsymbol{\Sigma}} - \rho(\boldsymbol{\Sigma}) \right)_{ij} \right| = \left| \frac{[\hat{\mathbf{S}}_{\boldsymbol{\Sigma}}]_{ij}}{[\hat{\mathbf{S}}_{\boldsymbol{\Sigma}}]_{ii}^{1/2} [\hat{\mathbf{S}}_{\boldsymbol{\Sigma}}]_{jj}^{1/2}} - \rho(\boldsymbol{\Sigma})_{ij} \right| \quad (105)$$

$$= \left| \frac{\frac{[\hat{\mathbf{S}}_{\boldsymbol{\Sigma}}]_{ij}}{\sqrt{\sigma_{*,ii}\sigma_{*,jj}}}}{\frac{[\hat{\mathbf{S}}_{\boldsymbol{\Sigma}}]_{ii}^{1/2} [\hat{\mathbf{S}}_{\boldsymbol{\Sigma}}]_{jj}^{1/2}}{\sqrt{\sigma_{*,ii}} \sqrt{\sigma_{*,jj}}}} - \rho(\boldsymbol{\Sigma})_{ij} \right| \quad (106)$$

$$\leq \left| \frac{\frac{[\hat{\mathbf{S}}_{\boldsymbol{\Sigma}}]_{ij}}{\sqrt{\sigma_{*,ii}\sigma_{*,jj}}} - \rho(\boldsymbol{\Sigma})_{ij}}{\frac{[\hat{\mathbf{S}}_{\boldsymbol{\Sigma}}]_{ii}^{1/2} [\hat{\mathbf{S}}_{\boldsymbol{\Sigma}}]_{jj}^{1/2}}{\sqrt{\sigma_{*,ii}} \sqrt{\sigma_{*,jj}}}} \right| + \left| \frac{\rho(\boldsymbol{\Sigma})_{ij}}{\frac{[\hat{\mathbf{S}}_{\boldsymbol{\Sigma}}]_{ii}^{1/2} [\hat{\mathbf{S}}_{\boldsymbol{\Sigma}}]_{jj}^{1/2}}{\sqrt{\sigma_{*,ii}} \sqrt{\sigma_{*,jj}}}} - \rho(\boldsymbol{\Sigma})_{ij} \right| \quad (107)$$

$$\begin{aligned}
&= \left| \frac{\sqrt{\sigma_{*,ii}}}{[\hat{\Sigma}_{\Sigma}]_{ii}^{1/2}} \frac{\sqrt{\sigma_{*,jj}}}{[\hat{\Sigma}_{\Sigma}]_{jj}^{1/2}} \right| \left| \frac{[\hat{\Sigma}_{\Sigma}]_{ij}}{\sqrt{\sigma_{*,ii}\sigma_{*,jj}}} - \rho(\Sigma)_{ij} \right| \\
&\quad + |\rho(\Sigma)_{ij}| \left| \frac{\sqrt{\sigma_{*,ii}}}{[\hat{\Sigma}_{\Sigma}]_{ii}^{1/2}} \frac{\sqrt{\sigma_{*,jj}}}{[\hat{\Sigma}_{\Sigma}]_{jj}^{1/2}} - 1 \right| \tag{108}
\end{aligned}$$

$$\begin{aligned}
&\leq \frac{1}{1 - \sum_{k=1}^K \tilde{\eta}_k} \left( \sum_{k=1}^K (\nu_{p_k}(1 + o(1)) + |\rho(\Sigma)_{ij}| \tilde{\mu}_k) \right) \\
&\quad + |\rho(\Sigma)_{ij}| \left| \frac{1}{1 - \sum_{k=1}^K \tilde{\eta}_k} - 1 \right| \tag{109}
\end{aligned}$$

$$= \sum_{k=1}^K \frac{\nu_{p_k}(1 + o(1))(1 + |\rho(\Sigma)_{ij}|) + 2|\rho(\Sigma)_{ij}| \tilde{\mu}_k}{1 - \sum_{k=1}^K \tilde{\eta}_k}. \tag{110}$$

as desired. Note that (109) follows from (101) and (104).  $\square$

## D.2 Main Result

We can now build on top of Theorem 7 and existing results to prove our main convergence result in Theorem 8, which is a generalization of Corollary 17.2 from Zhou (2014b). After this, we discuss two important consequences of Theorem 8 relating to eigenvectors and eigenvalues of the additive  $L_1$  correlation iPCA estimator.

**Theorem 8.** *Suppose that (A1)-(A4) hold and that  $\sqrt{n} \geq \frac{p}{\sqrt{p_k}}$  for each  $k = 1, \dots, K$ . Assume also that  $\eta \leq 1/4$ , and  $\lambda_{\Sigma}$  is chosen to be*

$$\lambda_{\Sigma} = \frac{2 \sum_{k=1}^K \tilde{\eta}_k}{\epsilon_1 (1 - \sum_{k=1}^K \tilde{\eta}_k)}, \quad \text{for some } \epsilon_1 \in (0, 1). \tag{111}$$

Then on the event  $\mathcal{E}^*$ ,

$$\| \hat{\Sigma} - \Sigma^* \|_2 \leq 2\tilde{C} \lambda_{\Sigma} \sigma_{*,\max} \kappa(\rho(\Sigma))^2 \sqrt{s_{\Sigma} \vee 1}, \tag{112}$$

$$\| \hat{\Sigma} - \Sigma^* \|_F \leq 2\tilde{C} \lambda_{\Sigma} \sigma_{*,\max} \kappa(\rho(\Sigma))^2 \sqrt{s_{\Sigma} \vee n}, \tag{113}$$

$$\| \hat{\Sigma}^{-1} - (\Sigma^*)^{-1} \|_2 \leq \frac{\tilde{C} \lambda_{\Sigma} \sqrt{s_{\Sigma} \vee 1}}{\sigma_{*,\min} \phi_{\min}^2(\rho(\Sigma))}, \tag{114}$$

$$\| \hat{\Sigma}^{-1} - (\Sigma^*)^{-1} \|_2 \leq \frac{\tilde{C} \lambda_{\Sigma} \sqrt{s_{\Sigma} \vee n}}{\sigma_{*,\min} \phi_{\min}^2(\rho(\Sigma))} \tag{115}$$

for some constant  $\tilde{C}$ .

*Proof.* Assume that  $\mathcal{E}^*$  holds throughout this proof.

Next, recall that from Theorem 7,

$$\max_{i \neq j} \left| \left( \hat{\mathbf{S}}_{\rho, \Sigma} - \rho(\Sigma) \right)_{ij} \right| \leq \omega := \frac{2 \sum_{k=1}^K \tilde{\eta}_k}{1 - \sum_{k=1}^K \tilde{\eta}_k} \leq \frac{2 \sum_{k=1}^K \eta_k}{1 - \sum_{k=1}^K \eta_k}. \quad (116)$$

By defining  $C_{p,k} := \frac{2 \|\rho(\mathbf{\Delta}_k)^{-1}\|_{1, \text{off}}}{\epsilon p} + \frac{\|\rho(\mathbf{\Delta}_k)^{-1}\|_1}{p}$ , it follows that  $\eta_k = \left( \nu_{p_k} + \frac{\alpha_k}{1 - \alpha_k} C_{p,k} \right) (1 + o(1))$ . Then because  $C_{p,k} \asymp 1$  under (A3) and  $\nu_{p_k} \rightarrow 0$  as  $n, p_k \rightarrow \infty$  under (A1) and (A2),

$$\frac{2 \sum_{k=1}^K \eta_k}{1 - \sum_{k=1}^K \eta_k} \asymp \sum_{k=1}^K \nu_{p_k} \rightarrow 0 \quad \text{as } n, p_k \rightarrow \infty. \quad (117)$$

Moreover, under (A1), we have  $\omega \sqrt{s_{\Sigma} \vee 1} = o(1)$ . Thus, we can apply Theorem 4.5 from Zhou (2014a) to obtain for some constant  $\tilde{C}$ ,

$$\| \hat{\Sigma}_{\rho} - \rho(\Sigma) \|_2 \leq \| \hat{\Sigma}_{\rho} - \rho(\Sigma) \|_F \leq \tilde{C} \kappa(\rho(\Sigma))^2 \lambda_{\Sigma} \sqrt{s_{\Sigma} \vee 1} \quad (118)$$

$$\text{and } \| \hat{\Sigma}_{\rho}^{-1} - \rho(\Sigma)^{-1} \|_2 \leq \| \hat{\Sigma}_{\rho}^{-1} - \rho(\Sigma)^{-1} \|_F \leq \tilde{C} \lambda_{\Sigma} \frac{\sqrt{s_{\Sigma} \vee 1}}{2 \phi_{\min}^2(\rho(\Sigma))}. \quad (119)$$

Now since we have a bound on the correlation estimates, the next step is to consider the covariance estimates. Let us define  $\mathbf{W}_{\Sigma} = \text{diag}(\Sigma^*)^{1/2} = \sqrt{\frac{n}{\text{tr}(\Sigma)}} \text{diag}(\Sigma)^{1/2}$ . By Lemma 5,

$$| \hat{\mathbf{W}}_{\Sigma, ii}^2 - \mathbf{W}_{\Sigma, ii}^2 | = | \hat{\mathbf{W}}_{\Sigma, ii}^2 - \sigma_{*, ii} | \leq \sigma_{*, ii} \sum_{k=1}^K \tilde{\eta}_k \quad \forall i. \quad (120)$$

Therefore,

$$\| \hat{\mathbf{W}}_{\Sigma} - \mathbf{W}_{\Sigma} \|_2 \leq \sqrt{\sigma_{*, \max}} \left[ \left( \sqrt{1 + \sum_{k=1}^K \tilde{\eta}_k} - 1 \right) \vee \left( 1 - \sqrt{1 - \sum_{k=1}^K \tilde{\eta}_k} \right) \right] \quad (121)$$

$$\leq \sqrt{\sigma_{*, \max}} \sum_{k=1}^K \tilde{\eta}_k \quad (122)$$

$$\text{and } \| \hat{\mathbf{W}}_{\Sigma}^{-1} - \mathbf{W}_{\Sigma}^{-1} \|_2 \leq \frac{1}{\sqrt{\sigma_{*, \max}}} \left[ \frac{\sqrt{1 + \sum_{k=1}^K \tilde{\eta}_k} - 1}{\sqrt{1 + \sum_{k=1}^K \tilde{\eta}_k}} \vee \frac{1 - \sqrt{1 - \sum_{k=1}^K \tilde{\eta}_k}}{\sqrt{1 - \sum_{k=1}^K \tilde{\eta}_k}} \right] \quad (123)$$

$$\leq \frac{1}{\sqrt{\sigma_{*, \max}}} \frac{\sum_{k=1}^K \tilde{\eta}_k}{\sqrt{1 - \sum_{k=1}^K \tilde{\eta}_k}}. \quad (124)$$

Using Proposition 15.2 in Zhou (2014b), (122), and (124), we obtain

$$\begin{aligned} \| \hat{\Sigma} - \Sigma^* \|_2 &= \| \hat{\mathbf{W}}_{\Sigma} \hat{\Sigma}_{\rho} \hat{\mathbf{W}}_{\Sigma} - \mathbf{W}_{\Sigma} \rho(\Sigma) \mathbf{W}_{\Sigma} \|_2 \\ &\leq \left( \| \hat{\mathbf{W}}_{\Sigma} - \mathbf{W}_{\Sigma} \|_2 + \| \mathbf{W}_{\Sigma} \|_2 \right)^2 \| \hat{\Sigma}_{\rho} - \rho(\Sigma) \|_2 \end{aligned} \quad (125)$$

$$+ \|\hat{\mathbf{W}}_{\Sigma} - \mathbf{W}_{\Sigma}\|_2 \left( \|\hat{\mathbf{W}}_{\Sigma} - \mathbf{W}_{\Sigma}\|_2 + 2 \right) \|\rho(\Sigma)\|_2 \quad (126)$$

$$\leq \left( \tilde{C}\kappa(\rho(\Sigma))^2 \lambda_{\Sigma} \sqrt{s_{\Sigma} \vee 1} \right) \sigma_{*,\max} \left( 1 + \sum_{k=1}^K \tilde{\eta}_k \right)^2 \\ + \sigma_{*,\max} \sum_{k=1}^K \tilde{\eta}_k \left( \sum_{k=1}^K \tilde{\eta}_k + 2 \right) \|\rho(\Sigma)\|_2. \quad (127)$$

And because  $\lambda_{\Sigma}$  was chosen to satisfy  $\sum_{k=1}^K \tilde{\eta}_k < \lambda_{\Sigma}(1 - \sum_{k=1}^K \tilde{\eta}_k)/2$  where  $\sum_{k=1}^K \tilde{\eta}_k \leq \sum_{k=1}^K \eta_k \leq 1/4$ , we have

$$\|\hat{\Sigma} - \Sigma^*\|_2 \leq \left( \tilde{C}\kappa(\rho(\Sigma))^2 \lambda_{\Sigma} \sqrt{s_{\Sigma} \vee 1} \right) \sigma_{*,\max} \left( 1 + \sum_{k=1}^K \tilde{\eta}_k \right)^2 \\ + \sigma_{*,\max} \frac{\lambda_{\Sigma}}{2} \left( 1 - \sum_{k=1}^K \tilde{\eta}_k \right) \left( \sum_{k=1}^K \tilde{\eta}_k + 2 \right) \|\rho(\Sigma)\|_2 \quad (128)$$

$$\leq 2\tilde{C}\kappa(\rho(\Sigma))^2 \sigma_{*,\max} \lambda_{\Sigma} \sqrt{s_{\Sigma} \vee 1}. \quad (129)$$

We can also bound the error on the Frobenius norm similarly. Using Proposition 15.2 in Zhou (2014b), (122), (124),  $\sum_{k=1}^K \tilde{\eta}_k < \lambda_{\Sigma}(1 - \sum_{k=1}^K \tilde{\eta}_k)/2$ , and  $\sum_{k=1}^K \tilde{\eta}_k \leq \sum_{k=1}^K \eta_k \leq 1/4$  we see that

$$\|\hat{\Sigma} - \Sigma^*\|_F \leq \left( \|\hat{\mathbf{W}}_{\Sigma} - \mathbf{W}_{\Sigma}\|_2 + \|\mathbf{W}_{\Sigma}\|_2 \right)^2 \|\hat{\Sigma}_{\rho} - \rho(\Sigma)\|_F \\ + \|\hat{\mathbf{W}}_{\Sigma} - \mathbf{W}_{\Sigma}\|_2 \left( \|\hat{\mathbf{W}}_{\Sigma} - \mathbf{W}_{\Sigma}\|_2 + 2 \right) \|\rho(\Sigma)\|_F \quad (130)$$

$$\leq \left( \tilde{C}\kappa(\rho(\Sigma))^2 \lambda_{\Sigma} \sqrt{s_{\Sigma} \vee 1} \right) \sigma_{*,\max} \left( 1 + \sum_{k=1}^K \tilde{\eta}_k \right)^2 \\ + \sigma_{*,\max} \sum_{k=1}^K \tilde{\eta}_k \left( \sum_{k=1}^K \tilde{\eta}_k + 2 \right) \sqrt{n} \|\rho(\Sigma)\|_2 \quad (131)$$

$$\leq 2\tilde{C}\kappa(\rho(\Sigma))^2 \sigma_{*,\max} \lambda_{\Sigma} \sqrt{s_{\Sigma} \vee n}. \quad (132)$$

The same logic can be used to prove (114) and (115), so we omit the details.  $\square$

To summarize the convergence results from Theorem 8, if we set

$$\lambda_k = \frac{2\alpha_k}{\epsilon(1 - \alpha_k)} \asymp \sqrt{\frac{\log(n \vee p_k)}{n}} \quad \forall k = 1, \dots, K, \quad (133)$$

$$\text{and } \lambda_{\Sigma} = \frac{2 \sum_{k=1}^K \tilde{\eta}_k}{\epsilon_1(1 - \sum_{k=1}^K \tilde{\eta}_k)} \asymp \sum_{k=1}^K \frac{p_k}{p} \sqrt{\frac{\log(n \vee p_k)}{p_k}}, \quad (134)$$

then according to Theorem 8, with probability  $1 - \sum_{k=1}^K \frac{8}{(n \vee p_k)^2}$ ,

$$\|\hat{\Sigma} - \Sigma^*\|_2 = O\left(\sum_{k=1}^K \frac{p_k}{p} \sqrt{\frac{(s_{\Sigma} \vee 1) \log(n \vee p_k)}{p_k}}\right), \quad (135)$$

$$\|\hat{\Sigma}^{-1} - (\Sigma^{-1})^*\|_2 = O\left(\sum_{k=1}^K \frac{p_k}{p} \sqrt{\frac{(s_{\Sigma} \vee 1) \log(n \vee p_k)}{p_k}}\right), \quad (136)$$

$$\|\hat{\Sigma} - \Sigma^*\|_F = O\left(\sum_{k=1}^K \frac{p_k}{p} \sqrt{\frac{(s_{\Sigma} \vee n) \log(n \vee p_k)}{p_k}}\right), \quad (137)$$

$$\|\hat{\Sigma}^{-1} - (\Sigma^{-1})^*\|_F = O\left(\sum_{k=1}^K \frac{p_k}{p} \sqrt{\frac{(s_{\Sigma} \vee n) \log(n \vee p_k)}{p_k}}\right). \quad (138)$$

*Remark.* The convergence proof above assume that  $\sqrt{n} \geq \frac{p}{\sqrt{p_k}} \forall k = 1, \dots, K$  (i.e. the “large  $n$ ” setting). If instead  $\sqrt{n} < \frac{p}{\sqrt{p_k}} \forall k = 1, \dots, K$  (i.e. the “large  $p$ ” setting), then we modify Algorithm 6 to first initialize an estimate of  $\Sigma$  assuming  $\hat{\Delta}_k = \mathbf{I}$  for each  $k$ . Call this initial estimate  $\hat{\Sigma}^1$ . Then estimate  $\hat{\Delta}_k$  given  $\hat{\Sigma}^1$ . Call this estimate  $\hat{\Delta}_k$ . Lastly, obtain the final estimate of  $\Sigma$  given  $\hat{\Delta}_1, \dots, \hat{\Delta}_K$ . Denote this final estimate of  $\Sigma$  by  $\hat{\Sigma}$ . Similar convergence rates can be obtained for the “large  $p$ ” setting by using this modified algorithm. Namely, if the penalty parameters  $\lambda_k$  and  $\lambda_{\Sigma}$  are chosen on the order of (133) and (134), we can obtain the same rates as (135)-(138). The only additional assumption required here is a bound on  $|\rho(\Sigma)_{ij}|$ , namely,  $|\rho(\Sigma)_{ij}| = O(\frac{\sqrt{np_k}}{p})$  for each  $k = 1, \dots, K$  and  $i \neq j$ . We omit this proof as it is a repetition of previous arguments with slight differences. A more thorough discussion of this scenario is presented in Zhou (2014a).

Thus, in either the large  $n$  or large  $p$  case, we have a variant of the additive  $L_1$  correlation Flip-Flop algorithm such that under certain assumptions, the estimate of  $\Sigma$  converges at a rate of  $O\left(\sum_{k=1}^K \frac{p_k}{p} \sqrt{\frac{(s_{\Sigma} \vee 1) \log(n \vee p_k)}{p_k}}\right)$  in the operator norm. As a result of convergence in the operator norm, we obtain consistency of the eigenvalues and eigenvectors of  $\hat{\Sigma}$ .

1. If we let  $\phi_i$  denote the  $i^{\text{th}}$  eigenvalue of  $\Sigma^*$  and  $\hat{\phi}_i$  denote the  $i^{\text{th}}$  eigenvalue of  $\hat{\Sigma}$ , where the eigenvalues are sorted in descending order, then by Weyl’s theorem (Horn and Johnson 2012), we have that

$$|\hat{\phi}_i - \phi_i| \leq \|\hat{\Sigma} - \Sigma^*\|_2 \quad \forall i. \quad (139)$$

From (135) and the fact that  $\sum_{k=1}^K \frac{p_k}{p} \sqrt{\frac{(s_{\Sigma} \vee 1) \log(n \vee p_k)}{p_k}}$  converges to 0 as  $n, p_1, \dots, p_K \rightarrow \infty$  under (A1), (139) gives us consistency of the eigenvalues of  $\hat{\Sigma}$ .

2. Since iPCA is focused on estimating an underlying subspace and the eigenvectors of  $\hat{\Sigma}$  define this subspace, we are most interested in the consistency of the eigenvectors. So let  $\mathbf{v}_i$  denote the eigenvector of  $\Sigma^*$  corresponding to the eigenvalue  $\phi_i$ , and let  $\hat{\mathbf{v}}_i$

be the eigenvector of  $\hat{\Sigma}$  with eigenvalue  $\hat{\phi}_i$ . Then by a variant of the Davis-Kahan sin  $\theta$  theorem given in Yu et al. (2015),

$$\|\hat{\mathbf{v}}_i - \mathbf{v}_i\|_2 \leq \frac{2^{3/2} \|\hat{\Sigma} - \Sigma^*\|_2}{\min(\phi_{i-1} - \phi_i, \phi_i - \phi_{i+1})} \quad \forall i \quad (140)$$

assuming that  $\min(\phi_{i-1} - \phi_i, \phi_i - \phi_{i+1}) \neq 0$  and  $\hat{\mathbf{v}}^T \mathbf{v} \geq 0$ . (Note that if  $\hat{\mathbf{v}}^T \mathbf{v} < 0$ , we can simply take the negative of  $\hat{\mathbf{v}}$  and apply the theorem to  $-\hat{\mathbf{v}}$  and  $\mathbf{v}$ .) As before, (135) and (A1) then imply the consistency of the eigenvectors of  $\hat{\Sigma}$ .

## E Selecting Penalty Parameters

Our missing data imputation framework for selecting penalty parameters is given in Algorithm 7. In the subsequent sections, we discuss algorithms to impute the missing data in step 4 of this algorithm. As one option, one could use the multi-cycle expectation-conditional maximization (MCECM) (Meng and Rubin 1993) algorithm, which iterates between taking conditional expectations in the E-step and maximizing with respect to one variable at a time in the M-step. We derive the full MCECM algorithm for iPCA in Appendix E.1. This method generalizes the MCECM imputation method proposed in Allen and Tibshirani (2010), which only considered the  $K = 1$  case. However, as Allen and Tibshirani (2010) pointed out, the full MCECM algorithm is computationally expensive, so in practice, we also advocate using a faster one-step approximation to the MCECM algorithm, which we discuss in Appendix E.2.

---

### Algorithm 7 Selecting Penalty Parameters via Missing Imputation Framework

---

**Given:** data  $\mathbf{X}_1, \dots, \mathbf{X}_K$ , space of penalty parameters  $\Lambda$ , type of penalized iPCA estimator

- 1: **for**  $k = 1, \dots, K$  **do**
  - 2:     Randomly leave out 5% of the elements in  $\mathbf{X}_k$ ; denote these scattered missing elements by  $\mathbf{X}_k^m$
  - 3: **for**  $\lambda$  in  $\Lambda$  **do**
  - 4:     Impute missing values (preferably by Algorithm 9); denote these imputed values by  $\hat{\mathbf{X}}_k^m$
  - 5: Select  $\lambda$  which minimizes  $\sum_{k=1}^K \frac{\|\hat{\mathbf{X}}_k^m - \mathbf{X}_k^m\|_F^2}{\|\mathbf{X}_k^m - \bar{\mathbf{X}}_k^m\|_F^2}$ , where  $\bar{\mathbf{X}}_k^m$  are the values of the column mean matrix  $\bar{\mathbf{X}}_k$  at the missing indicies.
- 

Following the notation in Allen and Tibshirani (2010), we write  $\mathbf{X}^o = (\mathbf{X}_1^o, \dots, \mathbf{X}_K^o)$  to denote the totality of observed entries of  $\mathbf{X} = (\mathbf{X}_1, \dots, \mathbf{X}_K)$ , and  $\mathbf{X}^m = (\mathbf{X}_1^m, \dots, \mathbf{X}_K^m)$  to denote the missing entries of  $\mathbf{X}$ . Also define  $\Theta = (\boldsymbol{\mu}_1, \dots, \boldsymbol{\mu}_K, \Sigma^{-1}, \Delta_1^{-1}, \dots, \Delta_K^{-1})$ , and let  $\Theta'$  be the current estimates of  $\Theta$ . Note that the MCECM and its one-step approximation for iPCA (where  $K \geq 1$ ) are generalizations of the imputation algorithms from Allen and Tibshirani (2010) (where  $K = 1$ ).

## E.1 Multi-Cycle Expectation-Conditional Maximization Algorithm

For concreteness, we will work with the multiplicative Frobenius penalty. The other penalized methods are very similar. We will proceed to derive the E-steps and M-steps with respect to each variable for the MCECM algorithm.

So first, in order to compute the E-steps, note that the  $Q$  function is

$$\begin{aligned}
Q(\Theta; \Theta') &:= \mathbb{E}_{\mathbf{X}^m | \mathbf{X}^o, \Theta'}[\ell(\Theta | \mathbf{X})] \\
&= p \log |\Sigma^{-1}| + n \sum_{k=1}^K \log |\Delta_k^{-1}| \\
&\quad - \mathbb{E}_{\mathbf{X}^m | \mathbf{X}^o, \Theta'} \left[ \sum_{k=1}^K \text{tr} \left( \Sigma^{-1} (\mathbf{X}_k - \mathbf{1}_n \boldsymbol{\mu}_k^T) \Delta_k^{-1} (\mathbf{X}_k - \mathbf{1}_n \boldsymbol{\mu}_k^T)^T \right) \right] \\
&\quad - \|\Sigma^{-1}\|_F^2 \sum_{k=1}^K \rho_k \|\Delta_k^{-1}\|_F^2
\end{aligned} \tag{141}$$

Thus, for the E-step with respect to  $\Sigma$ , we use linearity of the expectation and trace operators to obtain

$$\mathbb{E}_{\mathbf{X}^m | \mathbf{X}^o, \Theta'} \left[ \sum_{k=1}^K \text{tr} \left( \Sigma^{-1} (\mathbf{X}_k - \mathbf{1}_n \boldsymbol{\mu}_k^T) \Delta_k^{-1} (\mathbf{X}_k - \mathbf{1}_n \boldsymbol{\mu}_k^T)^T \right) \right] \tag{143}$$

$$= \text{tr} \left( \sum_{k=1}^K \mathbb{E}_{\mathbf{X}^m | \mathbf{X}^o, \Theta'} \left[ \Sigma^{-1} (\mathbf{X}_k - \mathbf{1}_n \boldsymbol{\mu}_k^T) \Delta_k^{-1} (\mathbf{X}_k - \mathbf{1}_n \boldsymbol{\mu}_k^T)^T \right] \right) \tag{144}$$

$$= \text{tr} \left( \Sigma^{-1} \sum_{k=1}^K \mathbb{E}_{\mathbf{X}^m | \mathbf{X}^o, \Theta'} \left[ (\mathbf{X}_k - \mathbf{1}_n \boldsymbol{\mu}_k^T) \Delta_k^{-1} (\mathbf{X}_k - \mathbf{1}_n \boldsymbol{\mu}_k^T)^T \right] \right). \tag{145}$$

Using the notation and proof of Proposition 3 in Allen and Tibshirani (2010), the conditional expectation reduces to

$$\mathbb{E}_{\mathbf{X}^m | \mathbf{X}^o, \Theta'} \left[ (\mathbf{X}_k - \mathbf{1}_n \boldsymbol{\mu}_k^T) \Delta_k^{-1} (\mathbf{X}_k - \mathbf{1}_n \boldsymbol{\mu}_k^T)^T \right] = \sum_{k=1}^K (\hat{\mathbf{X}}_k \Delta_k^{-1} \hat{\mathbf{X}}_k^T + F_k(\Delta_k^{-1})). \tag{146}$$

For the E-Step with respect to  $\Delta_k$ , a similar argument shows that

$$\mathbb{E}_{\mathbf{X}^m | \mathbf{X}^o, \Theta'} \left[ \sum_{k=1}^K \text{tr} \left( \Sigma^{-1} (\mathbf{X}_k - \mathbf{1}_n \boldsymbol{\mu}_k^T) \Delta_k^{-1} (\mathbf{X}_k - \mathbf{1}_n \boldsymbol{\mu}_k^T)^T \right) \right] \tag{147}$$

$$= \sum_{k=1}^K \text{tr} \left( \mathbb{E}_{\mathbf{X}^m | \mathbf{X}^o, \Theta'} \left[ (\mathbf{X}_k - \mathbf{1}_n \boldsymbol{\mu}_k^T)^T \Sigma^{-1} (\mathbf{X}_k - \mathbf{1}_n \boldsymbol{\mu}_k^T) \right] \Delta_k^{-1} \right), \tag{148}$$

and again from Allen and Tibshirani (2010), we have that

$$\mathbb{E}_{\mathbf{X}^m | \mathbf{X}^o, \Theta'} \left[ (\mathbf{X}_k - \mathbf{1}_n \boldsymbol{\mu}_k^T)^T \boldsymbol{\Sigma}^{-1} (\mathbf{X}_k - \mathbf{1}_n \boldsymbol{\mu}_k^T) \right] = \hat{\mathbf{X}}_k^T \boldsymbol{\Sigma}^{-1} \hat{\mathbf{X}}_k + G(\boldsymbol{\Sigma}^{-1}). \quad (149)$$

We next plug (146) and (149) back into the  $Q$  function and take partial derivatives to compute the M steps.

For the M-step with respect to  $\boldsymbol{\Sigma}$ , we have that

$$\frac{\partial Q}{\partial \boldsymbol{\Sigma}^{-1}} = p \boldsymbol{\Sigma} - \sum_{k=1}^K (\hat{\mathbf{X}}_k \boldsymbol{\Delta}_k^{-1} \hat{\mathbf{X}}_k^T + F_k(\boldsymbol{\Delta}_k^{-1})) - 2 \boldsymbol{\Sigma}^{-1} \sum_{k=1}^K \lambda_k \|\boldsymbol{\Delta}_k^{-1}\|_F^2 = 0,$$

so given  $\boldsymbol{\Delta}_k^{-1}$  from the previous iteration, we can update  $\boldsymbol{\Sigma}$  via an eigendecomposition of  $\sum_{k=1}^K (\hat{\mathbf{X}}_k \boldsymbol{\Delta}_k^{-1} \hat{\mathbf{X}}_k^T + F_k(\boldsymbol{\Delta}_k^{-1}))$ . (The form of this update is analogous to the Flip-Flop updates in the multiplicative Frobenius Flip-Flop algorithm.)

Similarly, for the M-step with respect to  $\boldsymbol{\Delta}_k$ ,

$$\frac{\partial Q}{\partial \boldsymbol{\Delta}_k^{-1}} = n \boldsymbol{\Delta}_k - (\hat{\mathbf{X}}_k^T \boldsymbol{\Sigma}^{-1} \hat{\mathbf{X}}_k + G(\boldsymbol{\Sigma}^{-1})) - 2 \lambda_k \boldsymbol{\Delta}_k^{-1} \|\boldsymbol{\Sigma}^{-1}\|_F^2 = 0,$$

so given  $\boldsymbol{\Sigma}^{-1}$  from the previous iteration, we can update  $\boldsymbol{\Delta}_k$  by an eigendecomposition of  $\hat{\mathbf{X}}_k^T \boldsymbol{\Sigma}^{-1} \hat{\mathbf{X}}_k + G(\boldsymbol{\Sigma}^{-1})$ .

Putting these E-steps and M-steps together, we provide the full MCECM algorithm to impute missing values in Algorithm 8.

---

**Algorithm 8** Full MCECM Algorithm for iPCA

---

- |  |   |
|--|---|
| <ol style="list-style-type: none"> <li>1: Set <math>\hat{\boldsymbol{\mu}}_k</math> to be the column means of <math>\mathbf{X}_k^o</math> for each <math>k = 1, \dots, K</math></li> <li>2: If <math>x_{ij}^k</math> is missing, set <math>x_{ij}^k = \hat{\boldsymbol{\mu}}_k^j</math>.</li> <li>3: Initialize <math>\hat{\boldsymbol{\Sigma}}^{-1}</math> and <math>\hat{\boldsymbol{\Delta}}_1^{-1} \dots \hat{\boldsymbol{\Delta}}_K^{-1}</math> to be symmetric positive definite.</li> <li>4: <b>while</b> not converged <b>do</b></li> <li>5:   Compute <math>\sum_{k=1}^K [\hat{\mathbf{X}}_k \hat{\boldsymbol{\Delta}}_k^{-1} \hat{\mathbf{X}}_k^T + F(\hat{\boldsymbol{\Delta}}_k^{-1})]</math> <span style="float: right;">▷ E-Step (<math>\boldsymbol{\Sigma}</math>)</span></li> <li>6:   Update <math>\hat{\boldsymbol{\mu}}_k</math> to be the column means of <math>\hat{\mathbf{X}}_k</math></li> <li>7:   Take eigendecomposition: <math>\sum_{k=1}^K [\hat{\mathbf{X}}_k \hat{\boldsymbol{\Delta}}_k^{-1} \hat{\mathbf{X}}_k^T + F(\hat{\boldsymbol{\Delta}}_k^{-1})] = \mathbf{U} \boldsymbol{\Gamma} \mathbf{U}^T</math></li> <li>8:   Regularize eigenvalues: <math>\phi_i = \frac{1}{2p} \left( \gamma_i + \sqrt{\gamma_i^2 + 8p \sum_{k=1}^K \lambda_k \ \hat{\boldsymbol{\Delta}}_k^{-1}\ _F^2} \right)</math> <span style="float: right;">} M-Step (<math>\boldsymbol{\Sigma}</math>)</span></li> <li>9:   Update <math>\hat{\boldsymbol{\Sigma}}^{-1} = \mathbf{U} \boldsymbol{\Phi}^{-1} \mathbf{U}^T</math></li> <li>10:   <b>for</b> <math>k = 1, \dots, K</math> <b>do</b></li> <li>11:     Compute <math>\hat{\mathbf{X}}_k^T \hat{\boldsymbol{\Sigma}}^{-1} \hat{\mathbf{X}}_k + G_k(\hat{\boldsymbol{\Sigma}}^{-1})</math> <span style="float: right;">▷ E-Step (<math>\boldsymbol{\Delta}_k</math>)</span></li> <li>12:     Update <math>\hat{\boldsymbol{\mu}}_k</math> to be the column means of <math>\hat{\mathbf{X}}_k</math></li> <li>13:     Take eigendecomposition: <math>\hat{\mathbf{X}}_k^T \hat{\boldsymbol{\Sigma}}^{-1} \hat{\mathbf{X}}_k + G_k(\hat{\boldsymbol{\Sigma}}^{-1}) = \mathbf{V} \boldsymbol{\Phi} \mathbf{V}^T</math></li> <li>14:     Regularize eigenvalues: <math>\gamma_i = \frac{1}{2n} \left( \phi_i + \sqrt{\phi_i^2 + 8n \lambda_k \ \hat{\boldsymbol{\Sigma}}^{-1}\ _F^2} \right)</math> <span style="float: right;">} M-Step (<math>\boldsymbol{\Delta}_k</math>)</span></li> <li>15:     Update <math>\hat{\boldsymbol{\Delta}}_k^{-1} = \mathbf{V} \boldsymbol{\Gamma}^{-1} \mathbf{V}^T</math></li> </ol> | <div style="font-size: 3em; line-height: 1;">}</div> <div style="font-size: 3em; line-height: 1;">}</div> |
|--|---|
-

## E.2 One-Step Approximation

Algorithm 8 is a generalization of the TRCMAimpute algorithm from Allen and Tibshirani (2010), and as discussed in Allen and Tibshirani (2010), it is computationally expensive to compute  $F(\hat{\Delta}_k^{-1})$  and  $G(\hat{\Delta}_k^{-1})$ . Hence, rather than using the full MCECM algorithm to impute the missing values in step 4 of Algorithm 7, we advocate, as in Allen and Tibshirani (2010), using a one-step approximation to the MCECM algorithm. We will empirically show that the one-step approximation is both a good approximation to the full MCECM algorithm and works well in practice.

The idea behind the one-step approximation is that since the first step of the MCECM algorithm typically gives the steepest decrease in the objective function, we will quickly approximate the MCECM algorithm by first obtaining a decent initial imputation and then stopping the algorithm after one M-step and one E-step. We detail the initial imputation step, M-step, and E-step as follows.

For the initial imputation step, we impute missing values assuming  $\Sigma = \mathbf{I}$ . If we assume  $\Sigma = \mathbf{I}$ , then  $\mathbf{X}_k \sim N_{n,p_k}(\mathbf{1}_n \boldsymbol{\mu}_k^T, \Sigma \otimes \Delta_k)$  for each  $k = 1, \dots, K$ , or equivalently,  $\mathbf{x}_1^k, \dots, \mathbf{x}_n^k \stackrel{iid}{\sim} N(\boldsymbol{\mu}_k, \Delta_k)$ , where  $x_i^k$  is the  $i^{\text{th}}$  row of  $\mathbf{X}_k$ . Since this reduces to the familiar multivariate case, we can initially impute the missing values in  $\mathbf{X}_k$  using any (regularized) multivariate normal imputation method such as RCMimpute from Allen and Tibshirani (2010) for each  $k = 1, \dots, K$ .

Given the initial imputation for  $\mathbf{X}_1, \dots, \mathbf{X}_K$  from the previous step, we next compute the M-step and estimate  $\boldsymbol{\mu}_1, \dots, \boldsymbol{\mu}_K, \Sigma, \Delta_1, \dots, \Delta_K$  using the penalized Flip-Flop algorithms derived in Appendix B.

In the next and final step, we take an E-step to impute the missing values by  $\hat{\mathbf{X}}_k^m = \mathbb{E}[\mathbf{X}_k^m | \mathbf{X}_k^o, \hat{\boldsymbol{\mu}}_k, \hat{\Sigma}, \hat{\Delta}_k]$  for each  $k = 1, \dots, K$ . This can be done using the Alternating Conditional Expectations Algorithm from Allen and Tibshirani (2010), applied to each  $\mathbf{X}_k$  separately. The only difference is that we specialize to the case where the mean matrix is  $\mathbf{M}_k = \mathbf{1}_n \boldsymbol{\mu}_k^T$ . We summarize this one-step approximation method for missing data imputation in Algorithm 9.

---

### Algorithm 9 One-Step MCECM Approximation

---

- 1: **for**  $k = 1, \dots, K$  **do** ▷ Initial Imputation // E-Step
  - 2:     Impute missing values in  $\mathbf{X}_k$  assuming  $\Sigma = \mathbf{I}$ ; call it  $\hat{\mathbf{X}}_{k,0}$ 
    - Use any regularized multivariate normal imputation method
  - 3: Estimate  $\boldsymbol{\mu}_1, \dots, \boldsymbol{\mu}_K, \Sigma, \Delta_1, \dots, \Delta_K$  given  $\hat{\mathbf{X}}_{1,0}, \dots, \hat{\mathbf{X}}_{K,0}$  via penalized MLE Flip-Flop algorithm ▷ M-Step
  - 4: **for**  $k = 1, \dots, K$  **do** ▷ E-Step
  - 5:     Set the missing values  $\hat{\mathbf{X}}_k^m = \mathbb{E}[\mathbf{X}_k^m | \mathbf{X}_k^o, \hat{\boldsymbol{\mu}}_k, \hat{\Sigma}, \hat{\Delta}_k]$  using the alternating conditional expectations algorithm as in Allen and Tibshirani (2010)
- 

In Figure 8, we compare the numerical convergence of the one-step approximation and the full MCECM algorithm for a small simulation. From this plot, we note two important observations. First, the initialization (assuming  $\Sigma = \mathbf{I}$ ) in the one-step approximation makes a significant difference, compared to initializing missing elements to their respective column means as in the full MCECM algorithm. Second, the first update of the

MCECM algorithm results in the largest increase in the log-likelihood function. As discussed in Allen and Tibshirani (2010), these two observations motivate the one-step approximation algorithm, which takes advantage of a good initialization and one update step to main sufficient accuracy while reducing the computational workload. Figure 8 also shows that the likelihood function after a good initialization and one iteration is on par with the full MCECM algorithm after 15 iterations. For a more detailed discussion on computation and timing comparisons between the one-step approximation and the full MCECM algorithm, we refer to Allen and Tibshirani (2010). Note that though Allen and Tibshirani (2010) only treats the  $K = 1$  case, the results are applicable to the  $K > 1$  case due to the separability of the log-likelihood function.

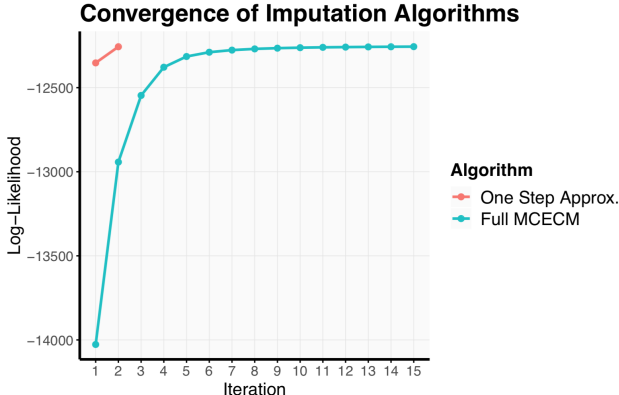


**Figure 8:** We use the same simulation as that in Figure 9 and randomly leave out 5% of the entries in each dataset. We impute the missing values using the full MCECM and one-step approximation algorithms with the multiplicative Frobenius penalty ( $\lambda = (1, 1)$ ), and we plot the log-likelihood value over each iterate. The log-likelihood obtained by the one-step approximation is on par with the log-likelihood after 15 iterations of the MCECM algorithm.

Figure 9 compares the average imputation errors from the full MCECM and the one-step approximation for a small simulation. In this case, for both the one-step approximation and the full MCECM,  $\lambda = (10^{-5}, 100) \approx (0.32, 100)$  gave the lowest average imputation error, and hence, both imputation methods selected  $\lambda = (10^{-5}, 100)$  for the multiplicative Frobenius iPCA estimator. This further supports the use of the one-step algorithm as an approximation to the full MCECM in practice. Moreover, we verified that the minimum subspace recovery error of 2.00 was obtained at  $\lambda^* = (0.01, 10^{1.5}) \approx (0.01, 31.62)$  and that  $\lambda = (10^{-5}, 100)$  yielded a similar subspace recovery error of 2.08. This preliminary empirical evidence leads us to believe that the one-step imputation algorithm is indeed a good approximation to the full MCECM algorithm.

## F Simulations

In order to check that the simulation results in Figure 3 are not heavily dependent on our choice of  $\Sigma$  and  $\Delta_1, \Delta_2, \Delta_3$ , we ran additional simulations, varying the dimension of the true underlying subspace  $\mathbf{U}$  and the number of datasets  $K$ . These simulation results are shown in Figure 10.

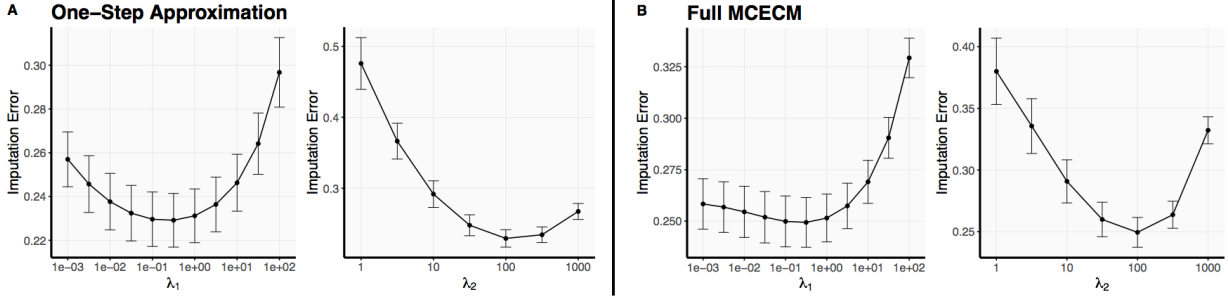


**Figure 9:** We simulated two coupled data matrices  $\mathbf{X}_1, \mathbf{X}_2$  with  $n = 50, p_1 = 60, p_2 = 70$  according to the iPCA model (2). Here, we took  $\Sigma$  to be as in the base simulation described in Section 4.1,  $\Delta_1$  to be an autoregressive Toeplitz matrix with the  $(ij)^{th}$  entry given by  $.9^{|i-j|}$ , and  $\Delta_2$  to be a block-diagonal matrix with five equal-sized blocks. Then, we randomly removed 5% of the elements in  $\mathbf{X}_1$  and  $\mathbf{X}_2$  and imputed these missing values using the full MCECM and the one-step approximation algorithms with the multiplicative Frobenius penalty. We plot the average imputation error  $\sum_{k=1}^K \|\hat{\mathbf{X}}_k^m - \mathbf{X}_k^m\|_F^2 / \|\mathbf{X}_k^m - \bar{\mathbf{X}}_k^m\|_F^2$  plus or minus one standard error, taken over 10 trials. In the left graph of each panel (A and B),  $\lambda_1$  varies while  $\lambda_2$  is fixed at its optimal value (i.e.  $\lambda_2 = 100$ ), and in the right graph of each panel,  $\lambda_2$  varies while  $\lambda_1$  is fixed at its optimal value (i.e.  $\lambda_1 = 10^{-.5}$ ). The minimum average imputation error is achieved at  $\lambda = (10^{-.5}, 100)$  for both imputation algorithms.

For the simulations in Figure 10A, we took  $\Delta_1, \Delta_2, \Delta_3$  to be the same as in the base simulation, and we put  $\Sigma$  to be of the form  $\mathbf{U}\mathbf{D}\mathbf{U}^T$ , where  $\mathbf{U}$  was a random  $n \times n$  orthogonal matrix, and  $\mathbf{D} = \text{diag}(d_1, \dots, d_n)$  was simulated by  $d_i \sim \text{Unif}(5, 75)$  for  $i = 1, \dots, D$ , and  $d_i = 1$  otherwise. Here,  $D$  is the dimension of the true underlying subspace of  $\Sigma$  (e.g.  $D$  was taken to be 2 in the base simulation). Then, like in the base simulation, we generated  $\mathbf{X}_k$  for each  $k = 1, 2, 3$  by  $\mathbf{X}_k \sim N(\mathbf{0}, \Sigma \otimes \Delta_k)$ , or equivalently  $\mathbf{X}_k = \Sigma^{1/2} \Omega \Delta_k^{1/2}$ , where  $\Omega$  is an  $n \times p_k$  random matrix with i.i.d.  $N(0, 1)$  entries.

For the simulations in Figure 10B, we took  $\Sigma$  to be the same as in the base simulation, and we generated  $\Delta_k$  from a random choice among the covariance types:

- (i) Autoregressive Toeplitz matrix with the  $(ij)^{th}$  entry given by  $\rho^{|i-j|}$ , where  $\rho \sim \text{Unif}(-.9, .9)$ ;
- (ii) Block diagonal matrix with  $B$  blocks of the entries  $q_1, \dots, q_B$ , where  $B \sim \text{Unif}(3, 10)$  and  $q_i \sim \text{Unif}(0, .9)$ ;
- (iii) Spiked covariance matrix  $\mathbf{U}\mathbf{D}\mathbf{U}^T$ , where  $\mathbf{U}$  is a random orthogonal matrix,  $d_i \sim \text{Unif}(5, 75)$  for  $i = 1, \dots, D$ ,  $d_i = 1$  for  $i = D + 1, \dots, p_k$ , and  $D \sim \text{Unif}(5, 50)$ ;
- (iv) Observed covariance matrix of real miRNA data from TCGA Ovarian Cancer. (Note that this covariance matrix can only be used for one  $k \in \{1, \dots, K\}$ )

The number of features was randomly selected by  $p_k \sim \text{Unif}(200, 500)$ , and we ensured that  $\|\Delta_k\|$  was larger than that of  $\Sigma$  so that the individual signal was larger than the joint signal.

As conveyed in Figure 10A, the Frobenius iPCA estimators outperformed its competitors regardless of the subspace dimension of  $\Sigma$ . It is also encouraging to see that the strong performance of the Frobenius iPCA estimators is not dependent on the cluster model for  $\Sigma$ , which was used in the simulations in Figure 3 but not in Figure 10A. Note that since the simulated  $\Sigma$  was dense, the additive  $L_1$  penalized iPCA estimator should perform poorly,

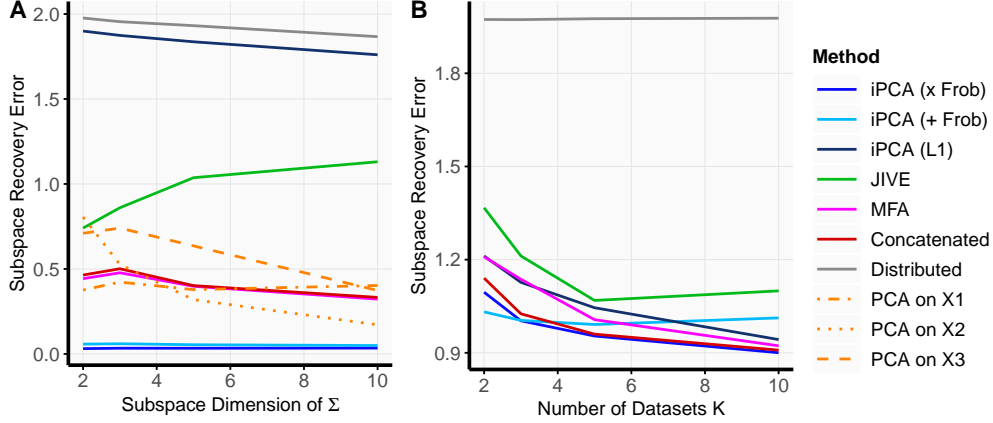


**Figure 10:** *Additional Simulations: (A) The Frobenius iPCA estimators yield the lower subspace recovery error regardless of the subspace dimension of  $\Sigma$ ; (B) As the number of integrated datasets increases, most methods tend to do better, with the multiplicative Frobenius iPCA penalty slightly outperforming the others when  $K = 10$ . Note that we did not run individual PCAs in (B) because the number of datasets is changing.*

as it does. We also point out that JIVE tends to do worse as the subspace dimension of  $\Sigma$  increases because JIVE tends to underestimate the rank of the joint variation matrix when the subspace dimension of  $\Sigma$  is larger. This is one of the disadvantages of matrix factorizations, as they require the rank of the factorized matrices to be chosen a priori.

In Figure 10B, we see that most of the methods perform better as the number of integrated datasets increases and that the multiplicative Frobenius iPCA estimator slightly outperforms all the other methods when  $K = 10$ . We speculate that the additive Frobenius iPCA estimator does worse for large values of  $K$  because the grid of possible penalty parameters was too coarse, and as  $K$  increase, so does the number of penalty parameters. Hence, it becomes more difficult to choose appropriate penalty parameters when  $K$  is large.

For the Laplacian simulations in Figure 4A, we generated  $\mathbf{X}_k$  for each  $k = 1, 2, 3$  by  $\mathbf{X}_k = \Sigma^{1/2} \Omega \Delta_k^{1/2} + \mathbf{E}$ , where  $\Sigma$  and  $\Delta_k$  were taken as in the base simulation, and  $\mathbf{E}$  was an  $n \times p_k$  random matrix with i.i.d. Laplace(0,  $b$ ) entries.

For the simulations in Figure 4B, we simulated three coupled datasets from an instance of the JIVE model: for each  $k = 1, 2, 3$ ,  $\mathbf{X}_k = \mathbf{J}_k + \mathbf{A}_k + \mathbf{E}_k$ , where  $\mathbf{J} = [\mathbf{J}_1, \mathbf{J}_2, \mathbf{J}_3]$  is the joint variation matrix of rank  $r = 5$ ,  $\mathbf{A}_1, \mathbf{A}_2, \mathbf{A}_3$  are the individual variation matrices of rank  $r_1 = 10$ ,  $r_2 = 15$ ,  $r_3 = 20$ , respectively, and  $\mathbf{E}_k$  are error matrices with independent entries from  $N(0, \sigma^2)$ . Similar to the simulations in Lock et al. (2013), we set  $\mathbf{J}$  and  $\mathbf{A}_k$  by  $\mathbf{J} = \mathbf{U} \mathbf{V}_k$  and  $\mathbf{A}_k = \mathbf{U}_k \mathbf{W}_k$ , where  $\mathbf{U} \in \mathbb{R}^{n \times r}$ ,  $\mathbf{V}_k \in \mathbb{R}^{r \times p_k}$ ,  $\mathbf{U}_k \in \mathbb{R}^{n \times r_k}$ , and  $\mathbf{W}_k \in \mathbb{R}^{r_k \times p_k}$ . Here,  $\mathbf{U}, \mathbf{U}_k, \mathbf{V}_k, \mathbf{W}_k$  are matrices whose entries are randomly generated i.i.d. from one of the following distributions:  $N(0, 1)$ ,  $\text{Unif}(0, 1)$ ,  $\text{Exp}(1)$ , and the discrete random variable  $\{-2, -1, 0, 1, 2\}$  with uniform probabilities. Note that under this JIVE model, the true joint covariance matrix is given by  $\Sigma = \mathbf{J} \mathbf{J}^T$ .

We finally note that other metrics such as canonical angles, which also quantify the distance between subspaces, these metrics behave similarly to the subspace recovery error, so we omitted the results for brevity. Other common metrics such as  $\|\|\hat{\Sigma}\|_2 - \|\Sigma\|_2\|$  or  $\|\hat{\Sigma} - \Sigma\|_F^2$  are not appropriate for our study because we are interested in the distance between subspaces of eigenvectors, and eigenvectors are scale-invariant while these metric

are not.

R code can be found at <https://github.com/DataSlingers/iPCA>.

## References

- Abdi, H., Williams, L. J., and Valentin, D. (2013). Multiple factor analysis: principal component analysis for multitable and multiblock data sets. *Wiley Interdisciplinary Reviews: Computational Statistics*, 5(2):149–179.
- Acar, E., Papalexakis, E. E., Gürdeniz, G., Rasmussen, M. A., Lawaetz, A. J., Nilsson, M., and Bro, R. (2014). Structure-revealing data fusion. *BMC Bioinformatics*, 15(1):239.
- Allen, G. I. and Tibshirani, R. (2010). Transposable regularized covariance models with an application to missing data imputation. *The Annals of Applied Statistics*, 4(2):764–790.
- Alter, O., Brown, P. O., and Botstein, D. (2003). Generalized singular value decomposition for comparative analysis of genome-scale expression data sets of two different organisms. *Proceedings of the National Academy of Sciences*, 100(6):3351–3356.
- Benidis, K., Sun, Y., Babu, P., and Palomar, D. P. (2016). Orthogonal sparse pca and covariance estimation via procrustes reformulation. *IEEE Transactions on Signal Processing*, 64(23):6211–6226.
- Carrette, O., Demalte, I., Scherl, A., Yalkinoglu, O., Corthals, G., Burkhard, P., Hochstrasser, D. F., and Sanchez, J. (2003). A panel of cerebrospinal fluid potential biomarkers for the diagnosis of alzheimer’s disease. *Proteomics*, 3(8):1486–1494.
- Dawid, A. (1981). Some matrix-variate distribution theory: notational considerations and a bayesian application. *Biometrika*, 68(1):265–274.
- Dutilleul, P. (1999). The mle algorithm for the matrix normal distribution. *Journal of Statistical Computation and Simulation*, 64(2):105–123.
- Escofier, B. and Pages, J. (1994). Multiple factor analysis. *Computational Statistics & Data Analysis*, 18(1):121–140.
- Espuny-Camacho, I., Arranz, A. M., Fiers, M., Snellinx, A., Ando, K., Munck, S., Bonnefont, J., Lambot, L., Corthout, N., Omodho, L., et al. (2017). Hallmarks of alzheimer’s disease in stem-cell-derived human neurons transplanted into mouse brain. *Neuron*, 93(5):1066–1081.
- Fan, J., Wang, D., Wang, K., and Zhu, Z. (2017). Distributed estimation of principal eigenspaces. *ArXiv e-prints*.
- Ghil, M. and Malanotte-Rizzoli, P. (1991). Data assimilation in meteorology and oceanography. In *Advances in Geophysics*, volume 33, pages 141–266. Elsevier.

- Greenewald, K. and Hero, A. O. (2015). Robust kronecker product pca for spatio-temporal covariance estimation. *IEEE Transactions on Signal Processing*, 63(23):6368–6378.
- Gupta, A. K. and Nagar, D. K. (1999). *Matrix variate distributions*. CRC Press.
- Han, P., Liang, W., Baxter, L. C., Yin, J., Tang, Z., Beach, T. G., Caselli, R. J., Reiman, E. M., and Shi, J. (2014). Pituitary adenylate cyclase-activating polypeptide is reduced in alzheimer’s disease. *Neurology*, 82(19):1724–1728.
- Hastie, T., Mazumder, R., Lee, J. D., and Zadeh, R. (2015). Matrix completion and low-rank svd via fast alternating least squares. *The Journal of Machine Learning Research*, 16(1):3367–3402.
- Horn, R. A. and Johnson, C. R. (2012). *Matrix analysis*. Cambridge university press.
- Hotelling, H. (1936). Relations between two sets of variates. *Biometrika*, pages 321–377.
- Hsieh, C. J., Dhillon, I. S., Ravikumar, P. K., and Sustik, M. A. (2011). Sparse inverse covariance matrix estimation using quadratic approximation. In *Advances in Neural Information Processing Systems*, pages 2330–2338.
- Johnson, W. E., Li, C., and Rabinovic, A. (2007). Adjusting batch effects in microarray expression data using empirical bayes methods. *Biostatistics*, 8(1):118–127.
- Li, Y., Chen, Z., Gao, Y., Pan, G., Zheng, H., Zhang, Y., Xu, H., Bu, G., and Zheng, H. (2017). Synaptic adhesion molecule pcdh- $\gamma$ c5 mediates synaptic dysfunction in alzheimer’s disease. *Journal of Neuroscience*, pages 1051–17.
- Lock, E. F., Hoadley, K. A., Marron, J. S., and Nobel, A. B. (2013). Joint and individual variation explained (jive) for integrated analysis of multiple data types. *The Annals of Applied Statistics*, 7(1):523.
- Meng, X. L. and Rubin, D. B. (1993). Maximum likelihood estimation via the ecm algorithm: A general framework. *Biometrika*, 80(2):267–278.
- Mostafavi, S., Gaiteri, C., Sullivan, S. E., White, C. C., Tasaki, S., Xu, J., Taga, M., Klein, H. U., Patrick, E., Komashko, V., et al. (2018). A molecular network of the aging human brain provides insights into the pathology and cognitive decline of alzheimer’s disease. *Nature Neuroscience*, 21(6):811–819.
- Network, T. C. G. A. R. (2011). Integrated genomic analyses of ovarian carcinoma. *Nature*, 474(7353):609.
- Ponnappalli, S. P., Saunders, M. A., Van Loan, C. F., and Alter, O. (2011). A higher-order generalized singular value decomposition for comparison of global mrna expression from multiple organisms. *PloS one*, 6(12):e28072.
- Rapcsák, T. (1991). Geodesic convexity in nonlinear optimization. *Journal of Optimization Theory and Applications*, 69(1):169–183.

- Rothman, A. J., Bickel, P. J., Levina, E., and Zhu, J. (2008). Sparse permutation invariant covariance estimation. *Electronic Journal of Statistics*, 2:494–515.
- Shivappa, S. T., Trivedi, M. M., and Rao, B. D. (2010). Audiovisual information fusion in human-computer interfaces and intelligent environments: A survey. *Proceedings of the IEEE*, 98(10):1692–1715.
- Singh, A. P. and Gordon, G. J. (2008). Relational learning via collective matrix factorization. In *Proceedings of the 14th ACM SIGKDD International Conference on Knowledge Discovery and Data Mining*, pages 650–658. ACM.
- Tseng, P. (2001). Convergence of a block coordinate descent method for nondifferentiable minimization. *Journal of Optimization Theory and Applications*, 109(3):475–494.
- Tsiligkaridis, T., Hero, A. O., and Zhou, S. (2013). On convergence of kronecker graphical lasso algorithms. *IEEE Transactions on Signal Processing*, 61:1743–1755.
- Vishnoi, N. K. (2018). Geodesic Convex Optimization: Differentiation on Manifolds, Geodesics, and Convexity. *ArXiv e-prints*.
- Westerhuis, J. A., Kourti, T., and MacGregor, J. F. (1998). Analysis of multiblock and hierarchical pca and pls models. *Journal of Chemometrics*, 12(5):301–321.
- Wiesel, A. (2012). Geodesic convexity and covariance estimation. *IEEE Transactions on Signal Processing*, 60(12):6182.
- Yin, J. and Li, H. (2012). Model selection and estimation in the matrix normal graphical model. *Journal of Multivariate Analysis*, 107:119–140.
- Yu, Y., Wang, T., and Samworth, R. J. (2015). A useful variant of the davis-kahan theorem for statisticians. *Biometrika*, 102(2):315–323.
- Zhang, H. and Sra, S. (2016). First-order methods for geodesically convex optimization. In *Conference on Learning Theory*, pages 1617–1638.
- Zhou, S. (2014a). Gemini: Graph estimation with matrix variate normal instances. *The Annals of Statistics*, 42(2):532–562.
- Zhou, S. (2014b). Supplement to “gemini: Graph estimation with matrix variate normal instances”.